Subduction IV
Global subduction modeling

Thorsten W Becker

University of Southern California

Short course at
Universita di Roma
TRE

April 18 – 20, 2011

Real slabs aren't free

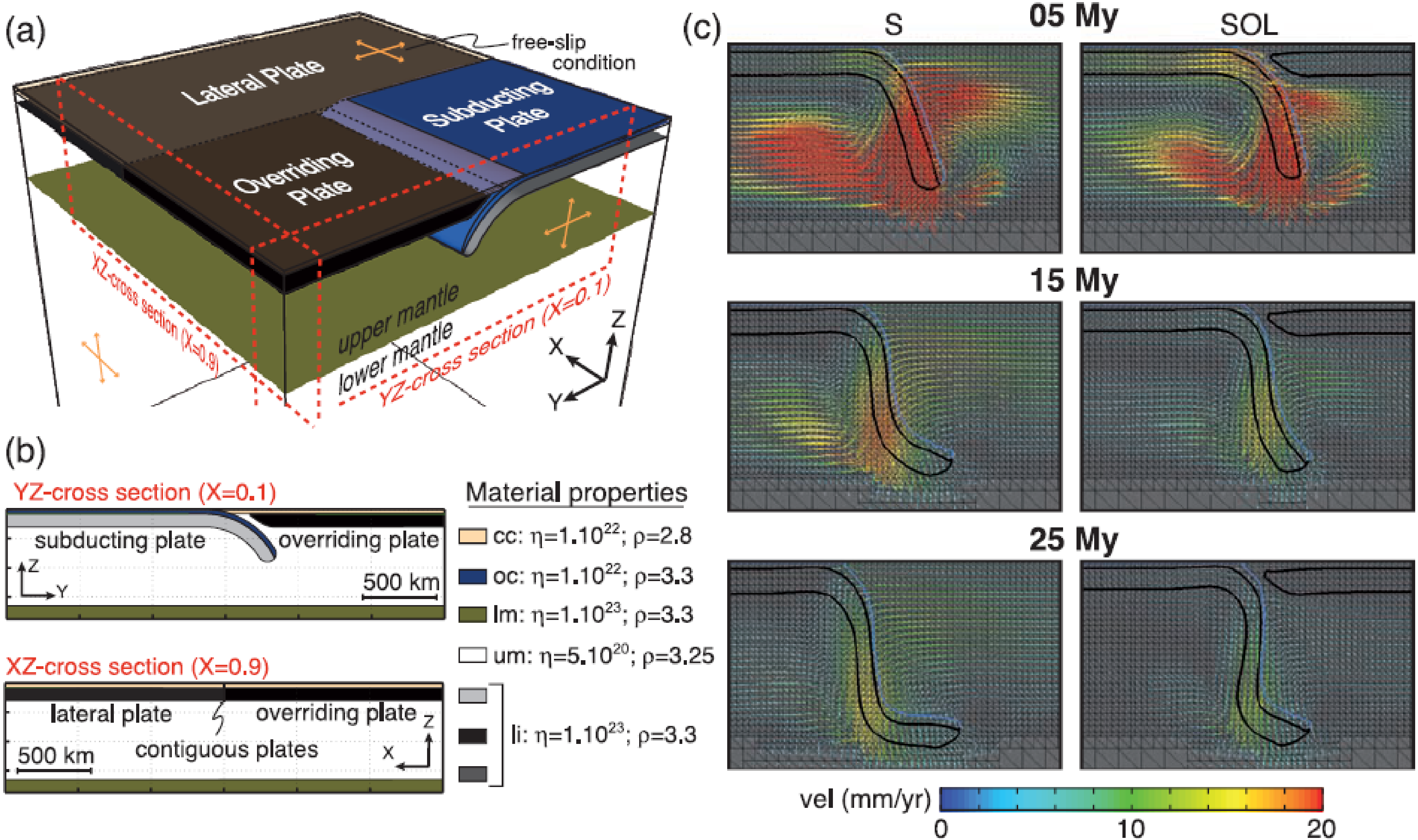

Yamato et el. (2009)

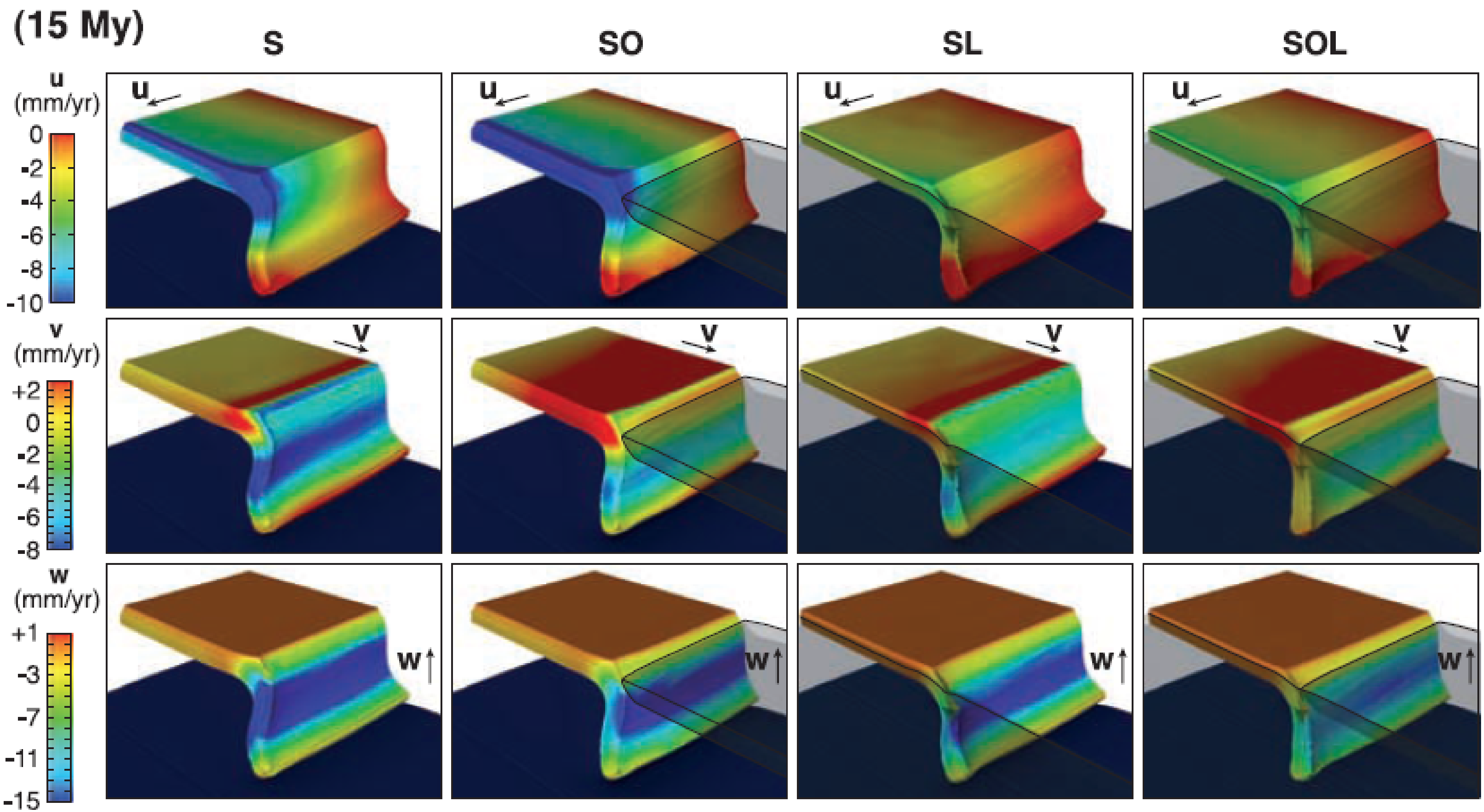

Yamato et el. (2009)

Regional subduction flowlines

- Stiff, dense slab (blue) drives flow

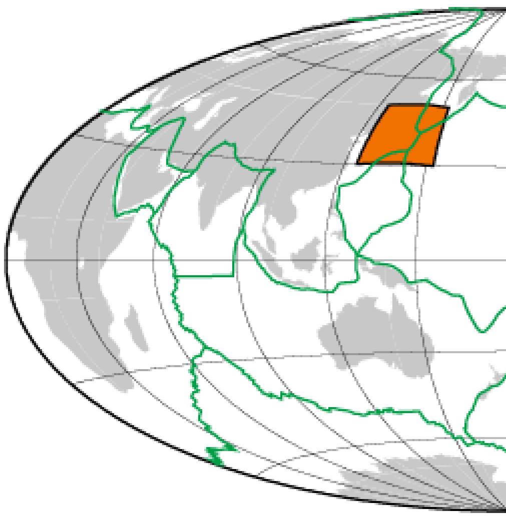

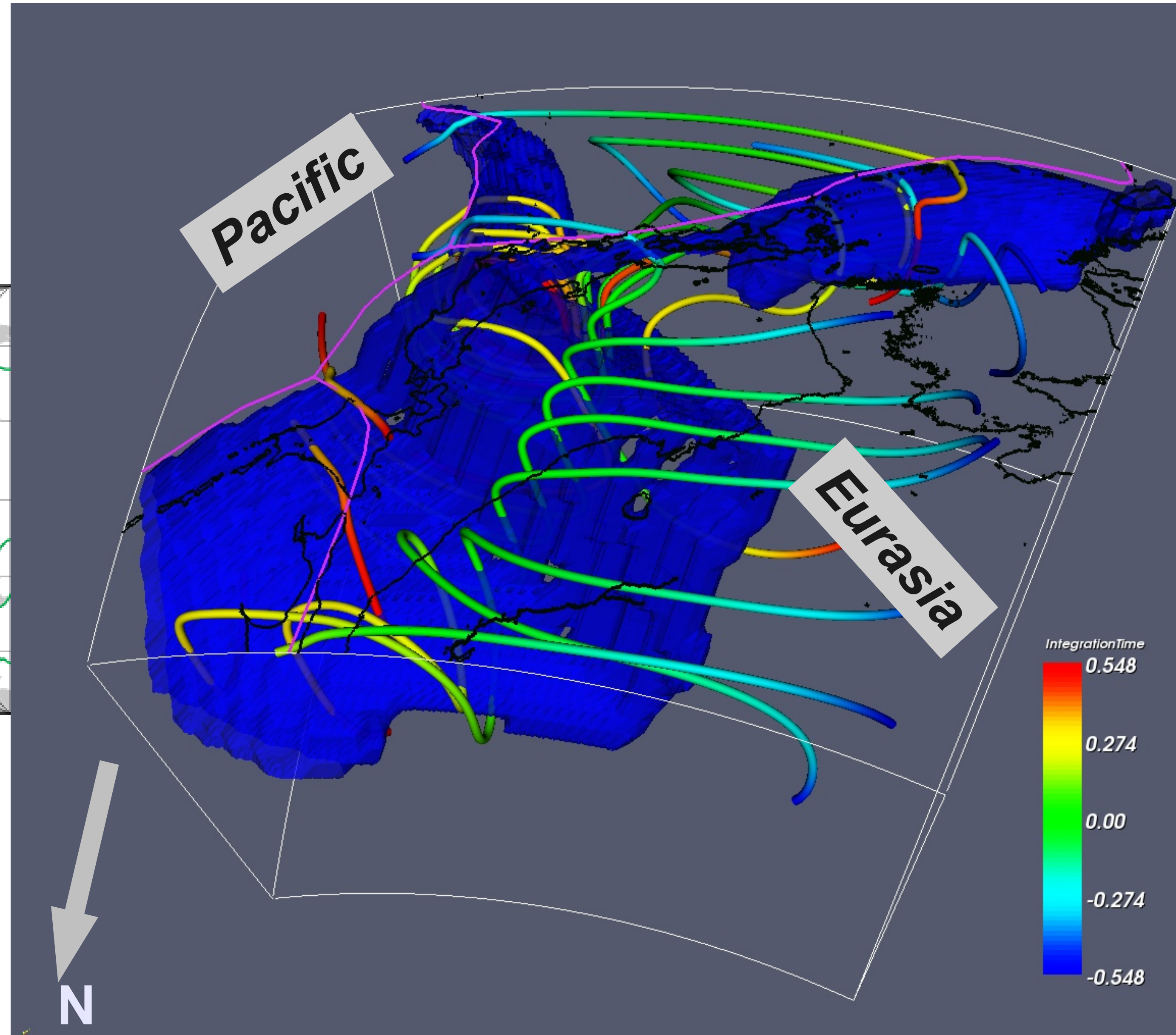

- Subduction rolls
- Streamlines don't match dip

Becker & Faccenna (2009)

Embedded (nested) subduction flow

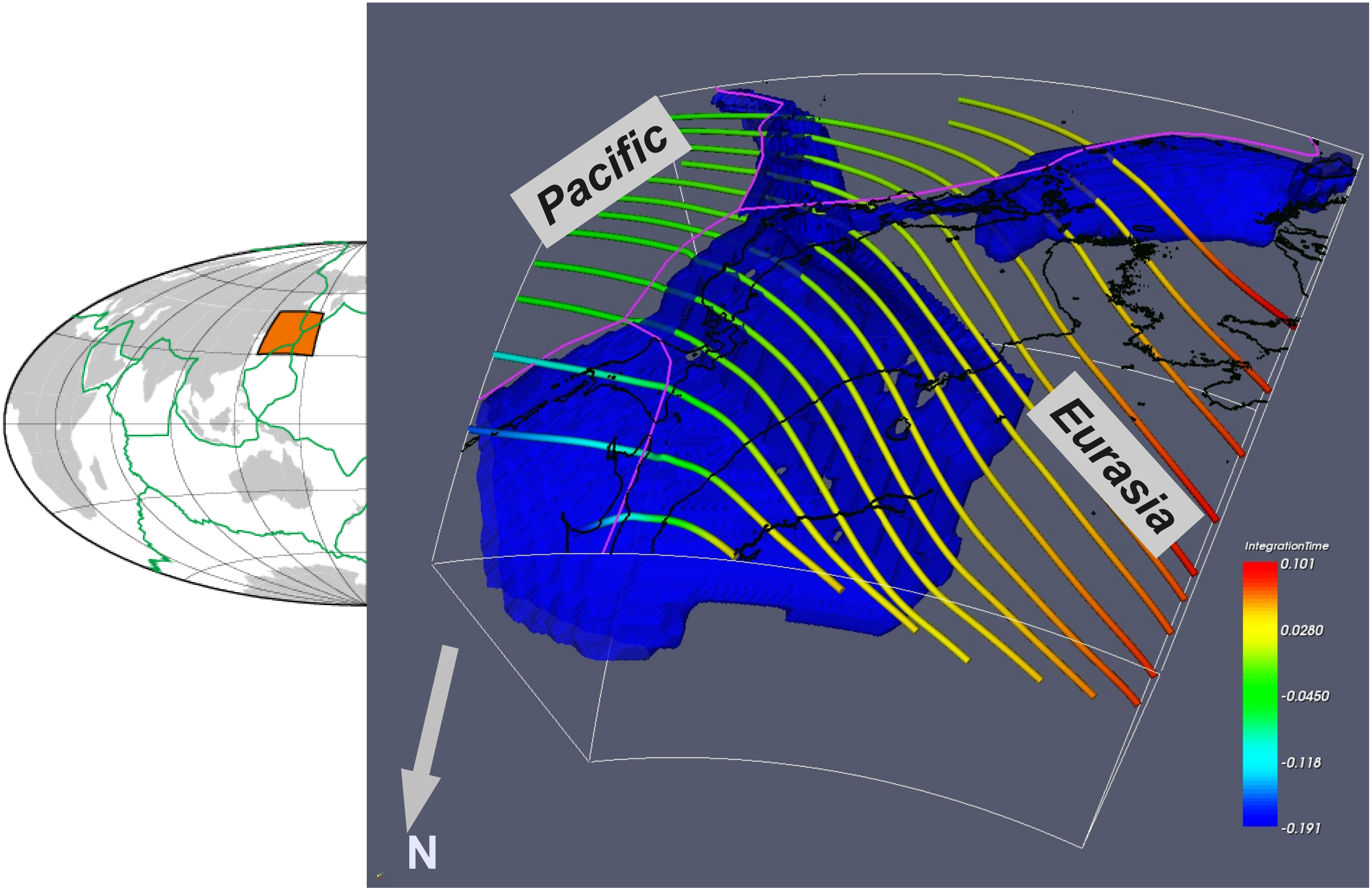

Becker & Faccenna (2009)

Plate motion histories and subduction

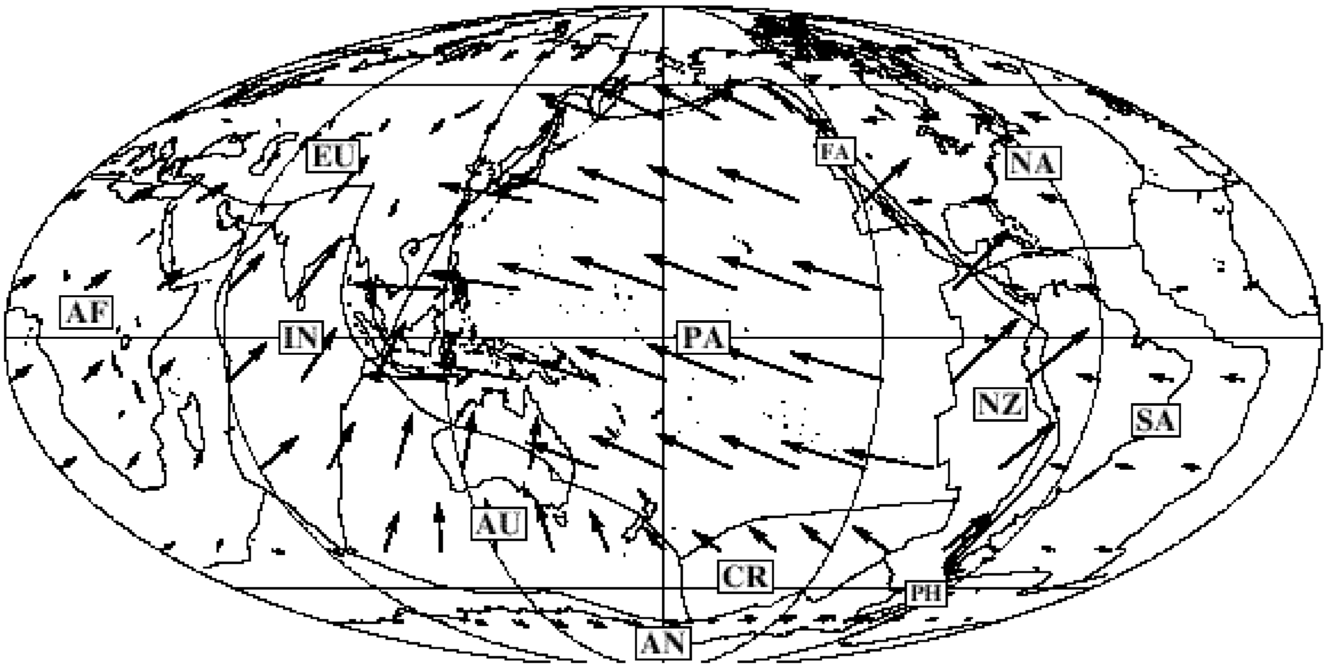

25-43 Ma

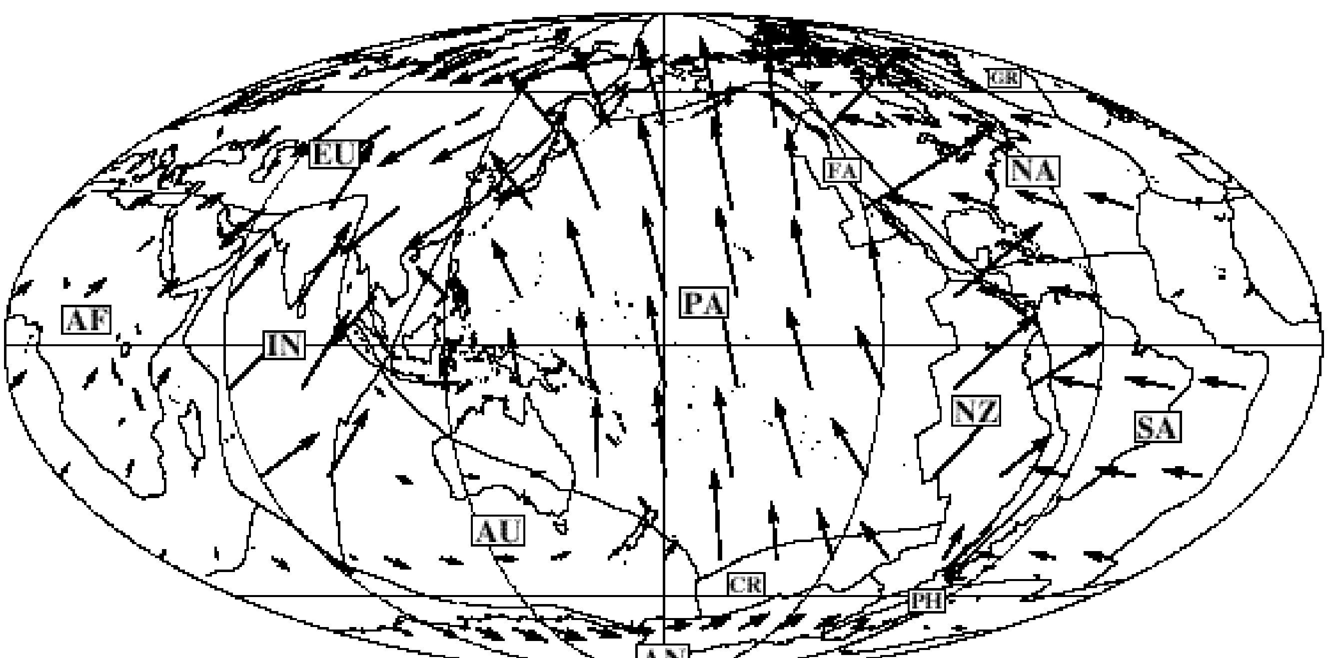

43-48 Ma

Lithgow-Bertelloni et al. (1993)

Direct Comparisons: Using Past Tectonics

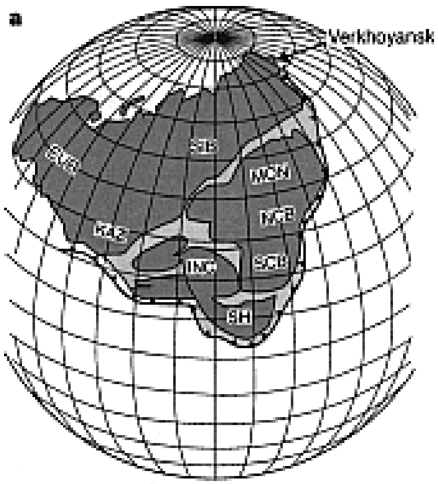

Early Cretaceous
(95-135 Myr)

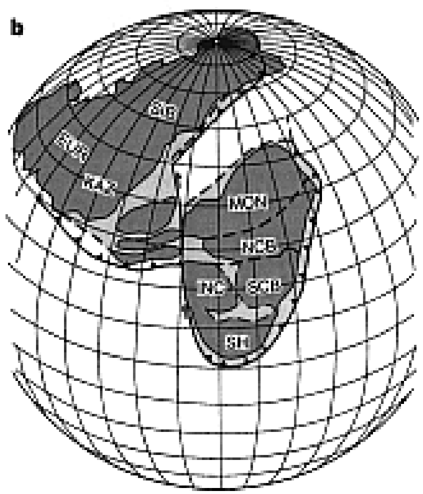

Late Jurassic
(135 - 155 Myr)

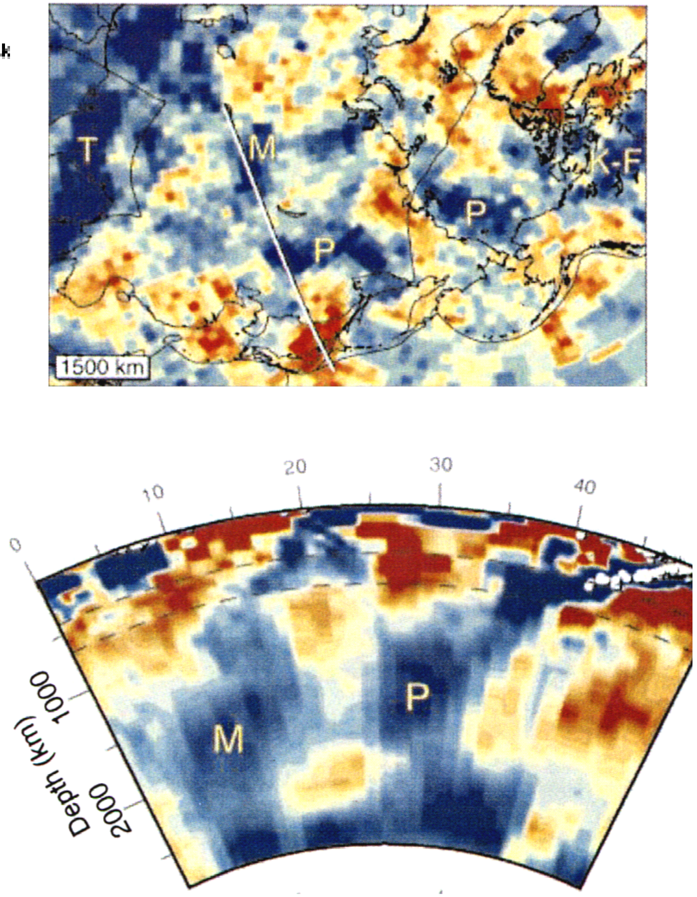

[*Voo et al.*, 1999]

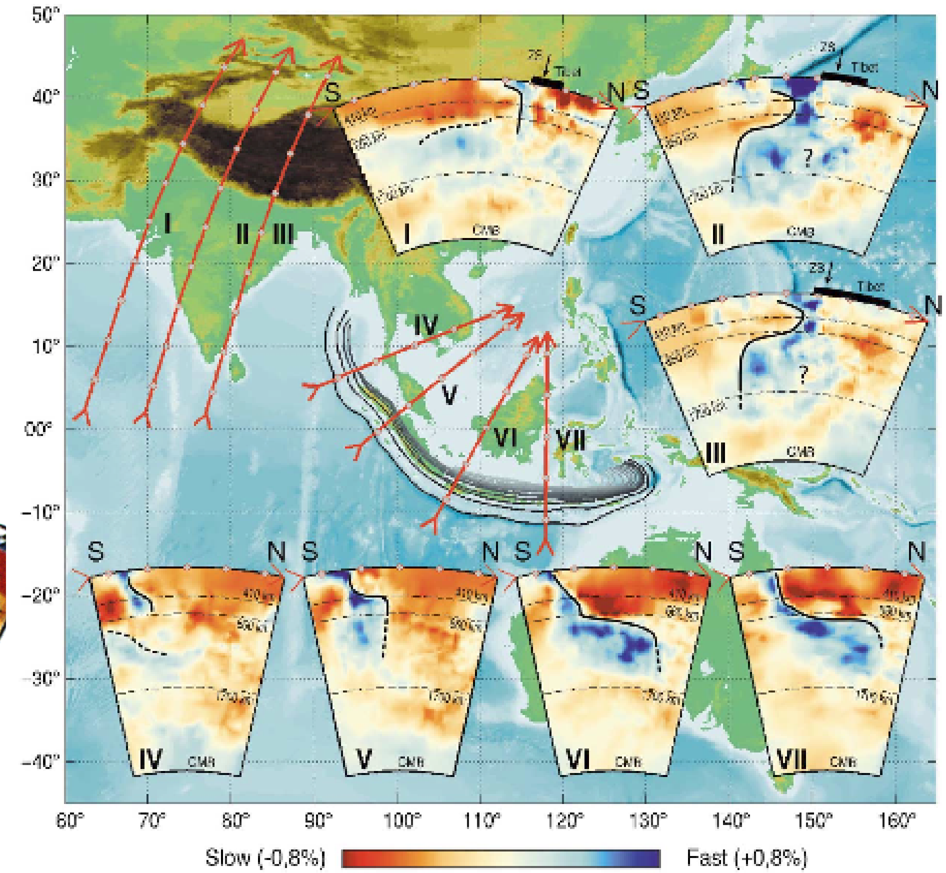

[*Replumaz et al.*, 2004]

Stokeslets

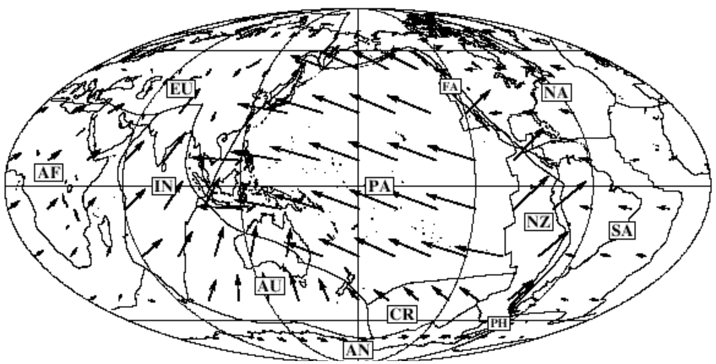

25-43 Ma

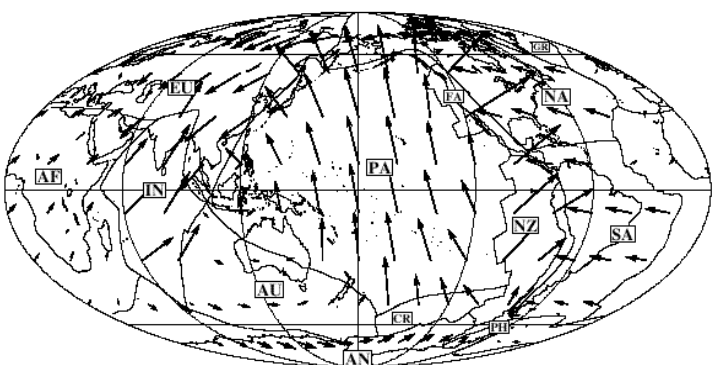

43-48 Ma

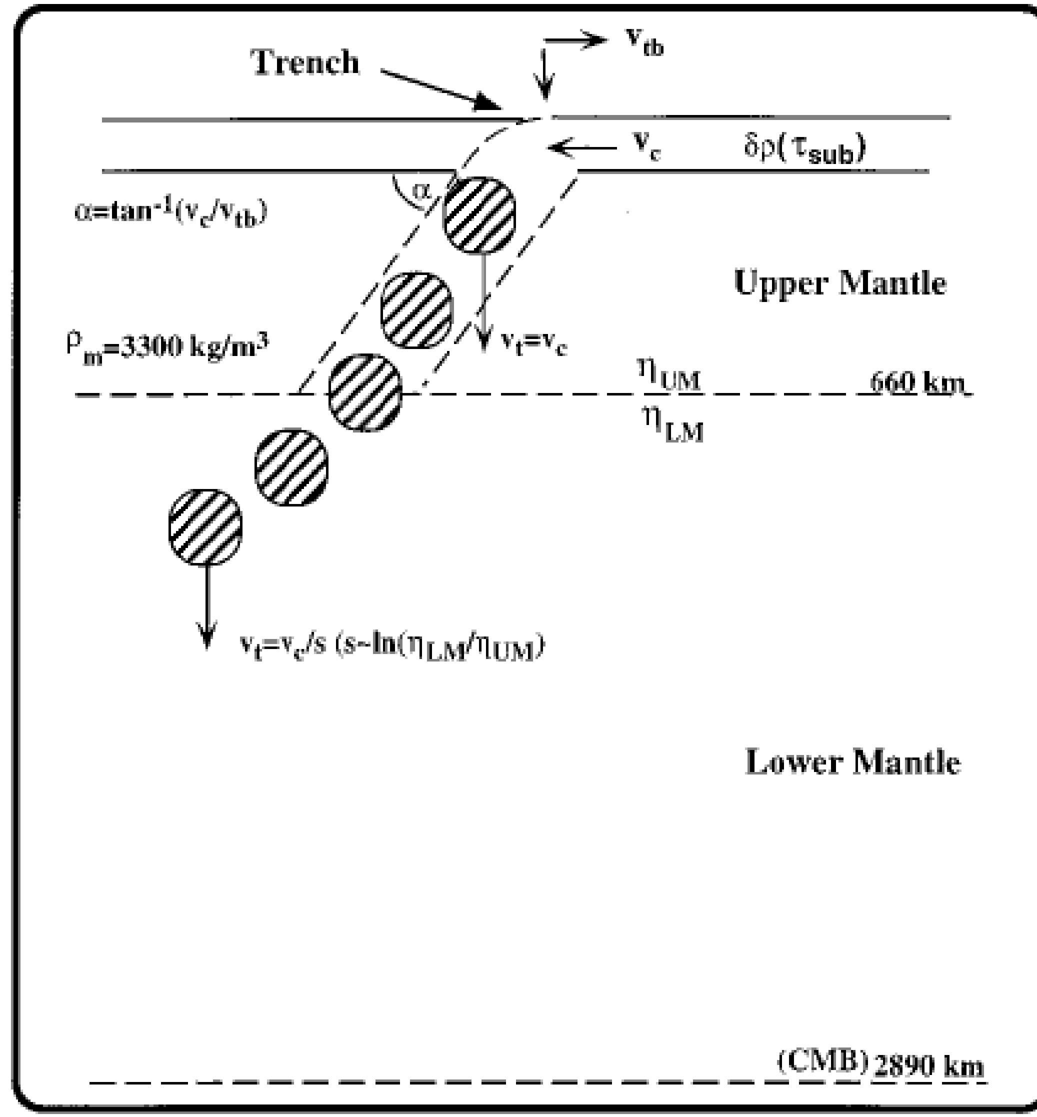

Ricard et al. (1993)

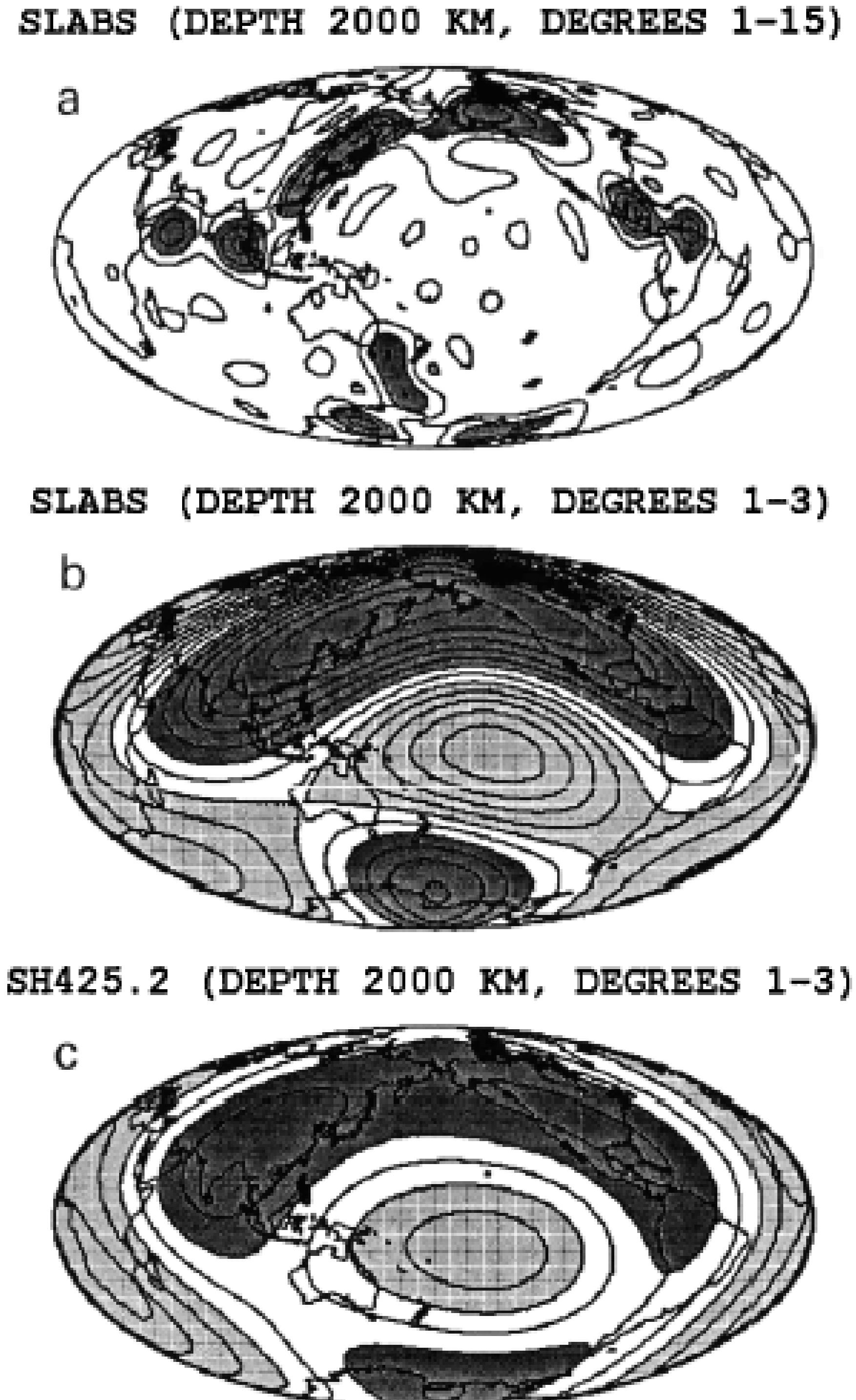

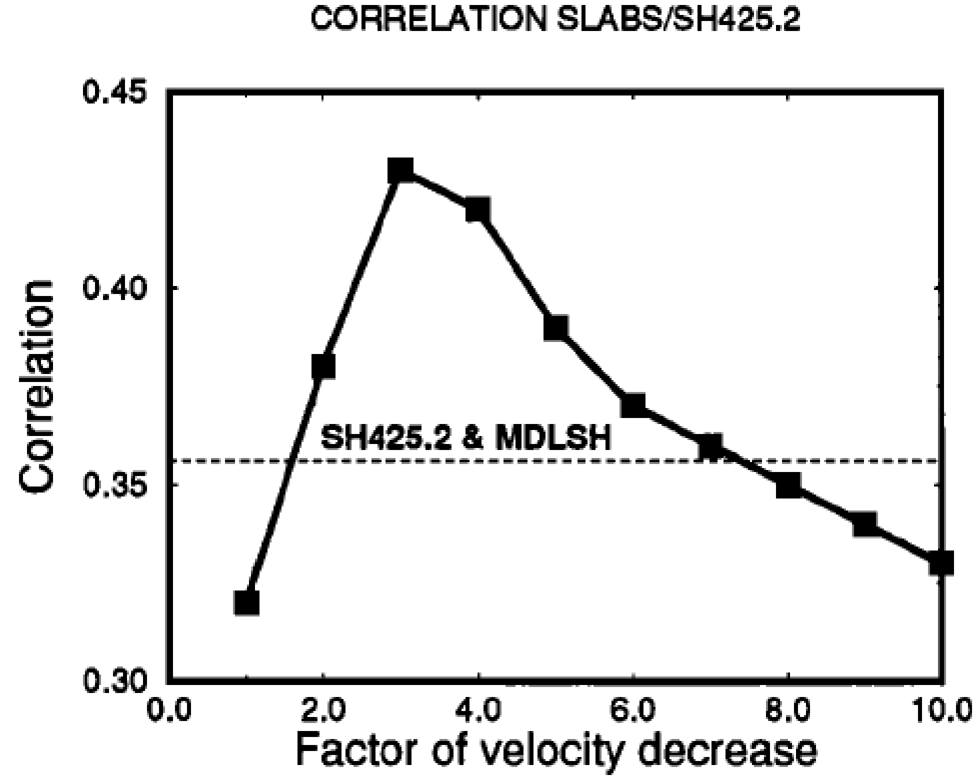

Ricard et al. (1993)

Subduction models over time

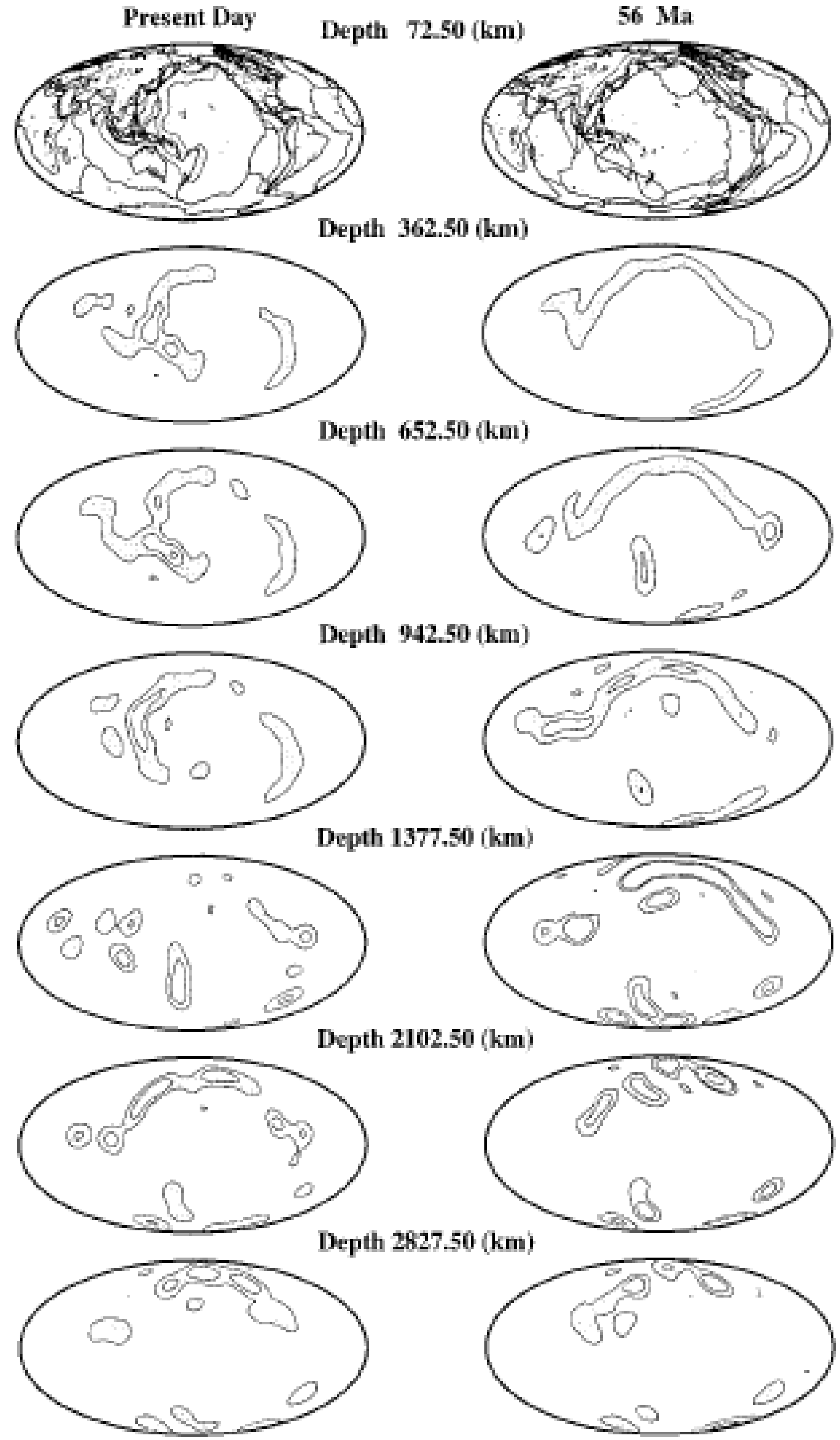

Ricard et al. (1993); Lithgow-Bertelloni & Richards (1998); Steinberger (2000); Spasojevich et al. (2009)

Tomography vs. advected slabs

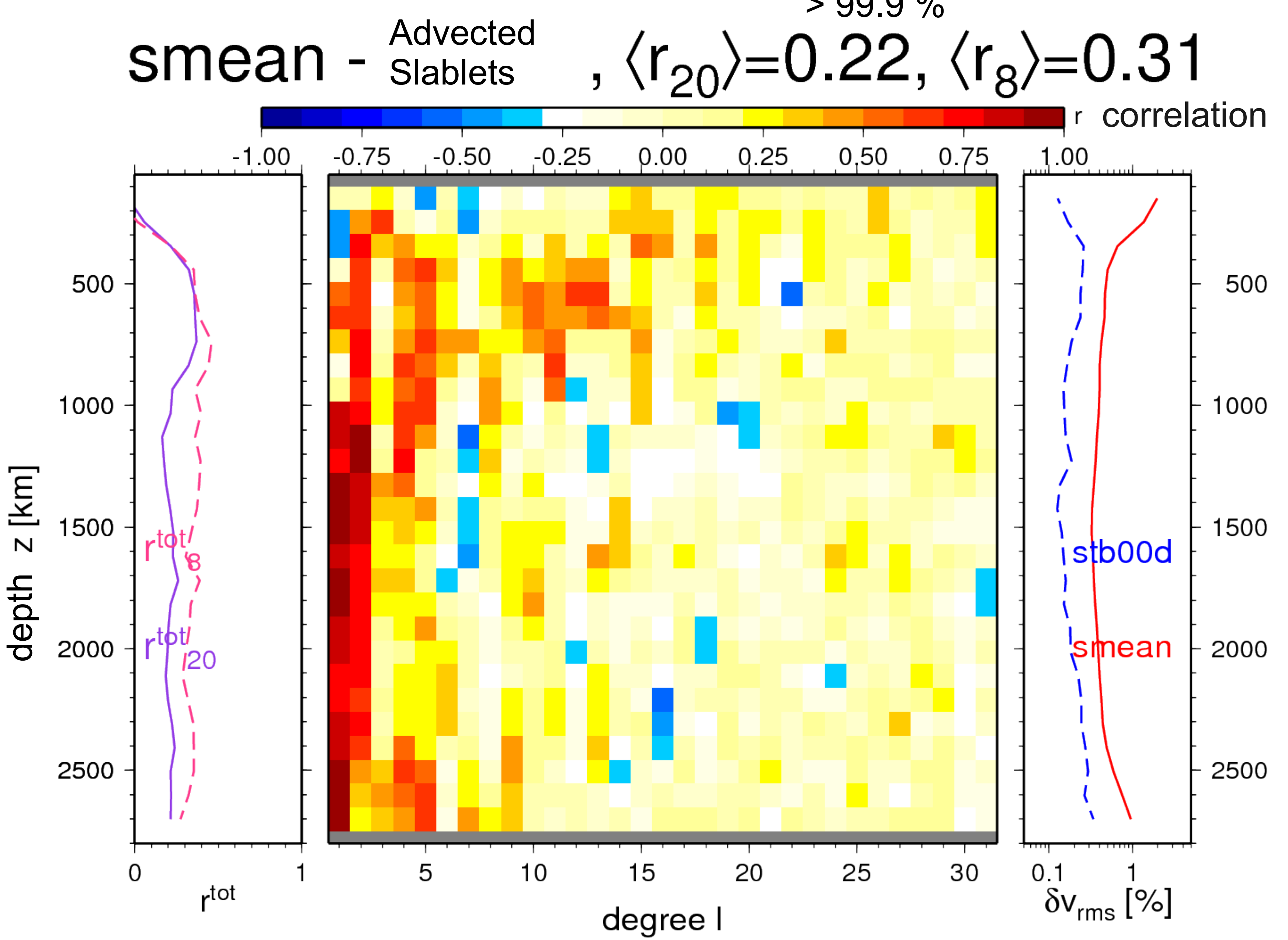

Becker & Boschi (2002)

Lithgow-Bertelloni & Richards (1998); Steinberger (2000); Bunge & Grand (2000); Spasojevic & Gurnis (2009)

Tomography vs. advected plumes

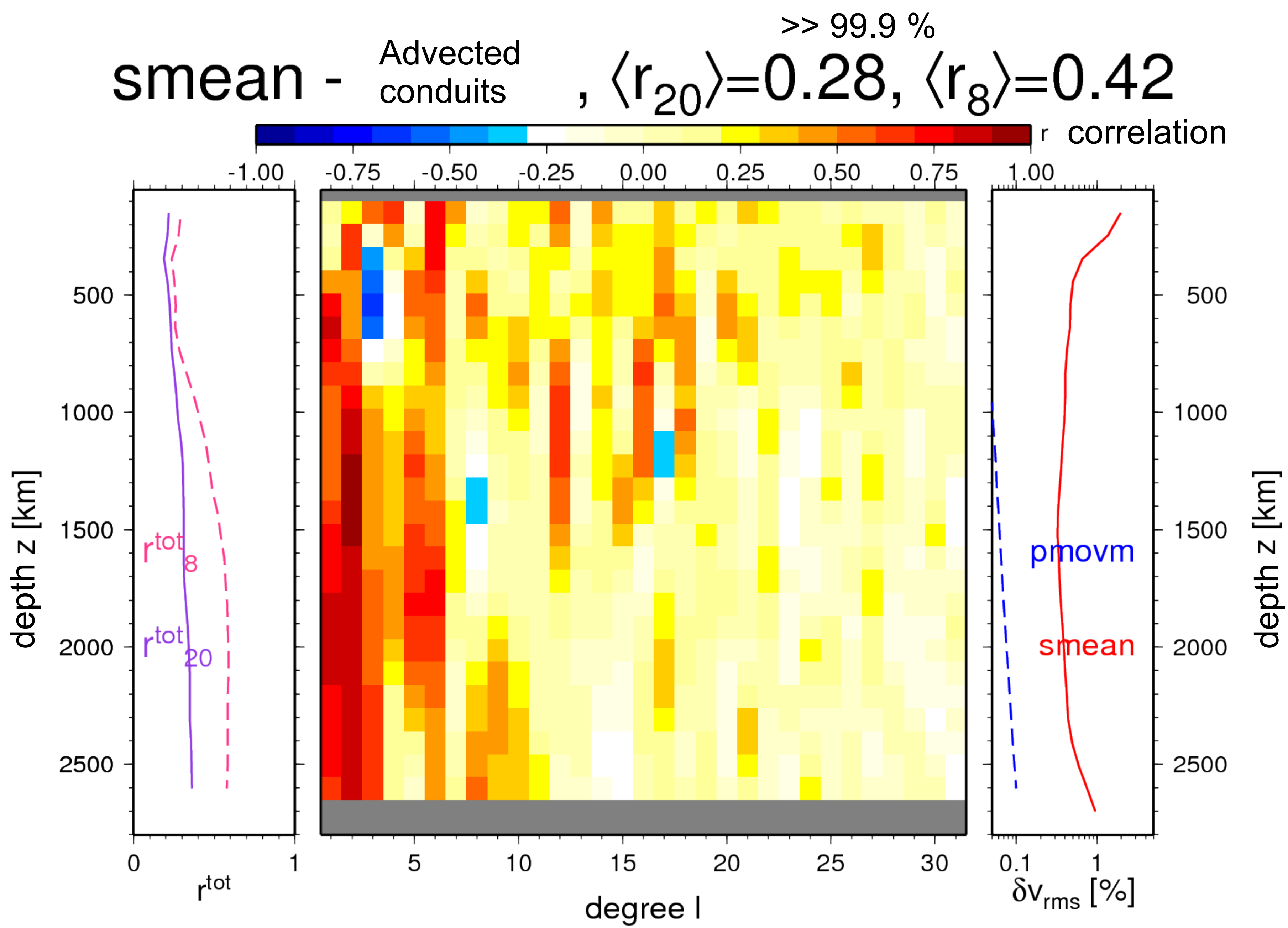

Boschi et al. (2007, 2008)

Input model

Correlation between input and output as a function of wavelength

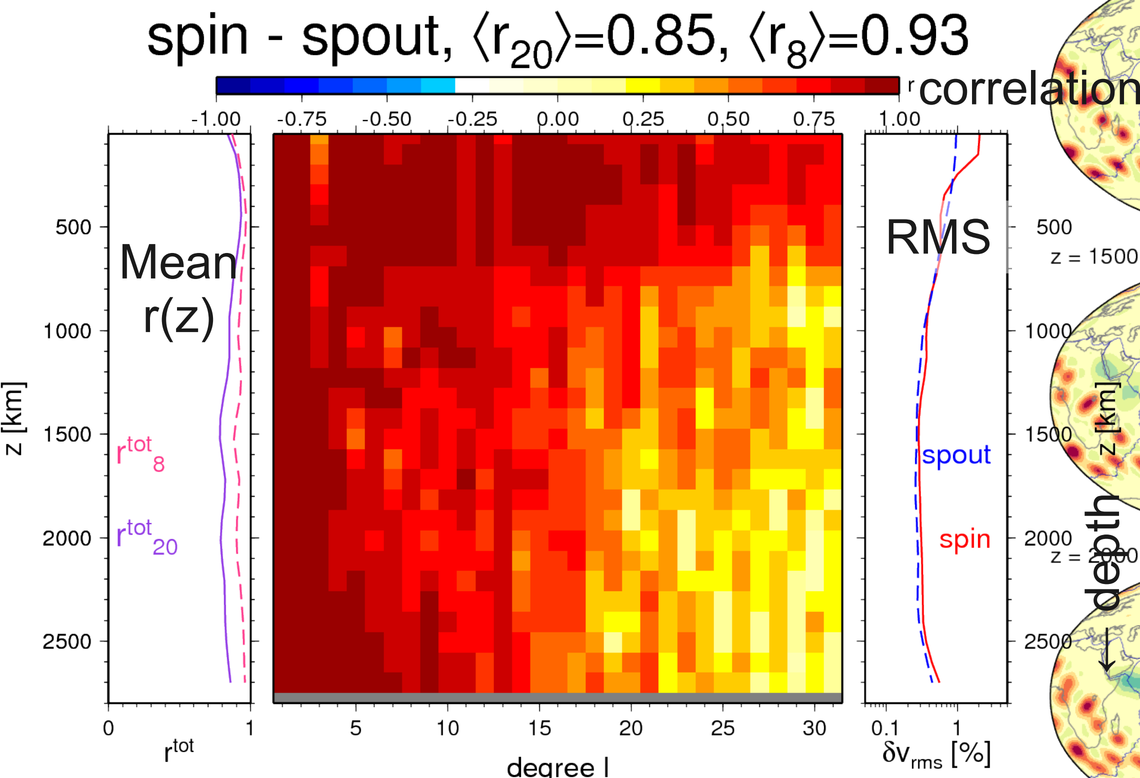

Shorter wavelengths →

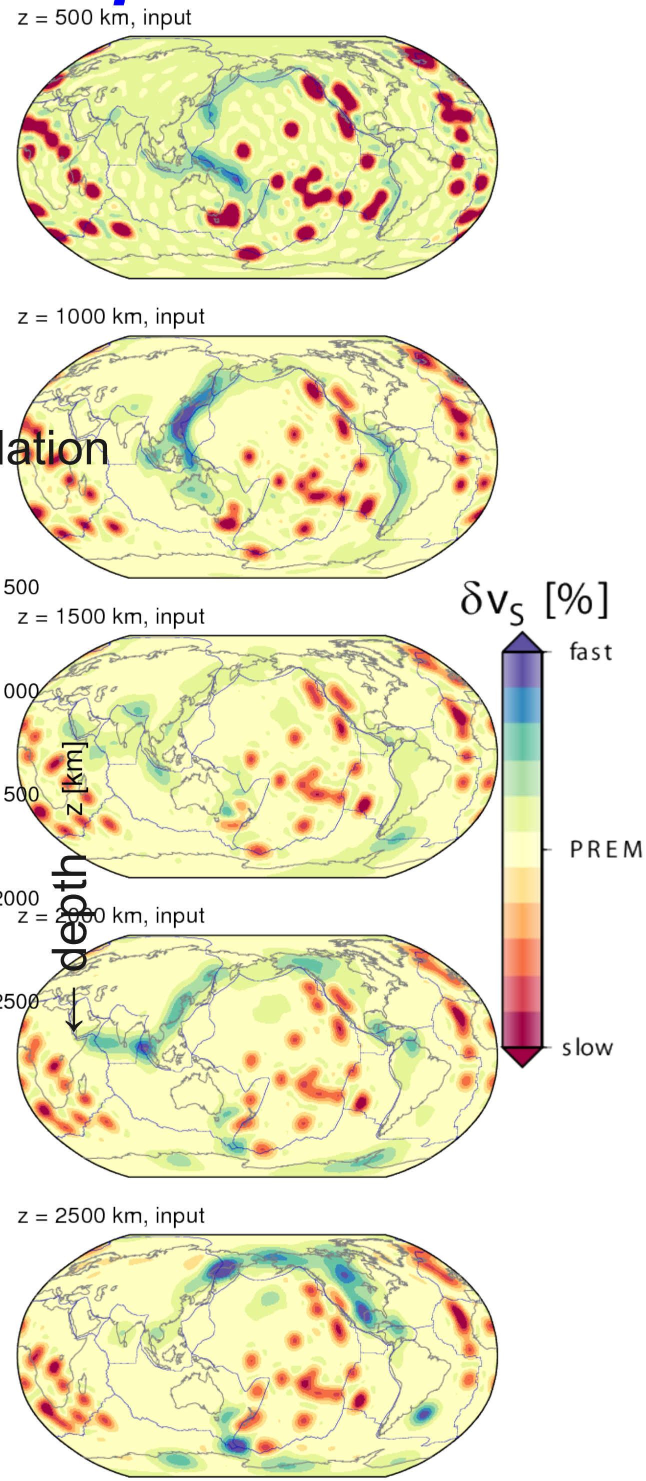

Inversion uses Simmons & Grand S body wave data, plus some noise

Absolute reference frame from slabs

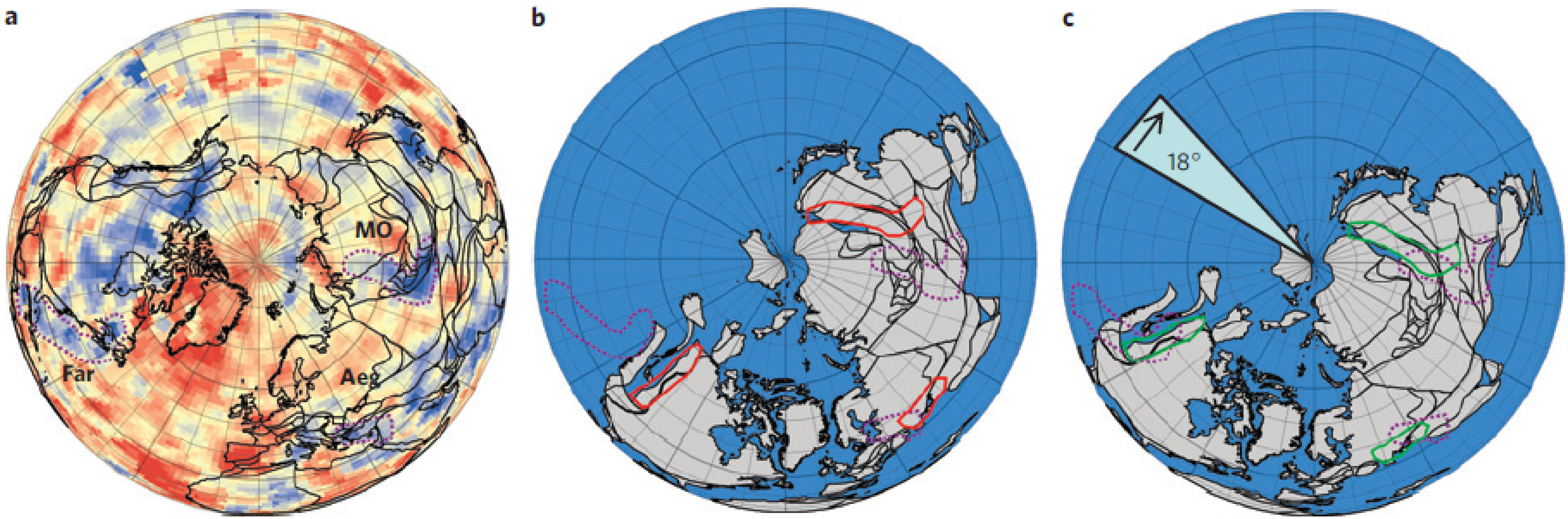

Figure 2 | Spatial longitude correction. North Pole orthographic projections. **a**, Tomographic depth slice[7] at 1,900 km, colour scale red (−0.4%) to blue (+0.4%) with present-day continents. Interpreted slabs are outlined in purple: Far, Farallon; Aeg, Aegean Tethys; MO, Mongol-Okhotsk. **b**, Unmodified reconstruction at 160 Myr. Offsets exist between the three slabs (purple) and their corresponding subduction complexes/sutures (red outlines). **c**, To obtain an improved fit between subduction complexes/sutures (green) and slab locations (purple), the plate tectonic reconstruction was shifted 18° westward.

Van der Meer et al. (2010)

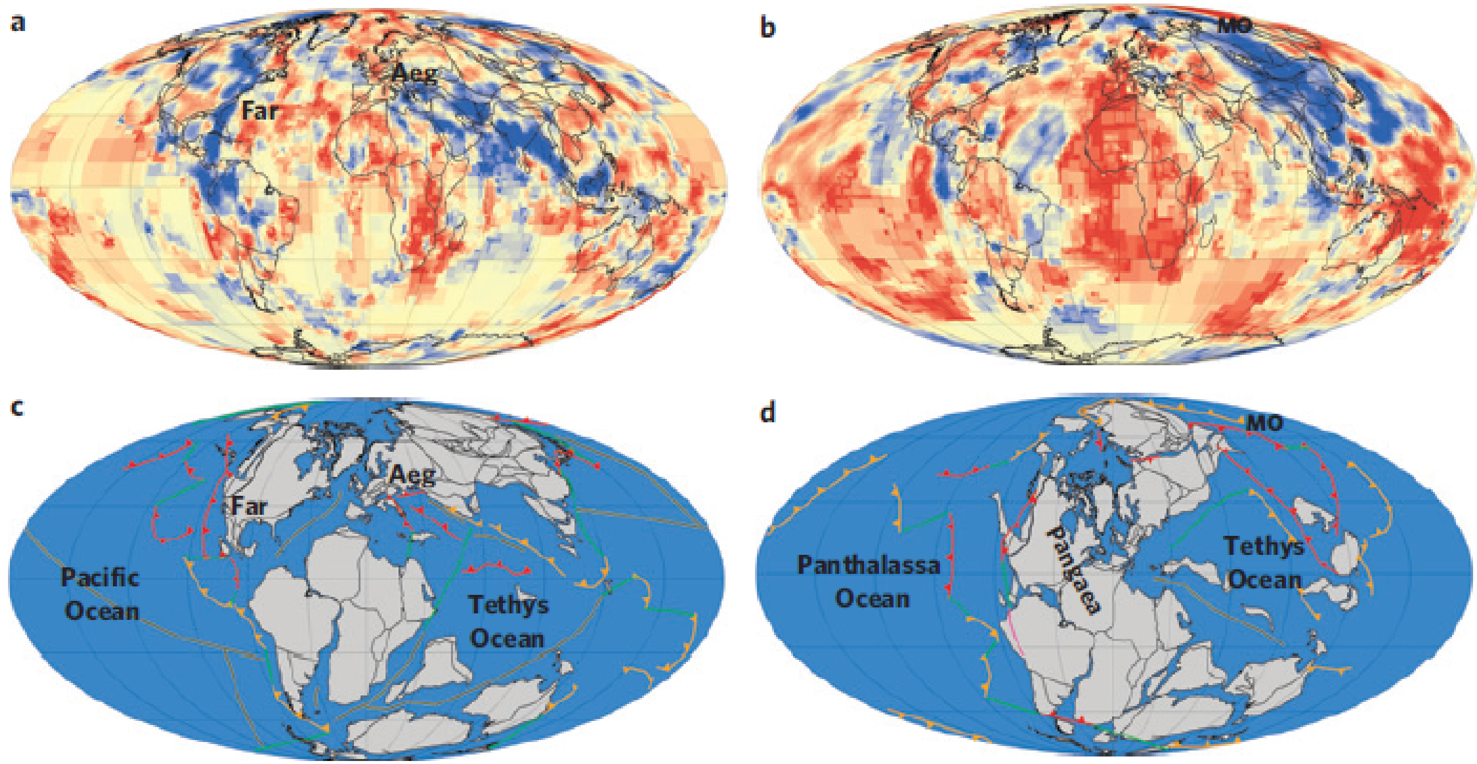

Figure 4 | Longitude-corrected plate tectonic reconstructions. The colour scale is given in Fig. 2 and slab name abbreviations are given in Table 1. **a–d**, A good fit is obtained between the tomographic depth slices[7] at 1,325 km (**a**) and 2,650 km (**b**) depth and the modified plate tectonic reconstructions[3,4] at 120 Myr (17° corrected) (**c**) and 240 Myr (10° corrected) (**d**). Tectonic interpretation: lines with triangles, subduction zone of the slab data set (red) and other slabs with only a qualitative interpretation (orange); green line, transform zone; yellow double line, spreading ridge. See Supplementary Figs S29–S40 for larger maps.

Van der Meer et al. (2010)

Global circulation models

- Mantle viscous Stokes flow, no inertia
  - Instantaneous solution for boundary conditions and internal loads
  - Semi-analytical, if viscosity is Newtonian and only depth dependent
- Force model
  - Plate motions prescribed
  - Evaluate mantle tractions and plate driving forces

Tractions from plate motions acting on asthenosphere

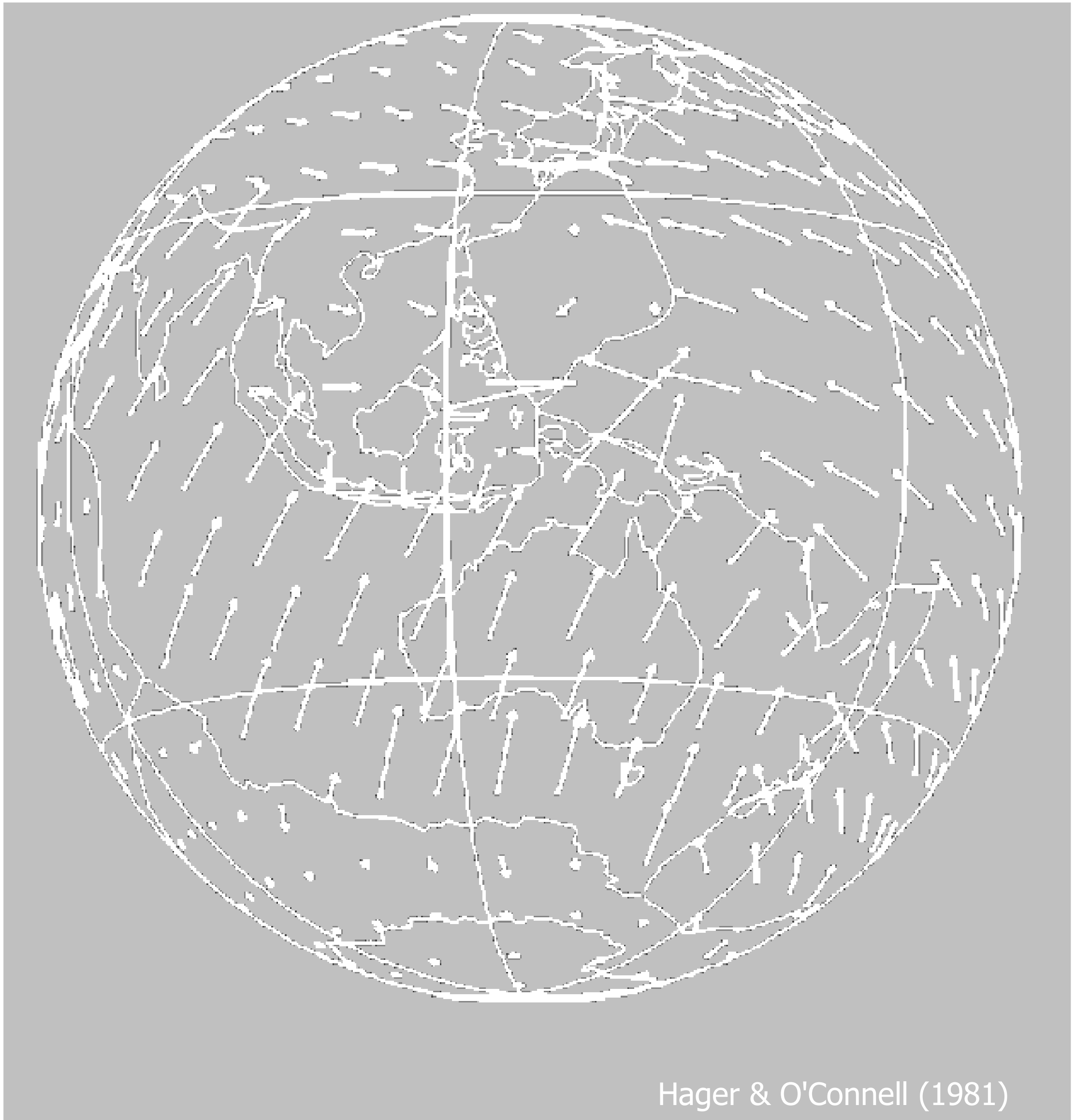

EGM360,
corrected for hydrostatic shape
of a rotating Earth (Nakiboglu, 1986)

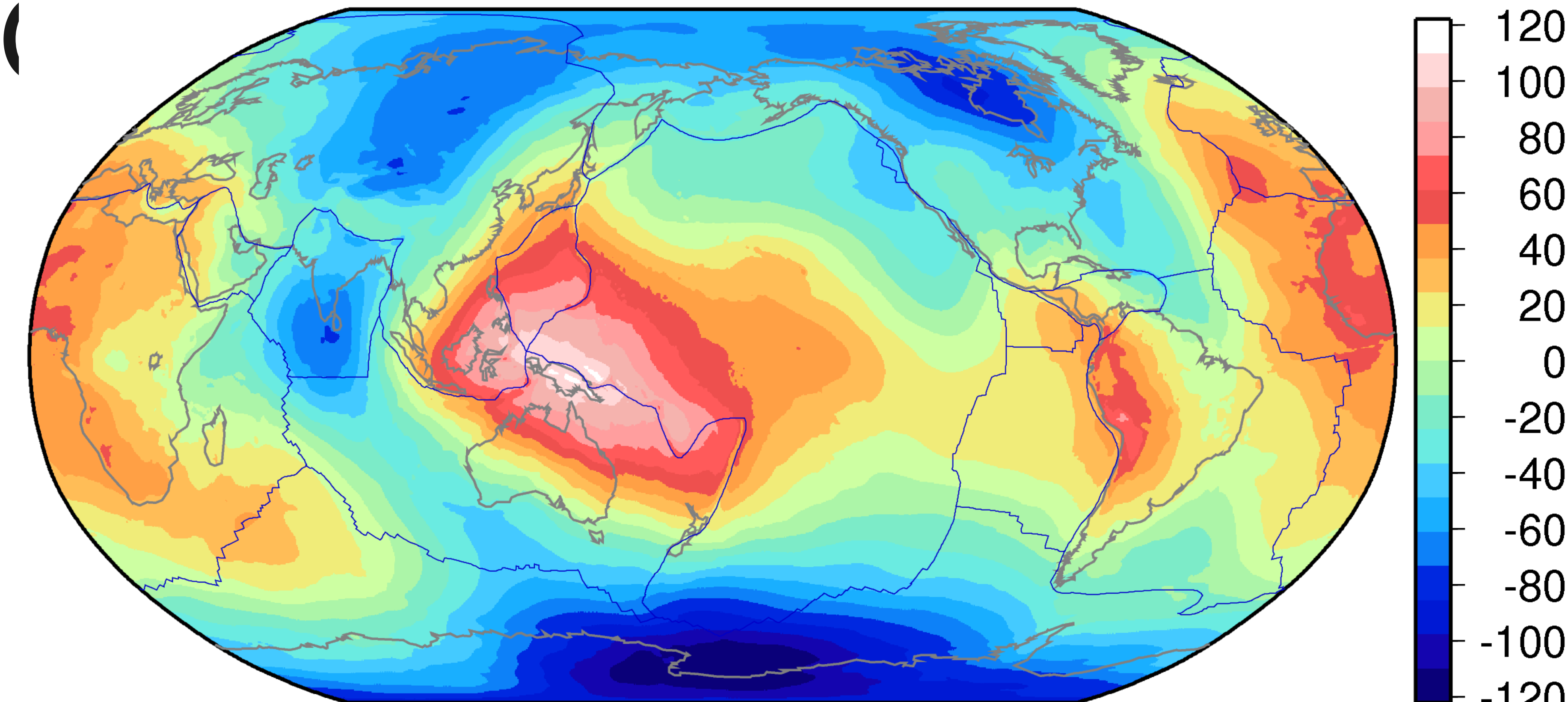

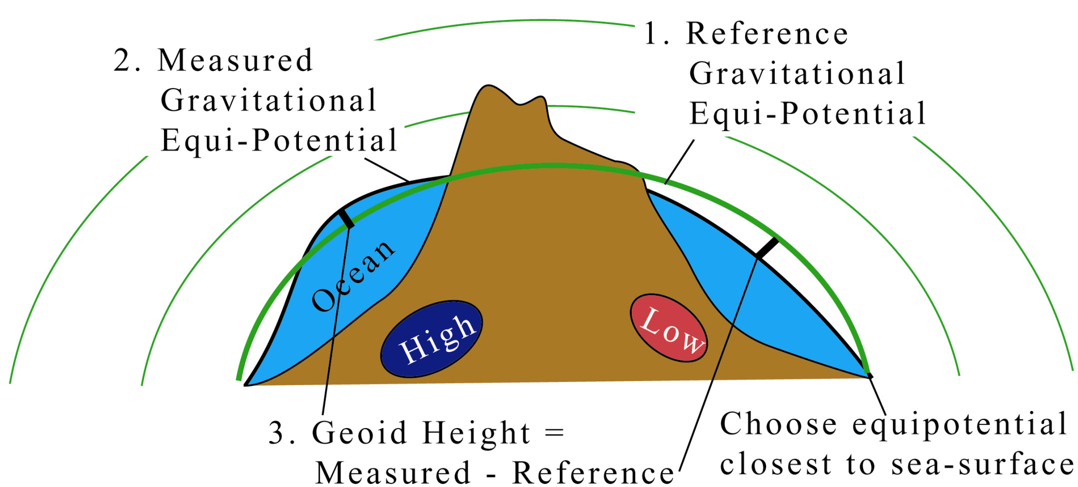

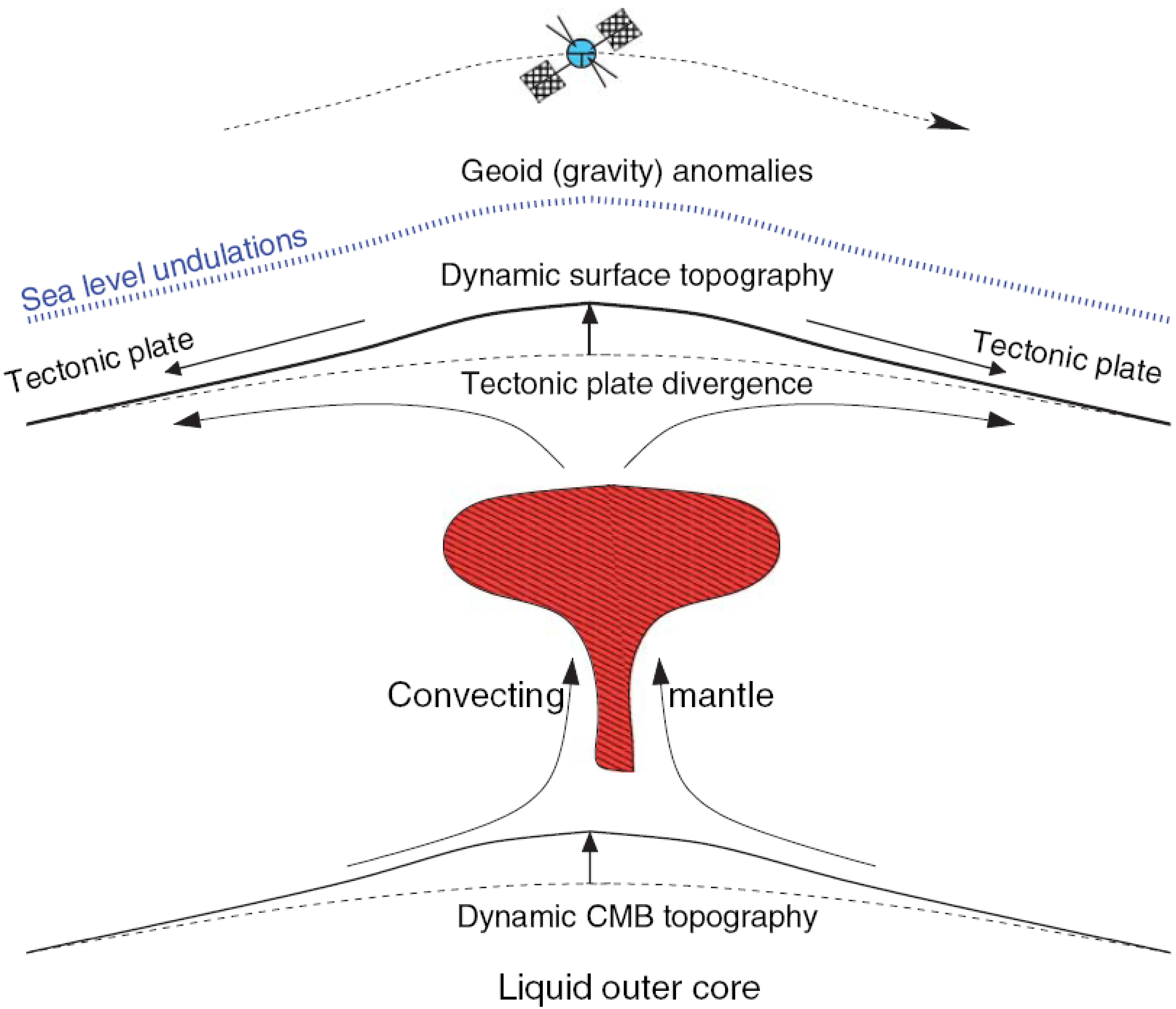

Geoid (gravity) anomalies
Sea level undulations
Dynamic surface topography
Tectonic plate
Tectonic plate
Tectonic plate divergence
Convecting
mantle
Dynamic CMB topography
Liquid outer core

Forte (2007)

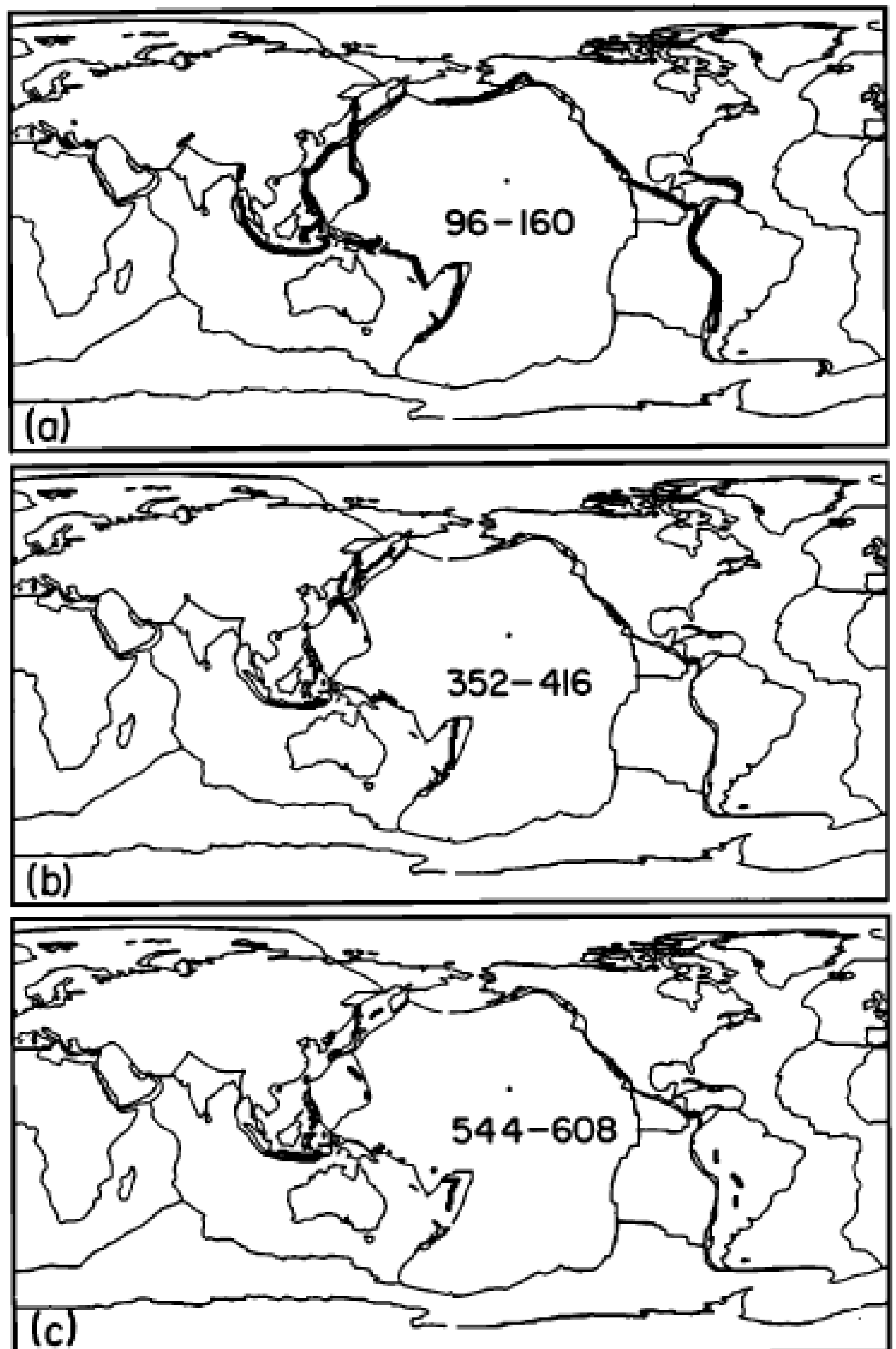

Hager (1984)

Mantle shear velocity anomalies

Map at 1200 km depth

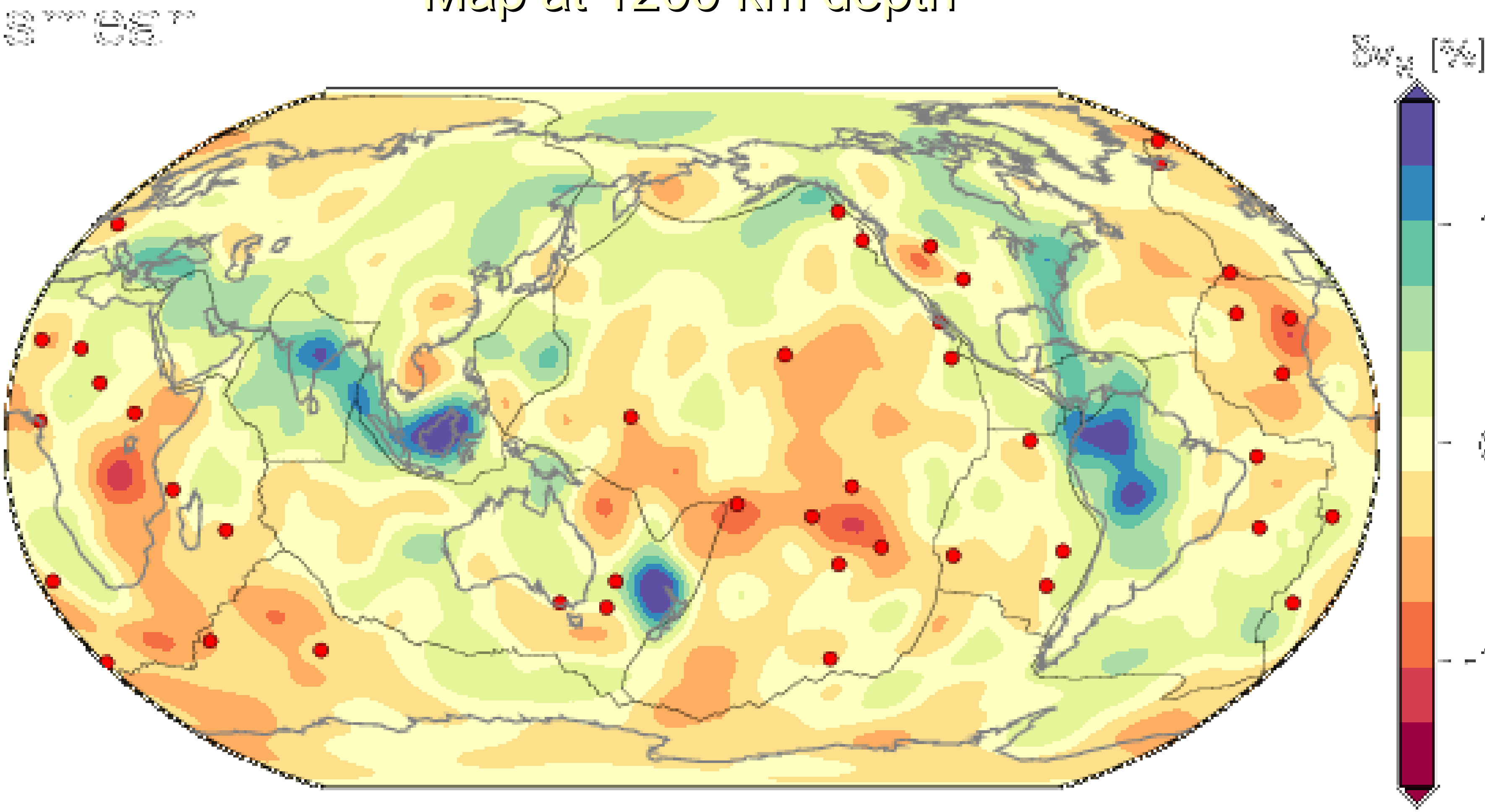

e.g. Grand and van der Hilst (1997); Fukao (2001); Romanowicz (2006); Becker and Boschi (2001); Nolet (2008)

Mantle temperature anomalies

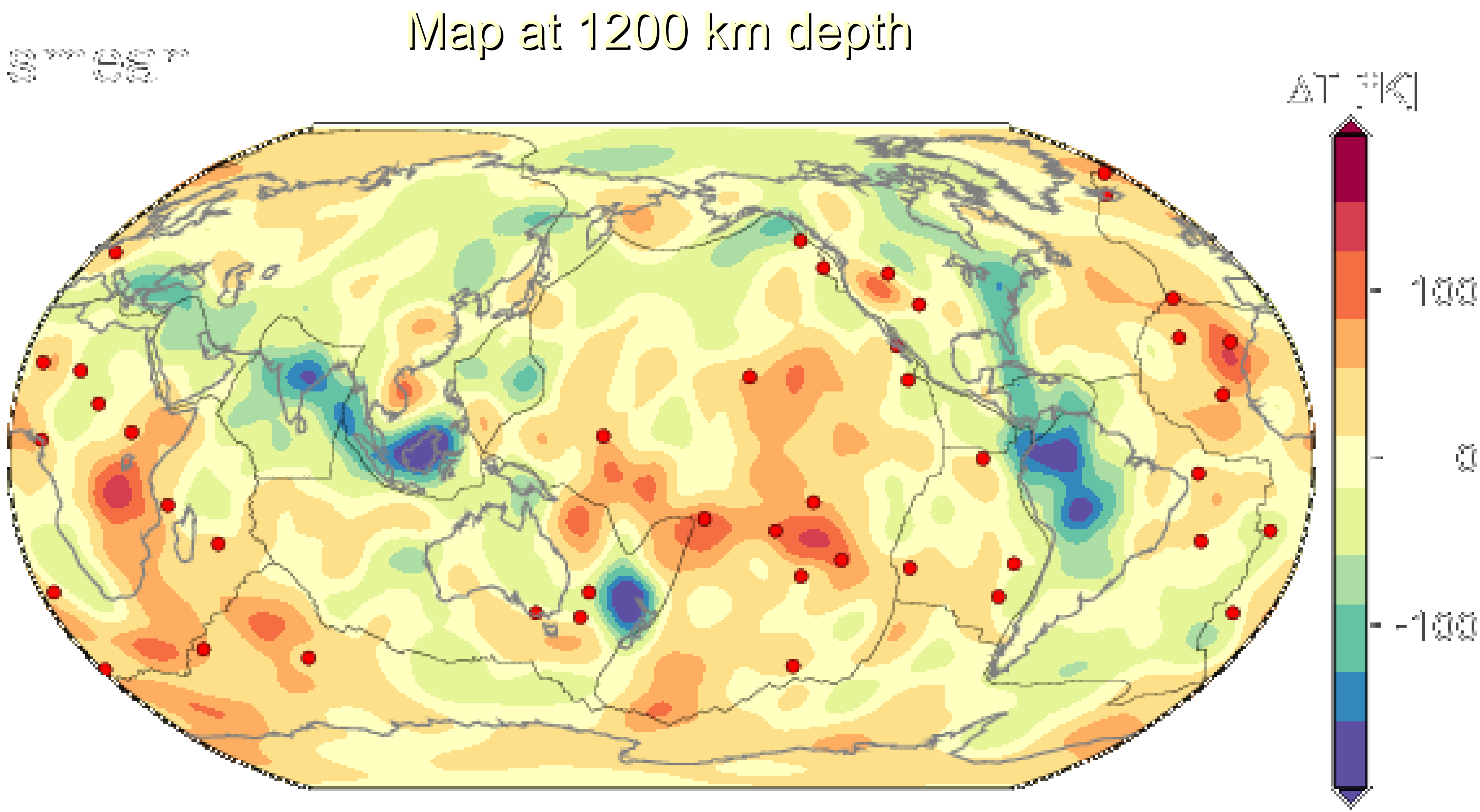

- Use mineral physics to convert velocity into temperature (density) anomalies

e.g. Hager (1984); Hager & Clayton (1989); Lithgow-Bertelloni & Richard (1998); Forte (2007)

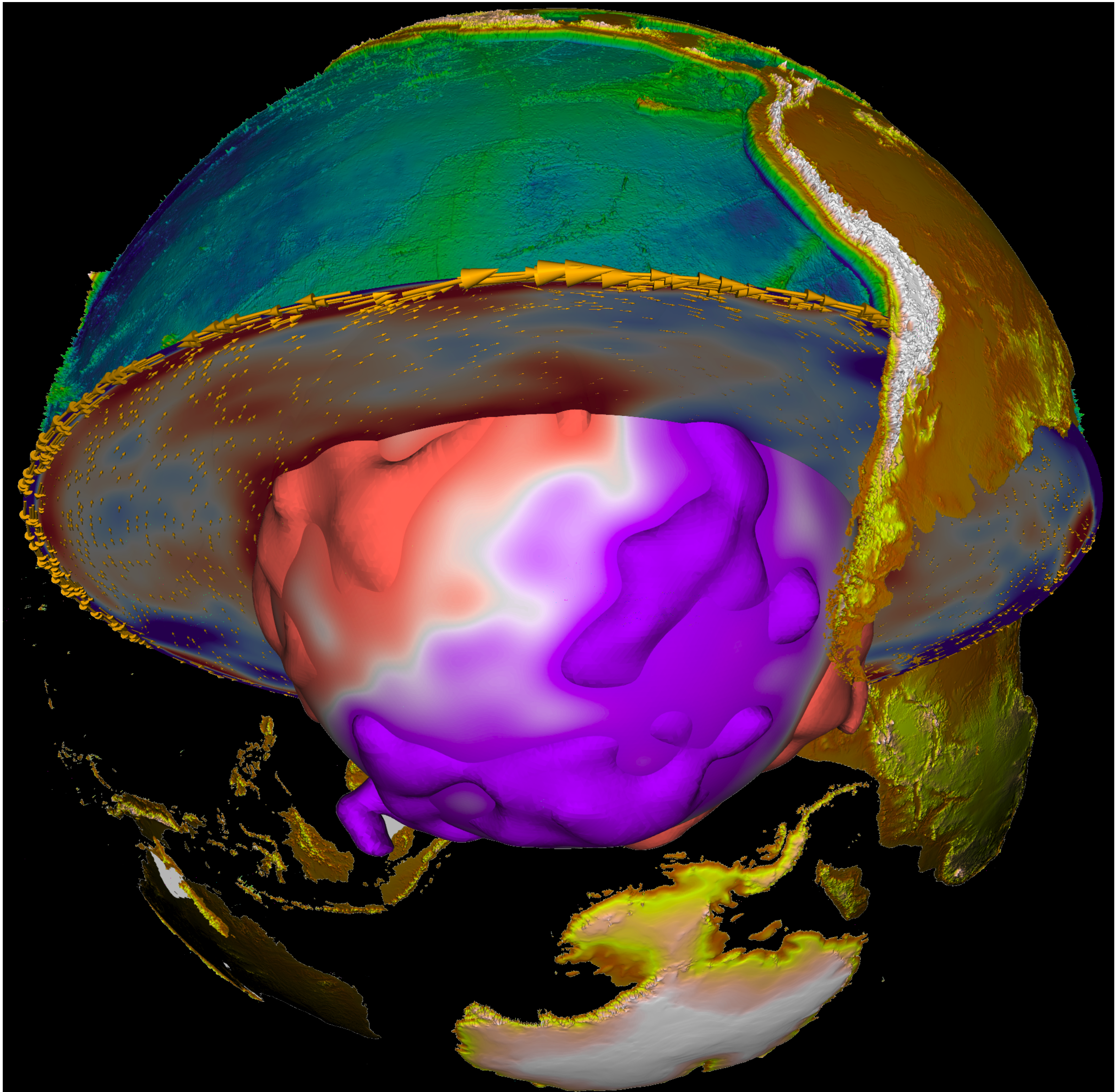

Becker (2010)

Geoid for tomography driven flow

- Isoviscous – free slip surface boundary condition

Constant
d ln ρ/d ln v_s

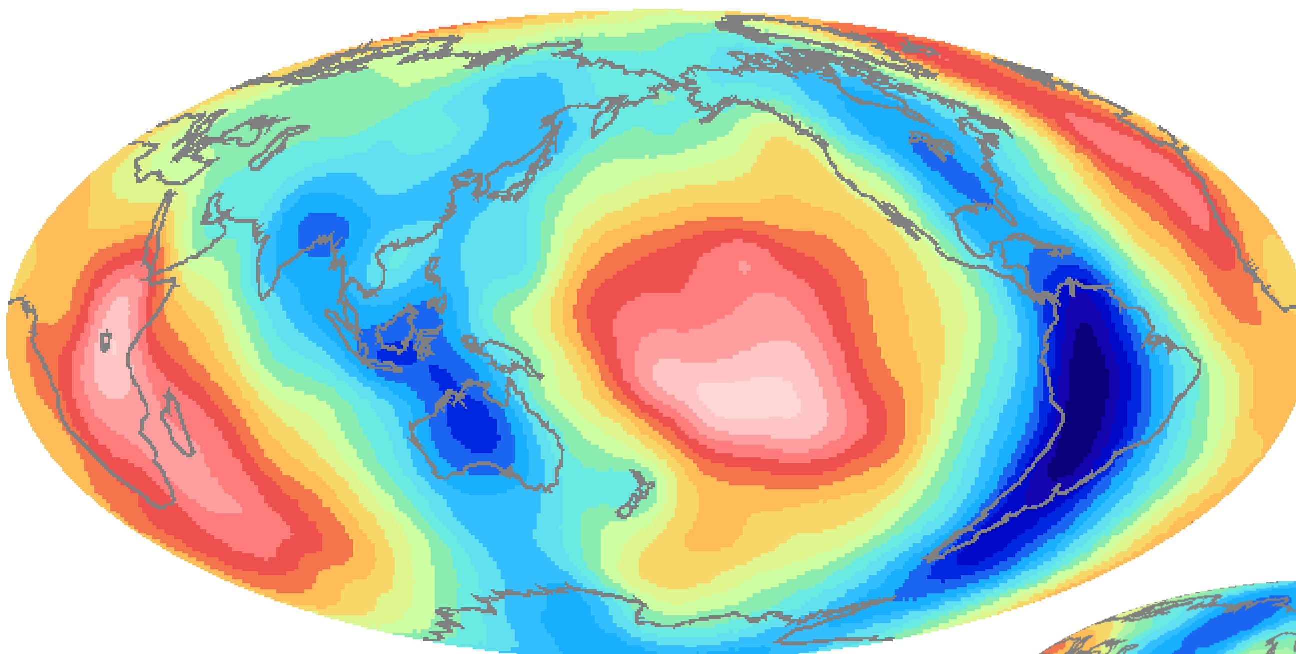

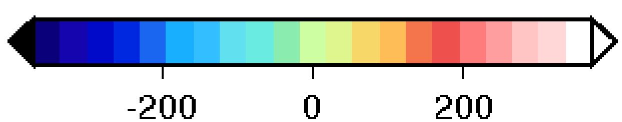

Tomography @ 1200 km

$r_{1\text{-}20} = 0.28$

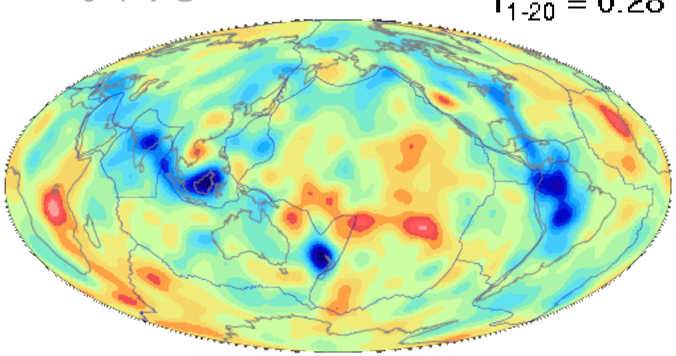

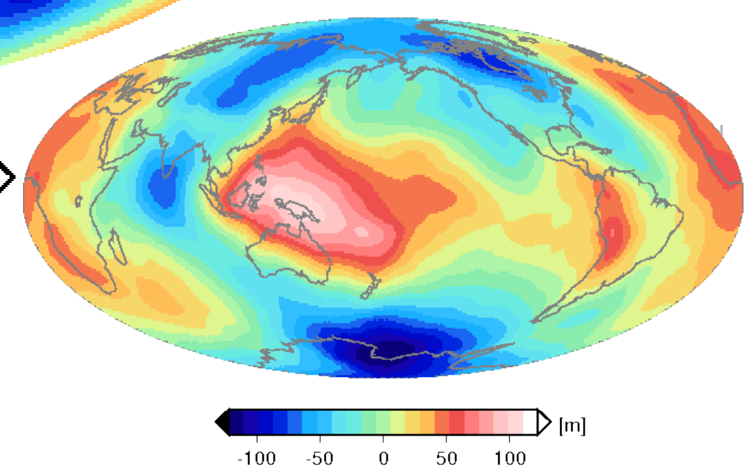

Geoid for tomography driven flow

- Lower mantle stiffer

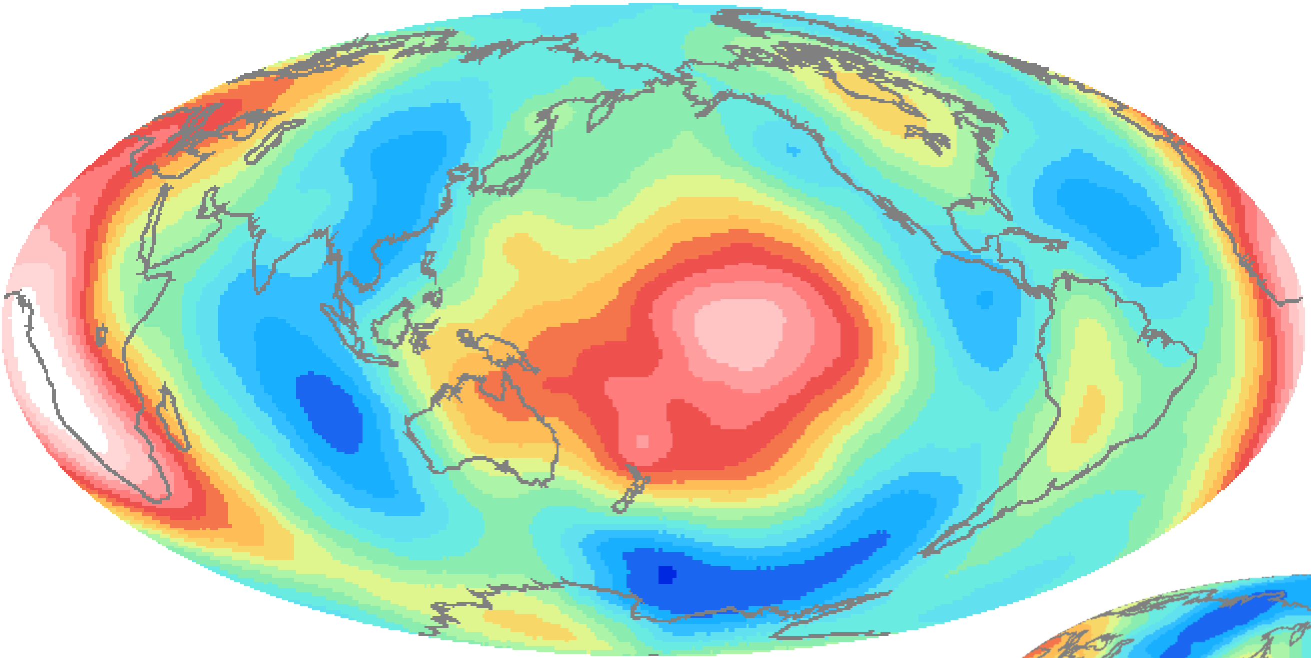

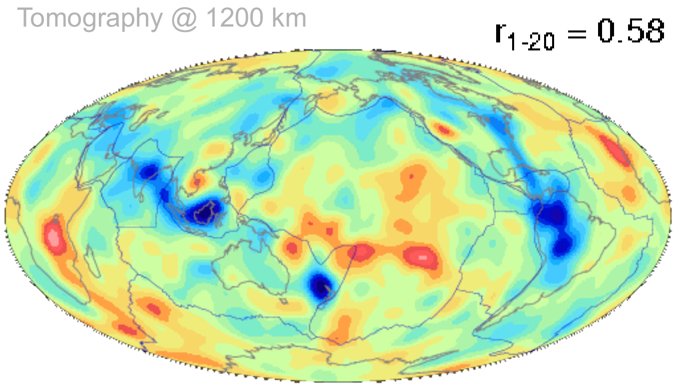

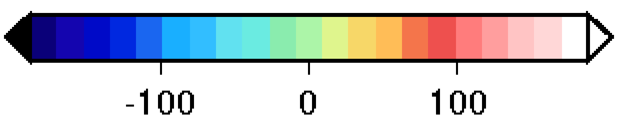

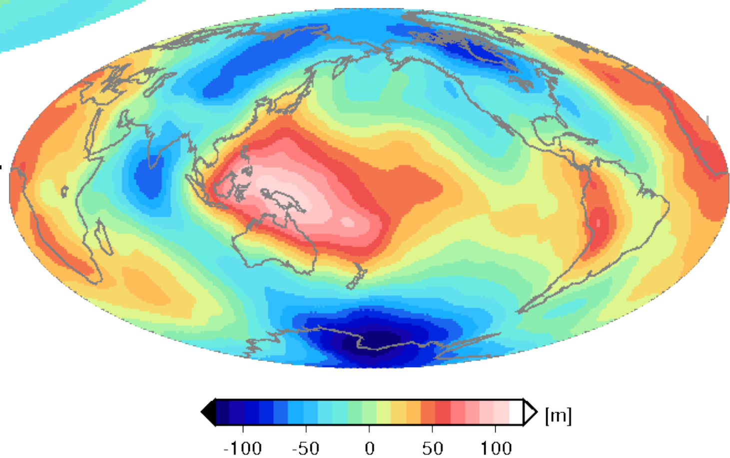

Geoid for tomography driven flow

- Four layer (~best-fit) model

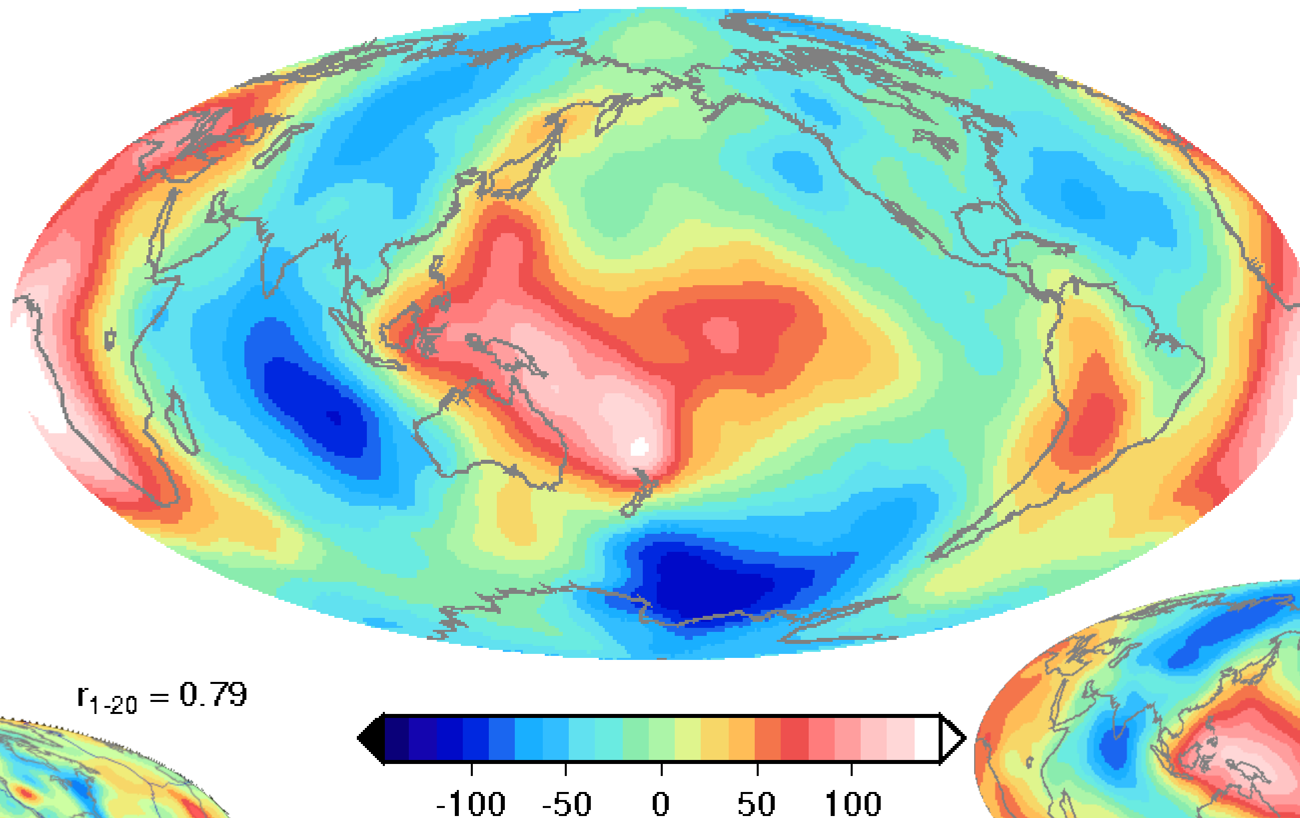

Tomography @ 1200 km

$r_{1\text{-}20} = 0.79$

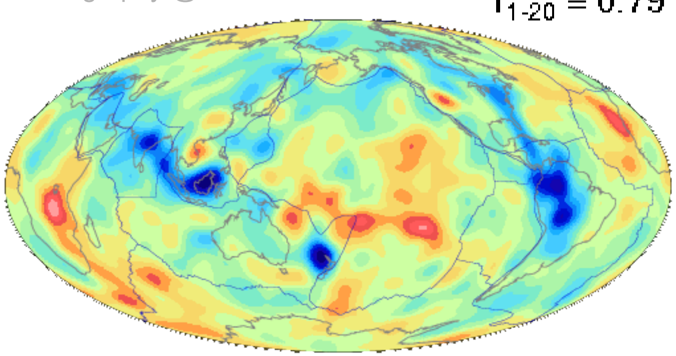

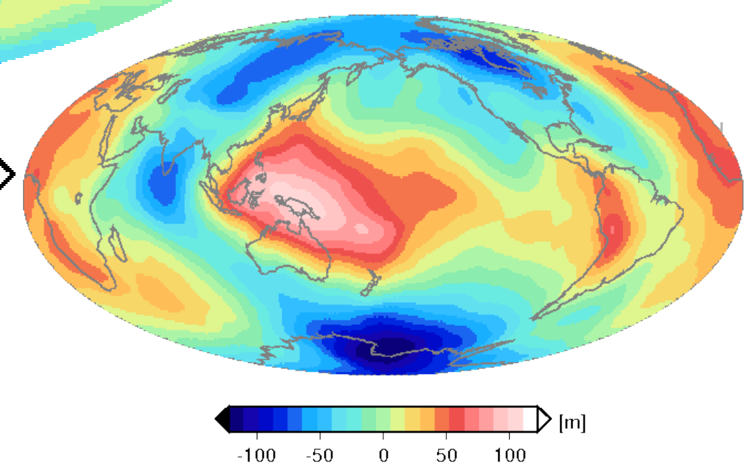

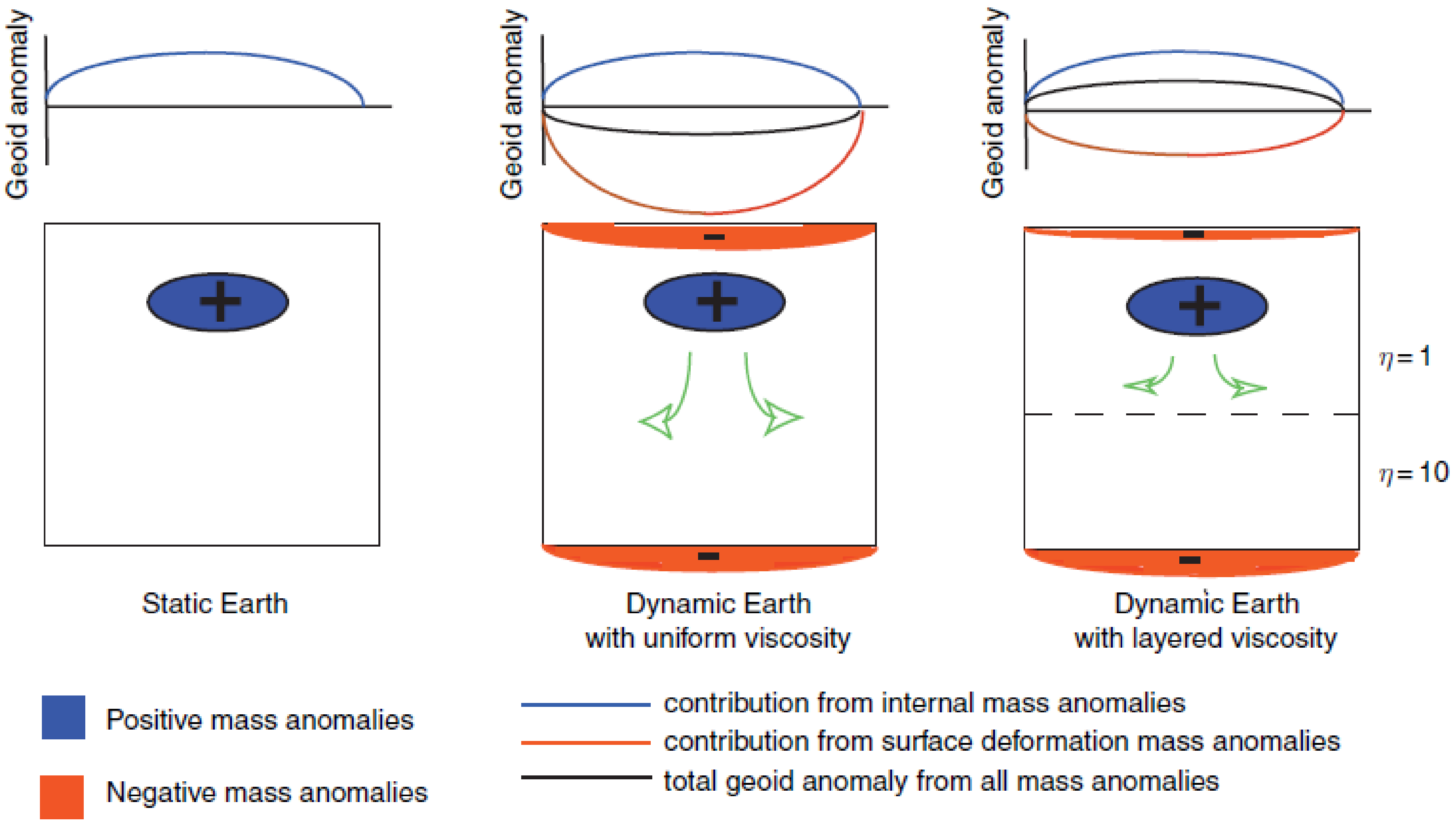
Geoid anomaly
Geoid anomaly
Geoid anomaly
$\eta = 1$
$\eta = 10$
Static Earth
Dynamic Earth
with uniform viscosity
Dynamic Earth
with layered viscosity
Positive mass anomalies
Negative mass anomalies
contribution from internal mass anomalies
contribution from surface deformation mass anomalies
total geoid anomaly from all mass anomalies

King (2007)

SEATREE - Trac - Mozilla Firefox

File Edit View History Bookmarks Tools Help

https://geosys.usc.edu/projects/seatree/wiki/

Search

Login | Settings | Help/Guide | About Trac

Wiki | Timeline | Roadmap | Browse Source | View Tickets | New Ticket | Search

Start Page | Index by Title | Index by Date | Last Change

Solid Earth Teaching and Research Environment

SEATREE is a modular and user-friendly software to facilitate using solid Earth research tools in the classroom and for interdisciplinary, scientific collaboration. We use python wrappers and make use of modern software design concepts, while remaining compatible with traditional scientific coding. Our goals are to provide a fully contained, yet transparent package that lets users operate in an easy, graphically supported "black box" mode, while also allowing to look under the hood. In the long run, we envision SEATREE to contribute to new ways of sharing scientific research, and making (numerical) experiments truly reproducible again. (Eos Article)

SEATREE is module based, and the current release includes tools for computing 2D mantle convection, 3D spherical mantle flow, for inverting for Earth structure by means of surface wave, phase velocity tomography, and a two-dimensional synthetic tomography teaching module. Additional modules for 3-D, body wave tomography and earthquake location are in the works. The main software design consists of transparent python wrappers that drive the modules, including a GMT plotting tool, and a graphical user interface.

SEATREE is freely available under the GNU license; a desktop installation is required to use SEATREE right now but we are planning on a web-based version as well. We encourage you to take the software for a test drive. If you want to use SEATREE in a classroom setting, we might be able to offer you some installation support and always welcome your feedback. Also, if you like to add your own module to SEATREE, please let us know; we might be able to provide some assistance.

Screenshots Illustrations of the softwares capabilities and design concepts.

Download and installation Instructions on how to obtain and install the whole package.

User Documentation User-level documentation of SEATREE and the modules.

Done

Local Folders/inbox - ... | SEATREE - Trac - Mozi... | fb10.pdf - Adobe Reader | USA | 00:42

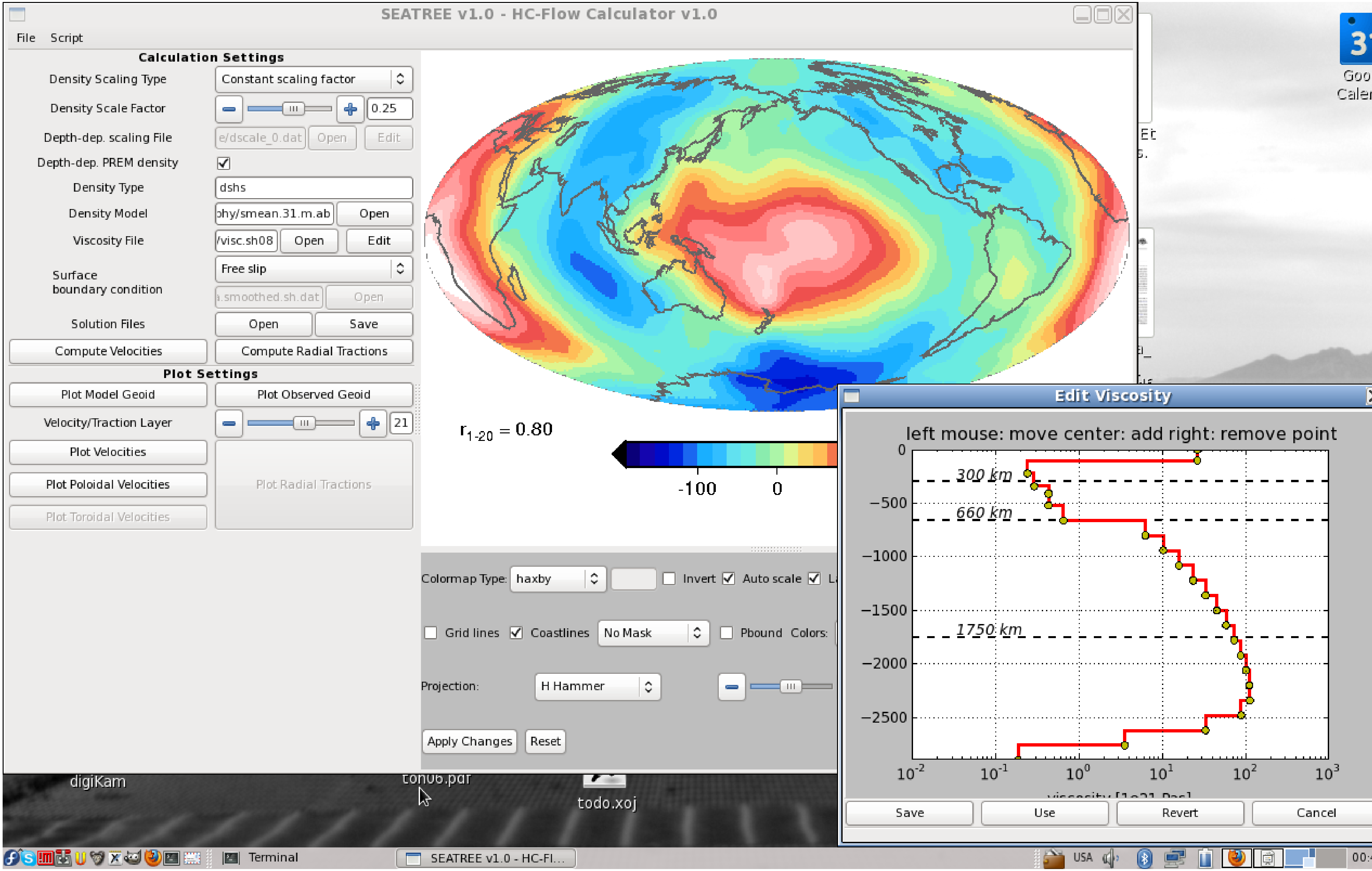
SEATREE v1.0 - HC-Flow Calculator v1.0
File
Script
Calculation Settings
Density Scaling Type
Constant scaling factor
Density Scale Factor
0.25
Depth-dep. scaling File
e/dscale_0.dat
Open
Edit
Depth-dep. PREM density
Density Type
dshs
Density Model
phy/smean.31.m.ab
Open
Viscosity File
/visc.sh08
Open
Edit
Surface boundary condition
Free slip
a.smoothed.sh.dat
Open
Solution Files
Open
Save
Compute Velocities
Compute Radial Tractions
Plot Settings
Plot Model Geoid
Plot Observed Geoid
Velocity/Traction Layer
21
Plot Velocities
Plot Poloidal Velocities
Plot Radial Tractions
Plot Toroidal Velocities
$r_{1\text{-}20} = 0.80$
-100
0
Colormap Type:
haxby
Invert
Auto scale
Grid lines
Coastlines
No Mask
Pbound
Colors:
Projection:
H Hammer
Apply Changes
Reset
Edit Viscosity
left mouse: move center: add right: remove point
300 km
660 km
1750 km
0
−500
−1000
−1500
−2000
−2500
10^{-2}
10^{-1}
10^{0}
10^{1}
10^{2}
10^{3}
Save
Use
Revert
Cancel
digiKam
todo.xoj
Terminal
SEATREE v1.0 - HC-Fl...
USA
00:43

Issues: Plate velocities as a constraint for lateral viscosity variations

Flow model with only radial viscosity variations

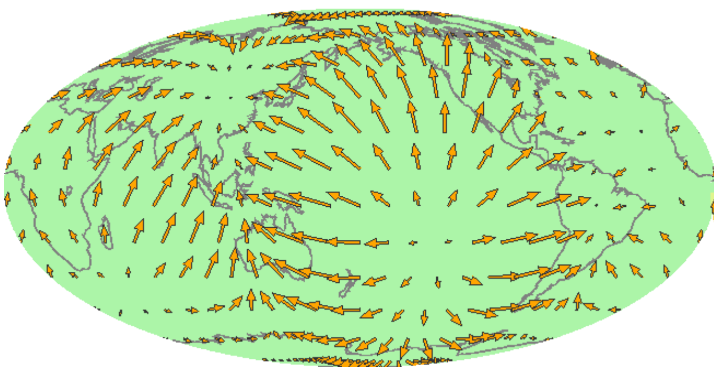

Poloidal component

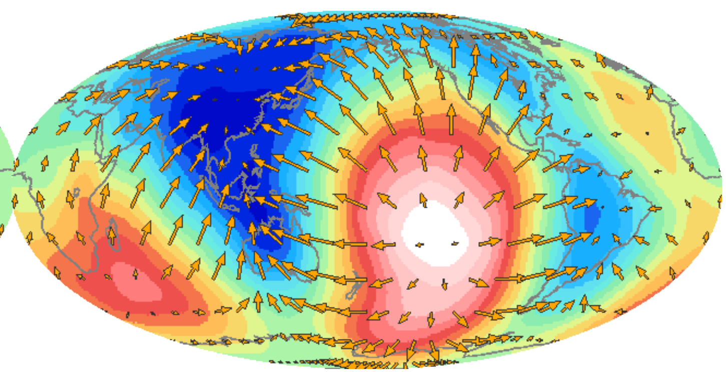

- No toroidal flow without lateral viscosity variations (no PT coupling)
- Strain-rates not very plate-like

Observed plate velocities in hot spot reference frame

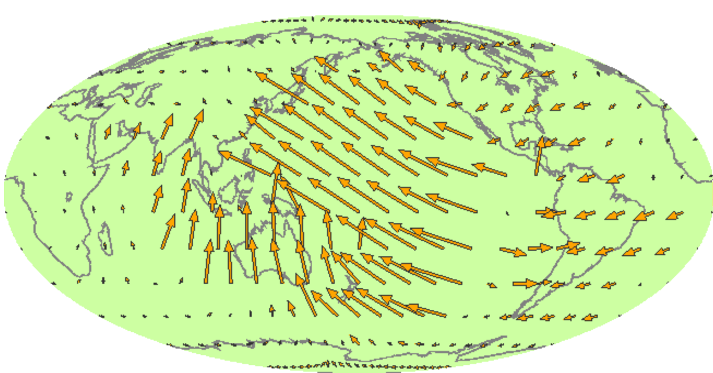

Poloidal component

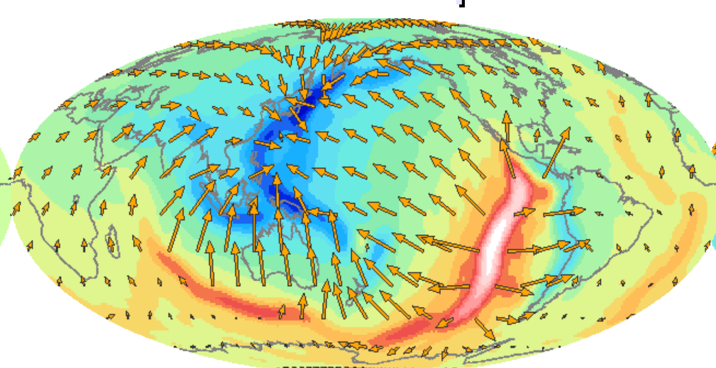

Sources and sinks

Toroidal component

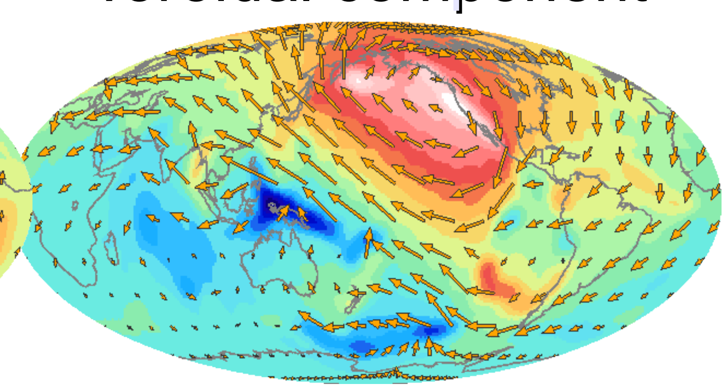

Strike slip motion, spin

O'Connell et al. (1991); Ricard et al. (1991); Ribe (1993); Forte & Peltier (1993); Thoraval & Richards (1997); Moucha et al. (2008); Ghosh et al. (2009)

The role of the plate boundaries

- Velocity model
  - Prescribe weak plate boundaries
  - Compute plate drag coupling and driving torques
  - Solve for Euler vectors for rigid plates
- Correlations good, but oceanic plates move as fast as continental ones

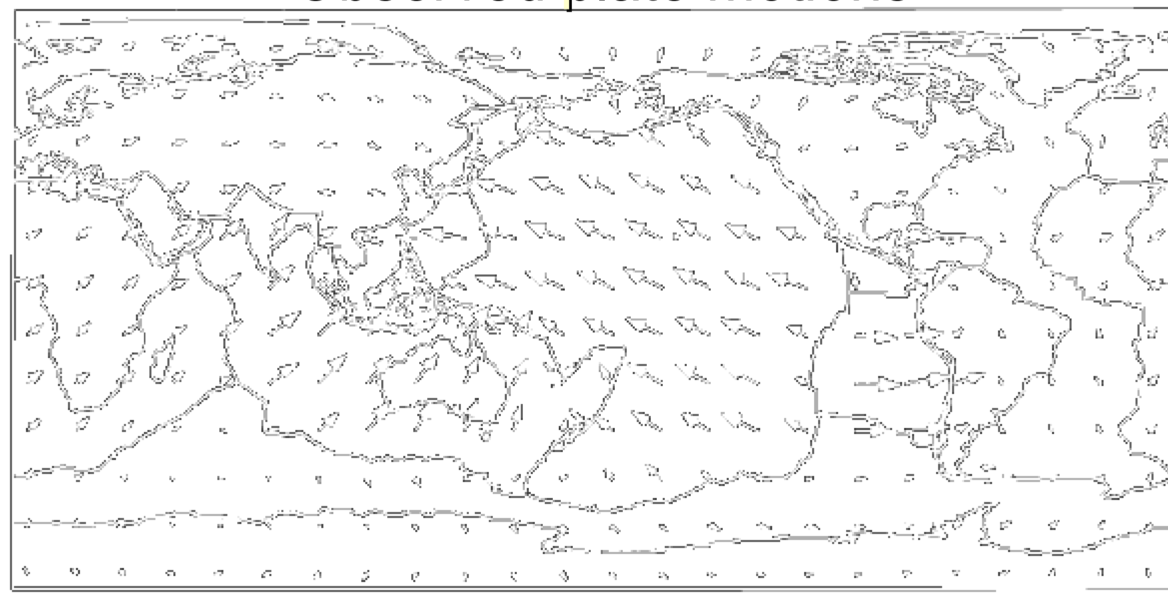

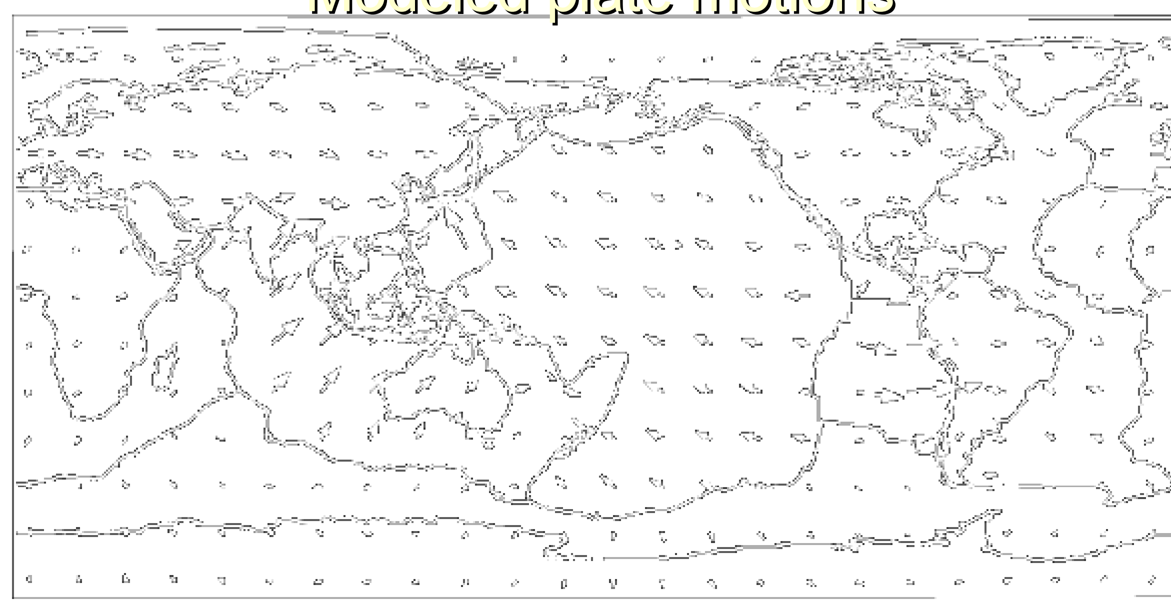

Ricard & Vigny (1989)

Ricard & Vigny (1989); Lithgow-Bertelloni & Richards (1998); Becker & O'Connell (2001); Conrad & Lithgow-Bertelloni (2002); Becker (2006)

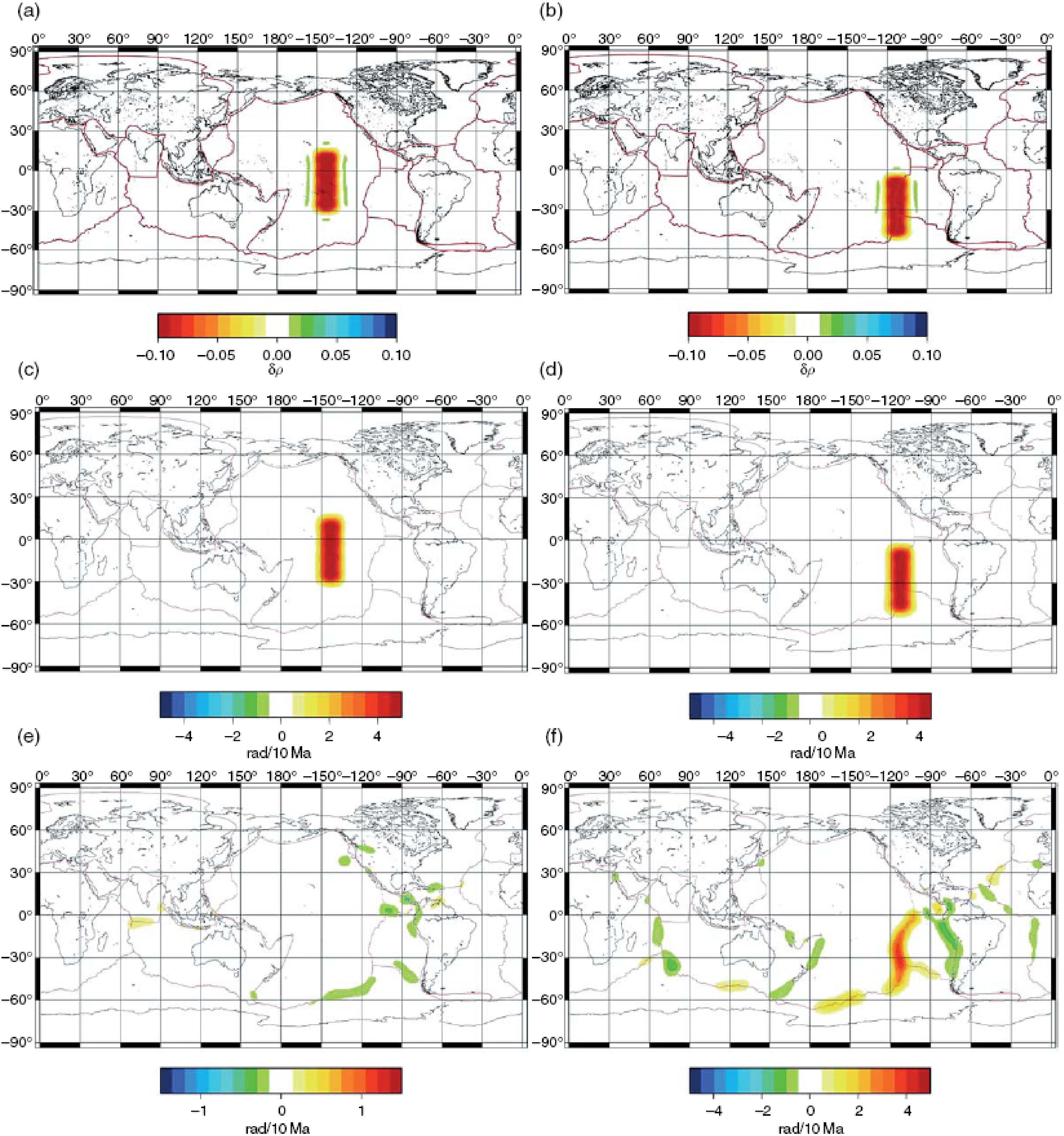

Forte (2008)

Geoid and LVVs

- Free slip surface
- Four layer viscosity (not optimized)
- SMEAN tomography

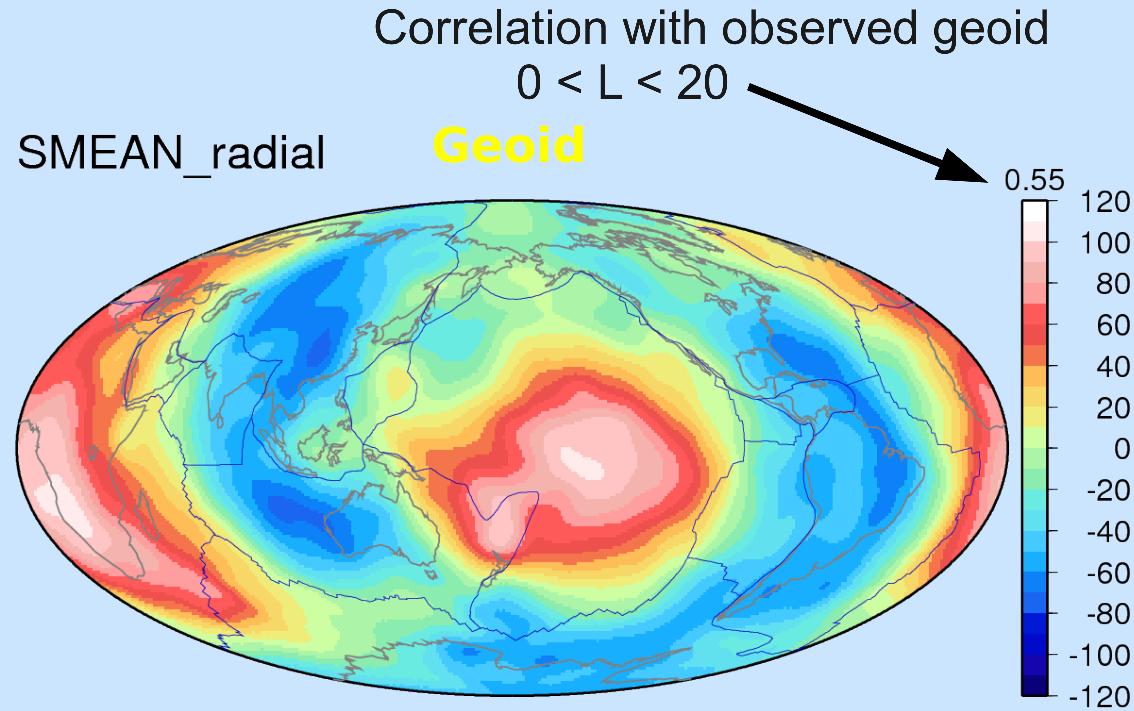

Surface velocities with viscosity in background

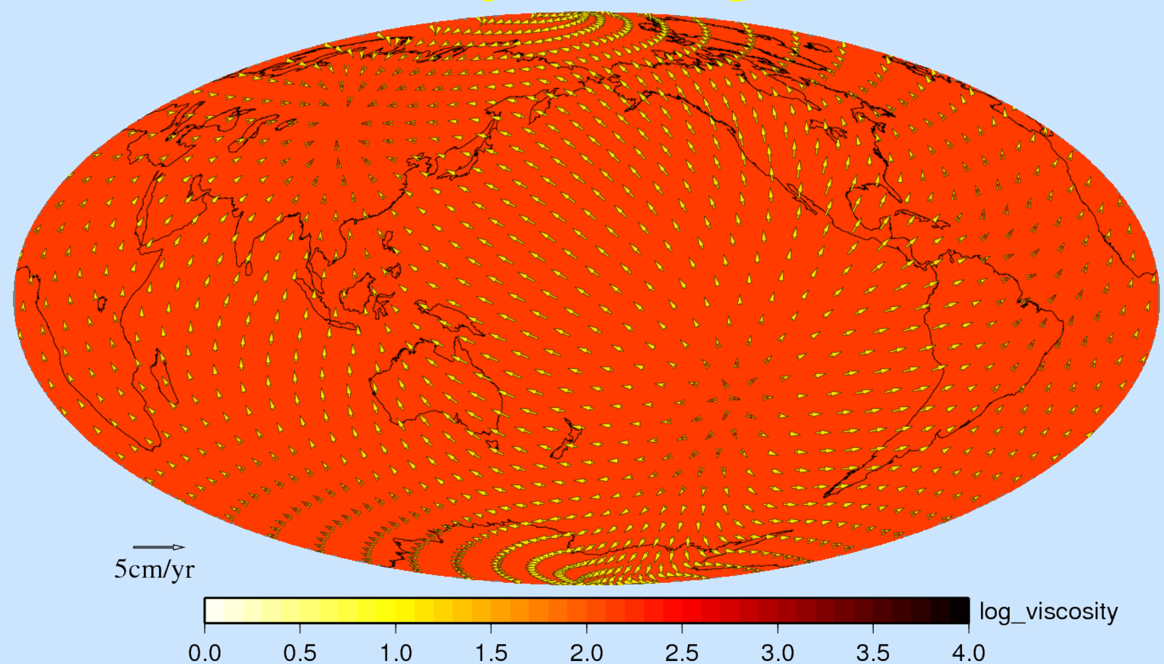

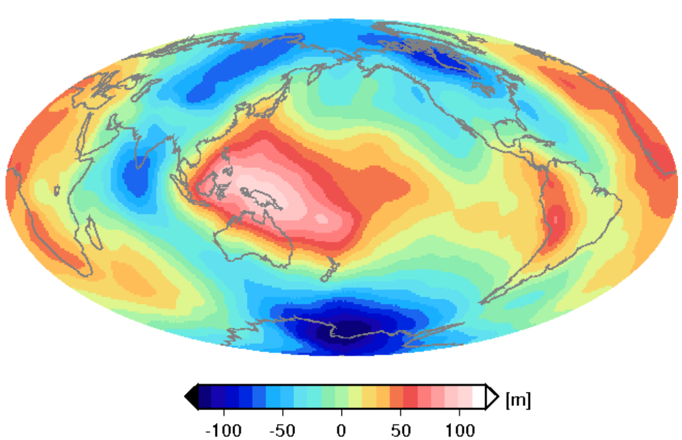

Geoid and LVVs

- Free slip surface
- Weak zones, stiff keels

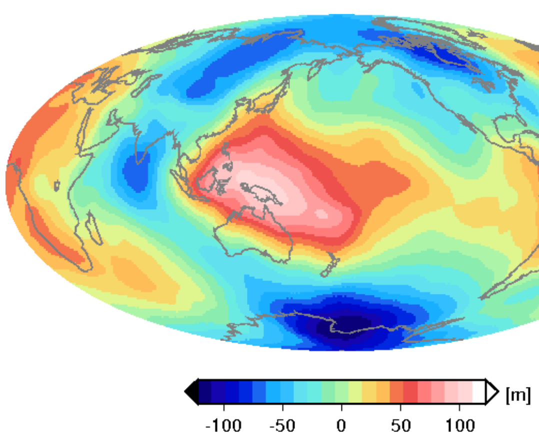

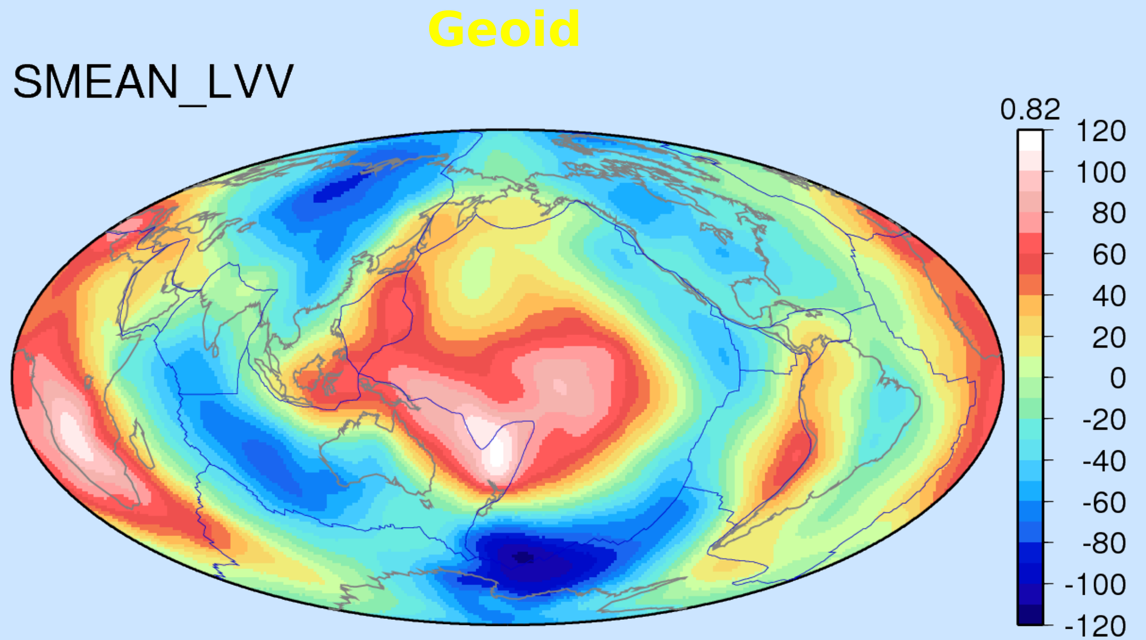

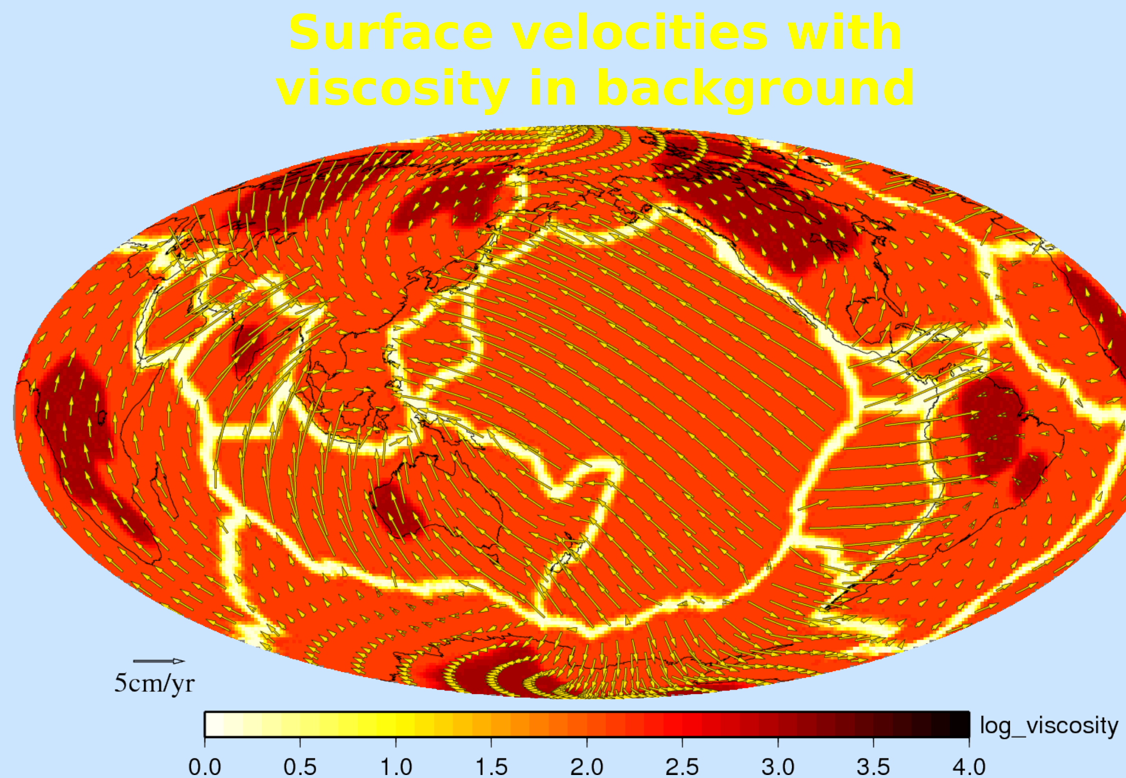

Geoid and LVVs

- Prescribed plate motions

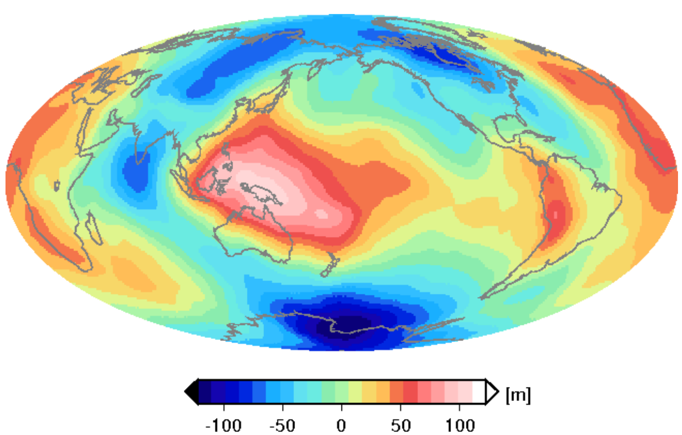

Geoid

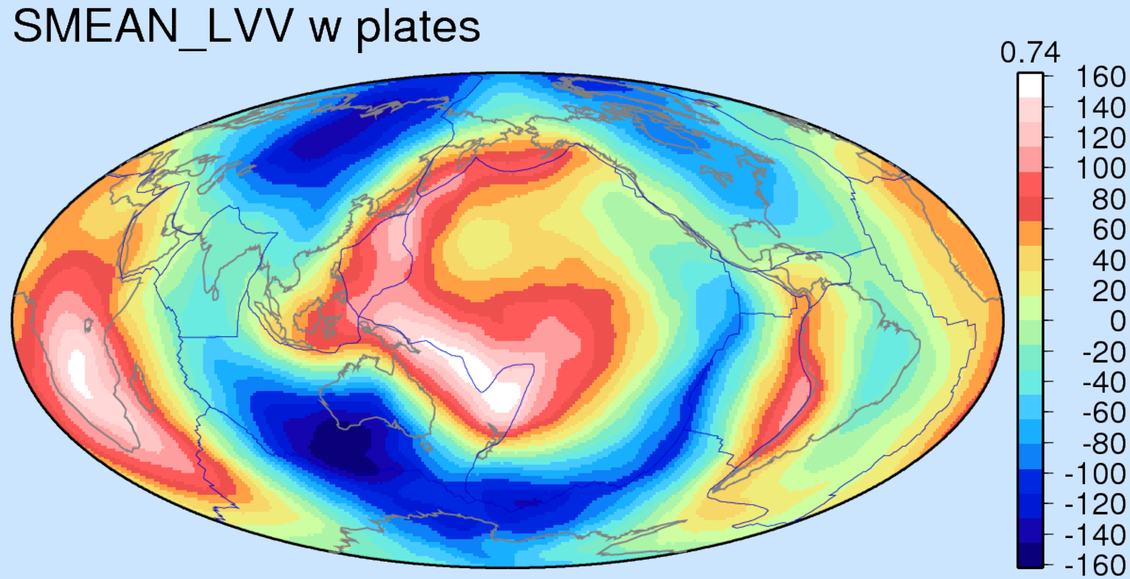

Surface velocities with viscosity in background

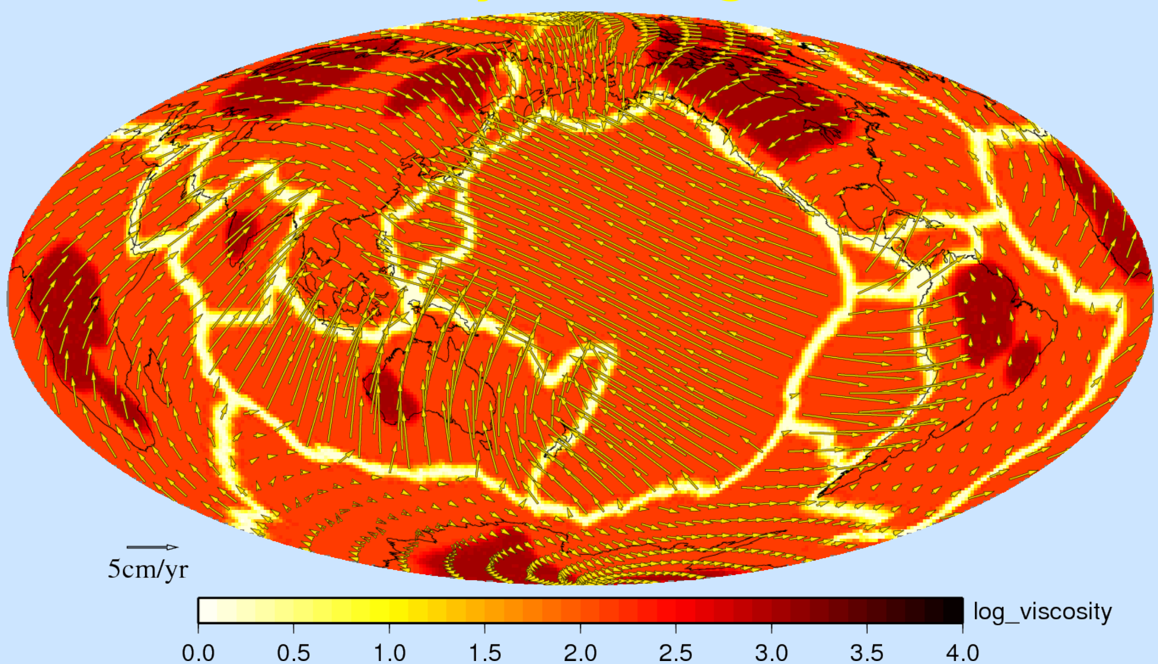

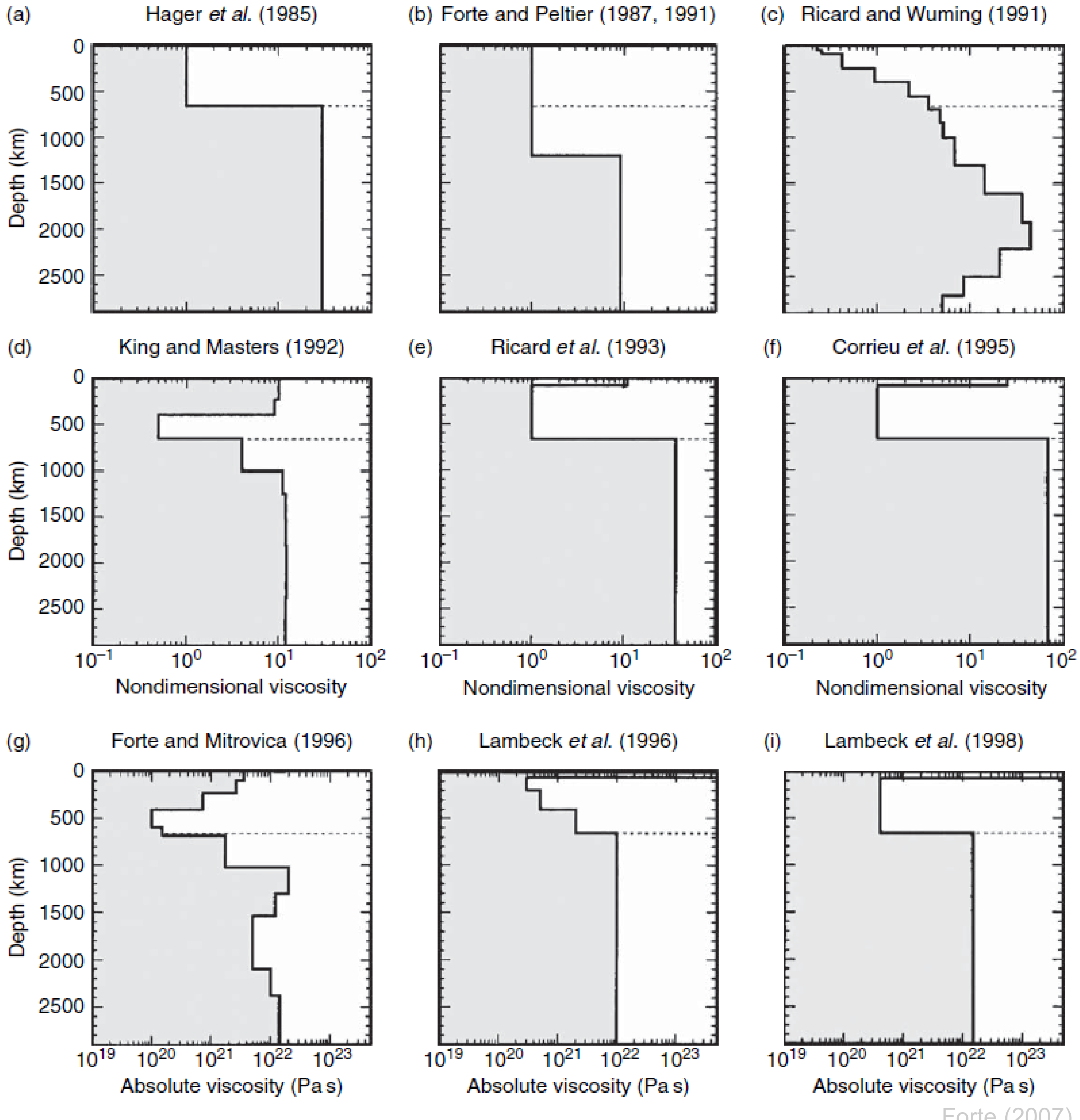

(a) Hager et al. (1985)
(b) Forte and Peltier (1987, 1991)
(c) Ricard and Wuming (1991)
(d) King and Masters (1992)
(e) Ricard et al. (1993)
(f) Corrieu et al. (1995)
(g) Forte and Mitrovica (1996)
(h) Lambeck et al. (1996)
(i) Lambeck et al. (1998)
Depth (km)
0
500
1000
1500
2000
2500
Nondimensional viscosity
10^{-1} 10^{0} 10^{1} 10^{2}
Absolute viscosity (Pa s)
10^{19} 10^{20} 10^{21} 10^{22} 10^{23}
Forte (2007)

Plate "velocity" and gravity kernels

- Physical insight
- Useful for inversions

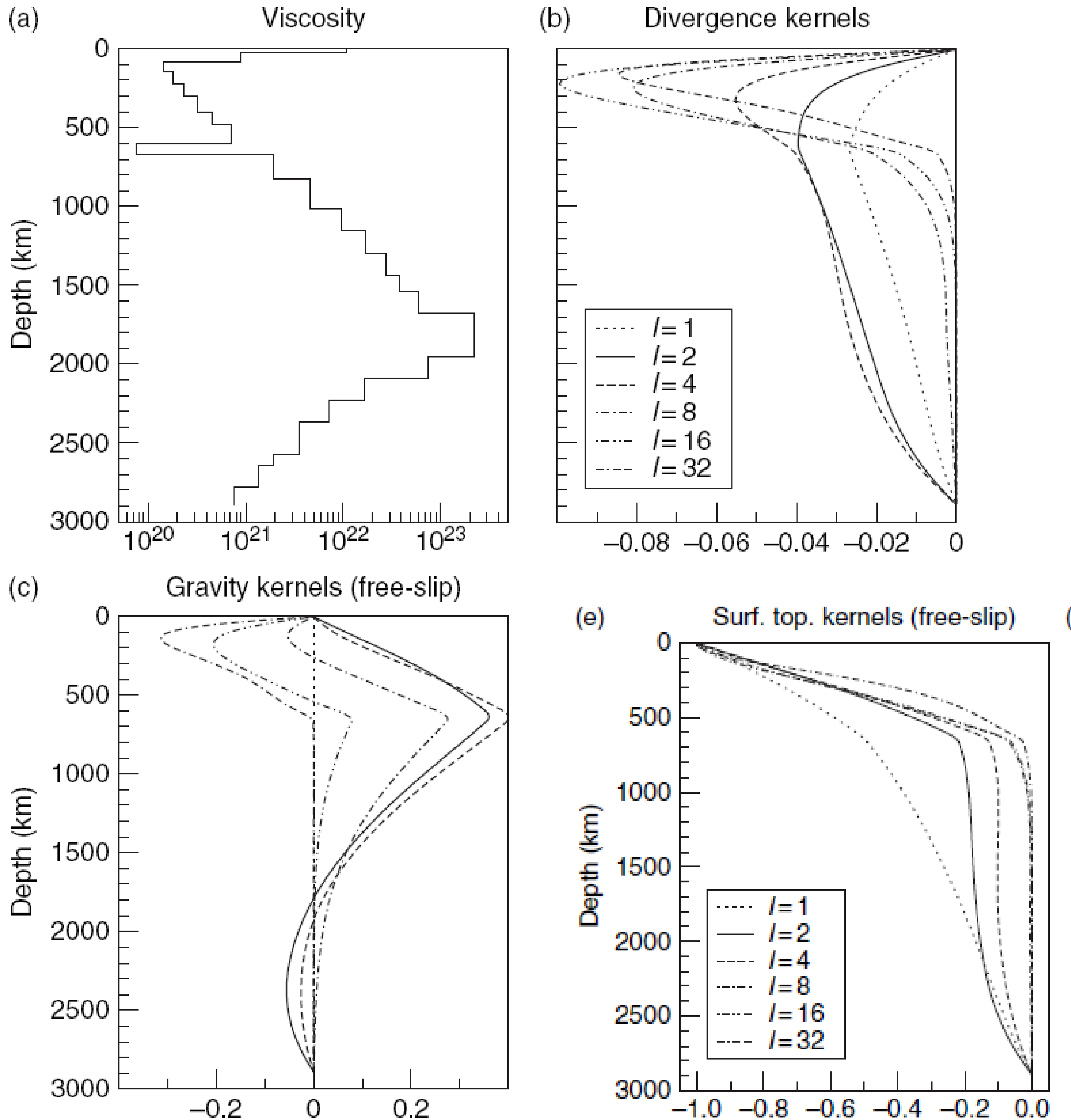

Forte (2007)

Combining GIA and geoid

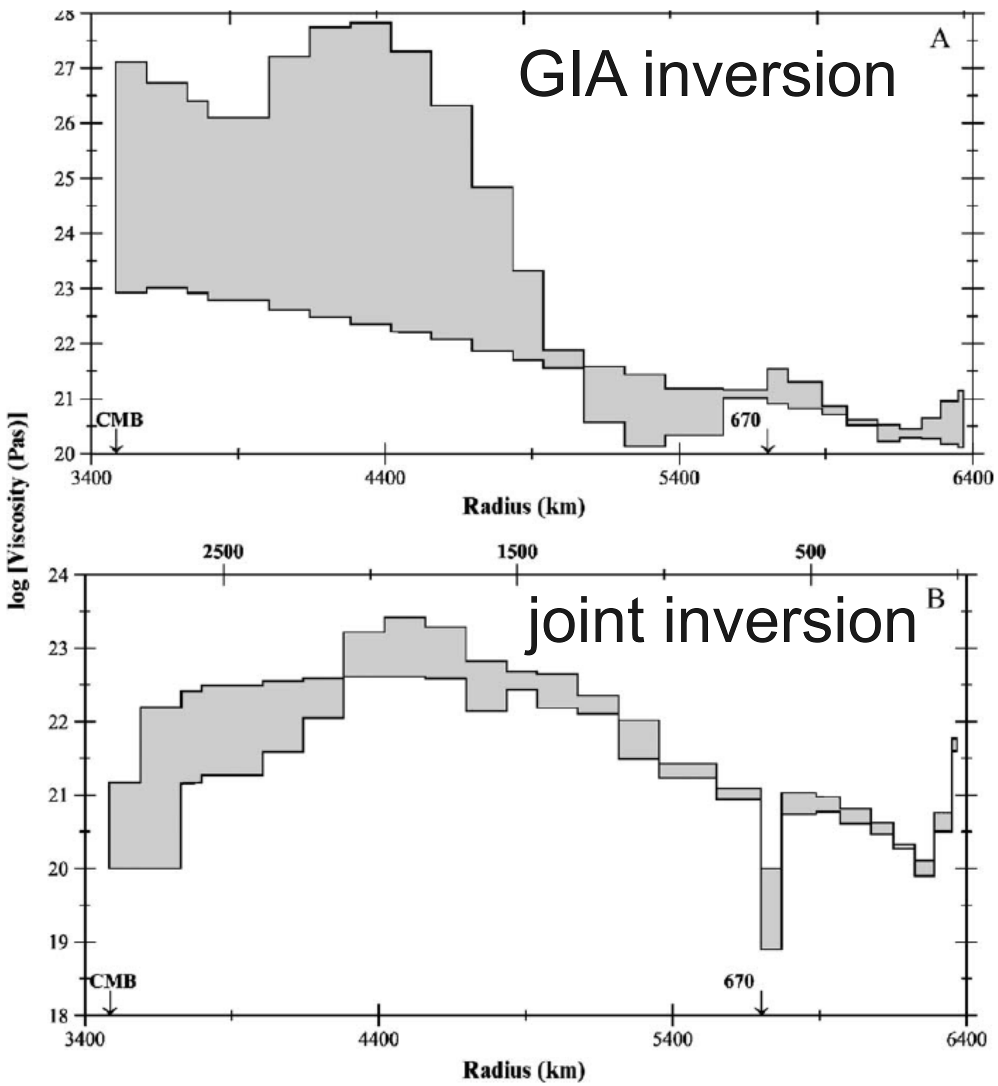

Mitrovica & Forte (2004)

Fig. 4. Range of viscosity profiles mapped out by varying the smoothing constraint (given by the smoothing weight, μ) in the Occam-style inversions. (A) The upper and lower bound, within each model layer, of viscosity inferences obtained by inverting only the GIA data using a suite of smoothing weights in the range 10^{-9} (roughest) to 10^{-5} (smoothest). (B) Bounds obtained by jointly inverting the GIA and convection data, for smoothing weights in the range 10^{-5}–10^{-1}, where the convection data are interpreted in the context of a viscous flow calculation based on Grand's [54] tomography model. The results shown in Fig. 3 are also part of the suite of models used to map out the viscosity bounds.

Alternative viscosity solutions

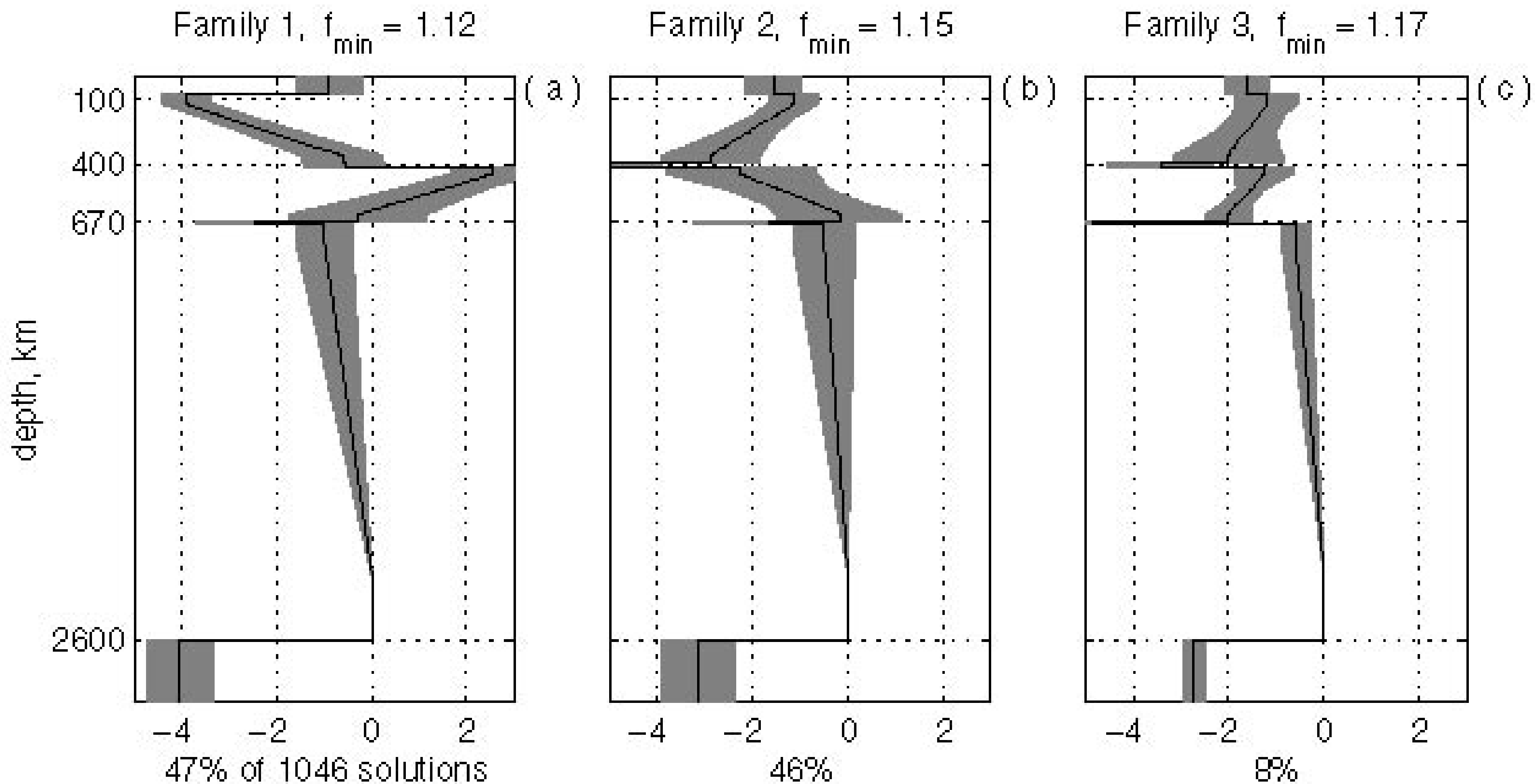

Panasyuk & Hager (2000)

Best-fit scaling factors

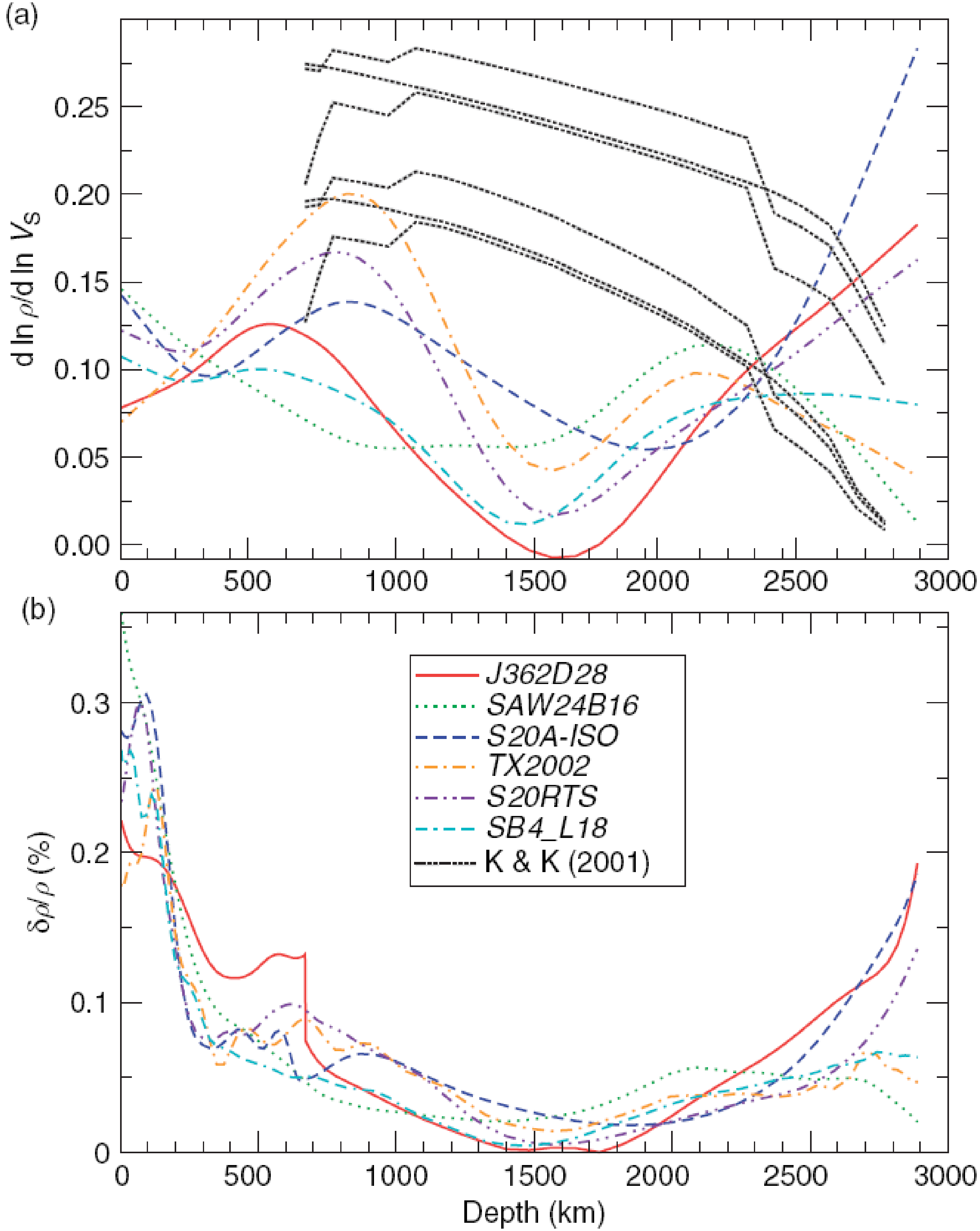

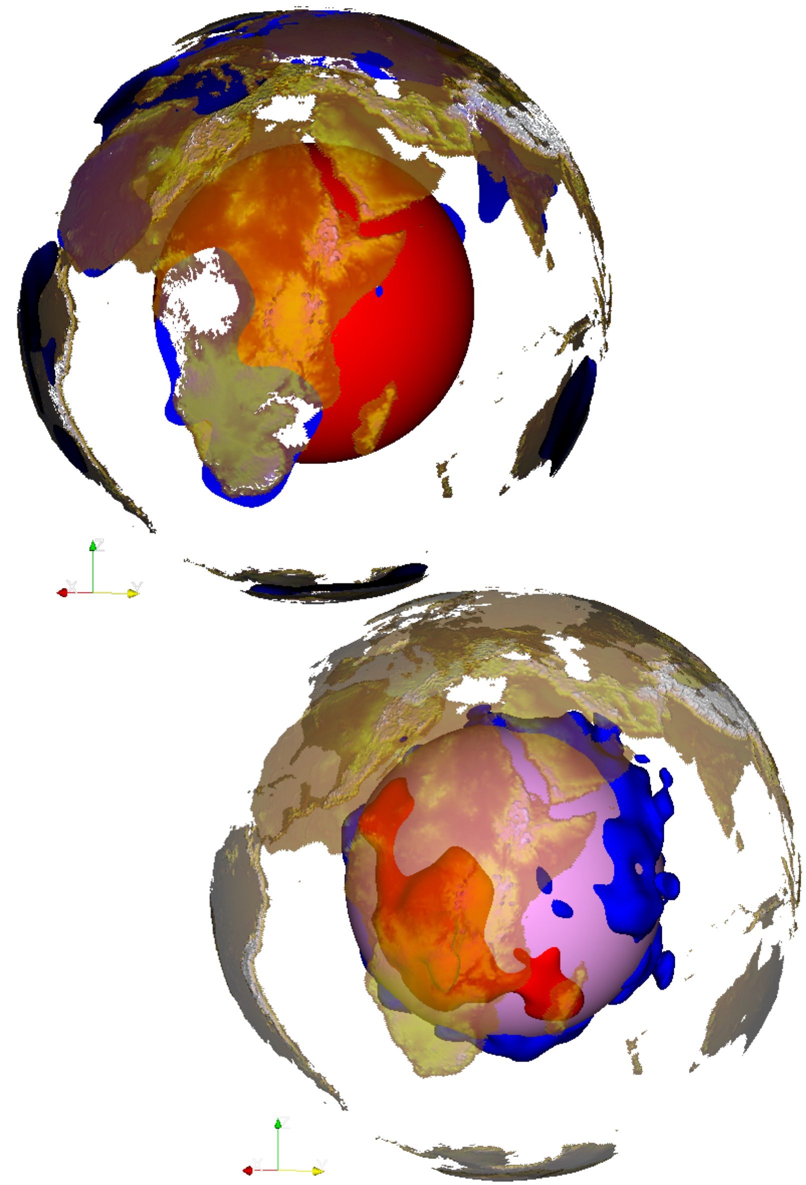

Forte (2008)

Issues: How to scale velocities to density anomalies?

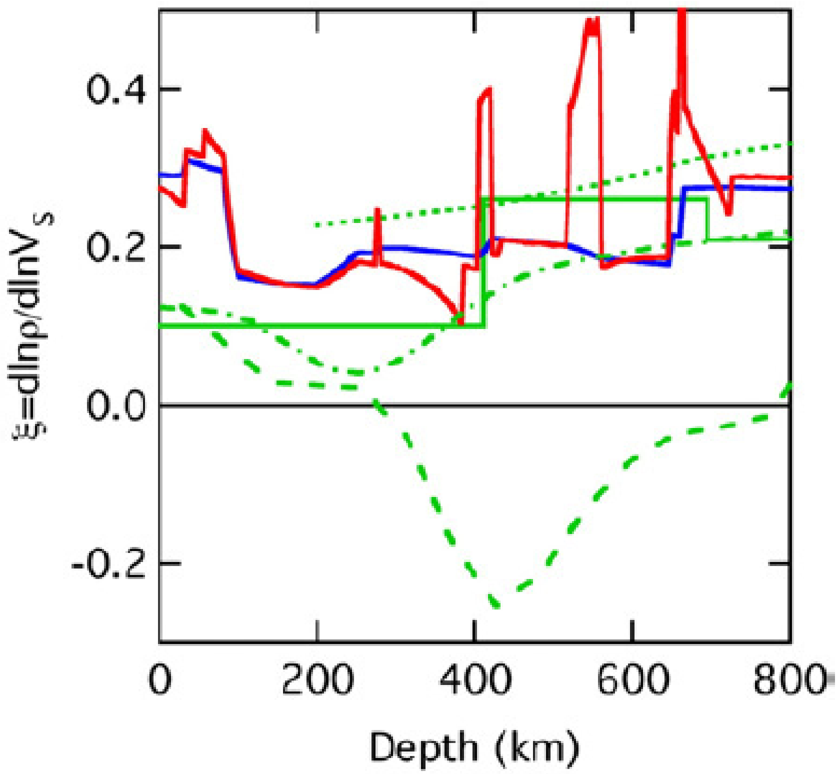

Fig. 8. Relative variations of density and shear wave velocity ξ (red) and the isomorphic contribution to ξ (blue) compared with the results of: (short-dashed green) Karato (1993), (solid green) Forte et al. (1994), (long-dashed green) Ishii and Tromp (2001) and (dash-dot green) Forte and Mitrovica (2001). (For interpretation of the references

Karato & Karki (2001); Forte & Mitrovica (2001); Steinberger & Calderwood (2006); Stixrude & Lithgow-Bertelloni (2007)

Seeing the slab

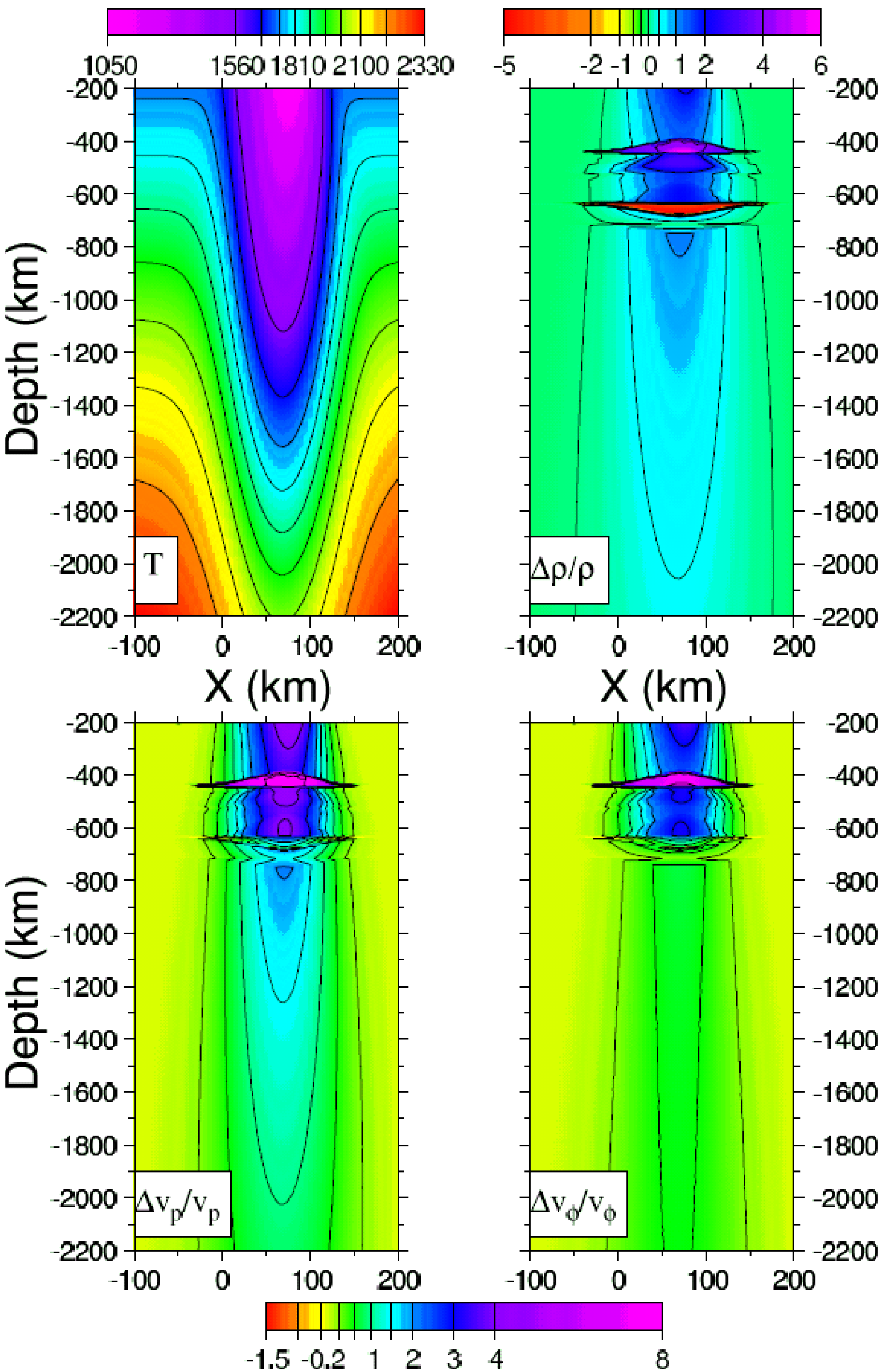

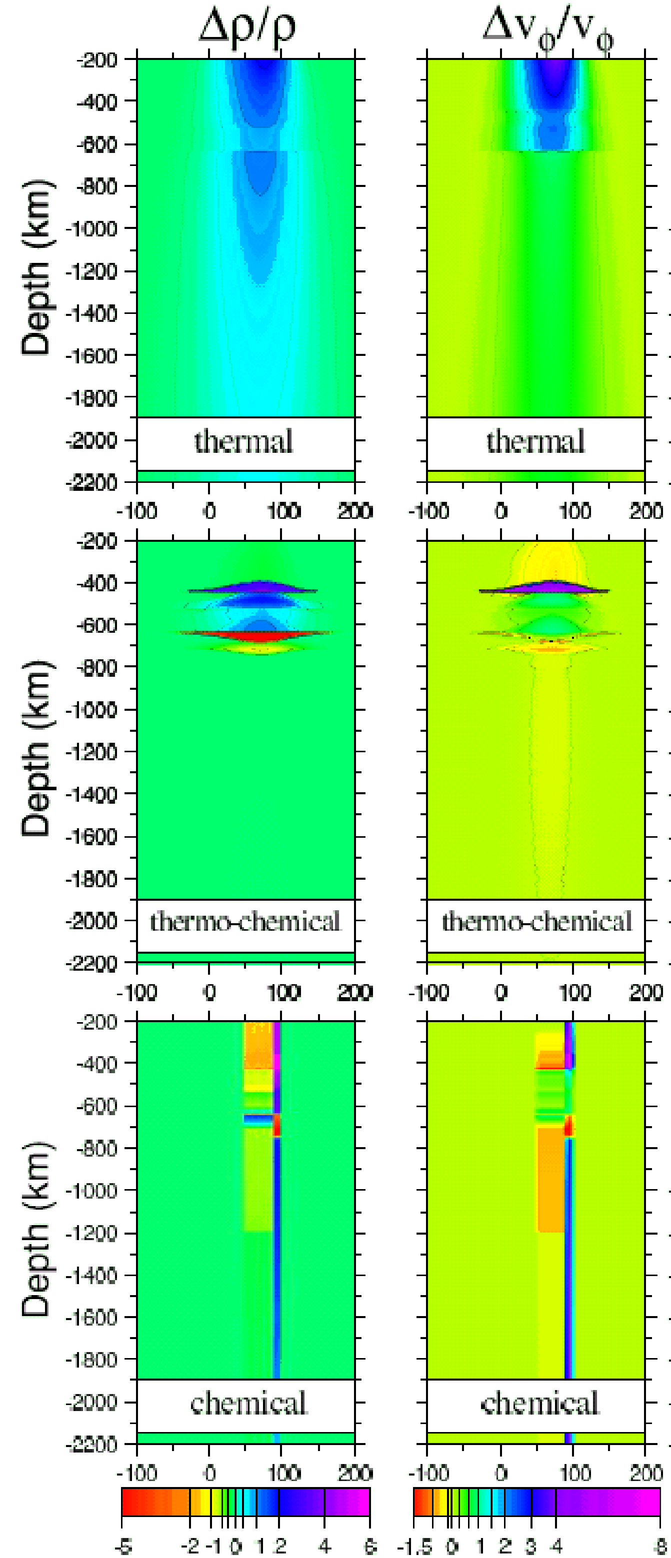

Ricard et al.
(2005)

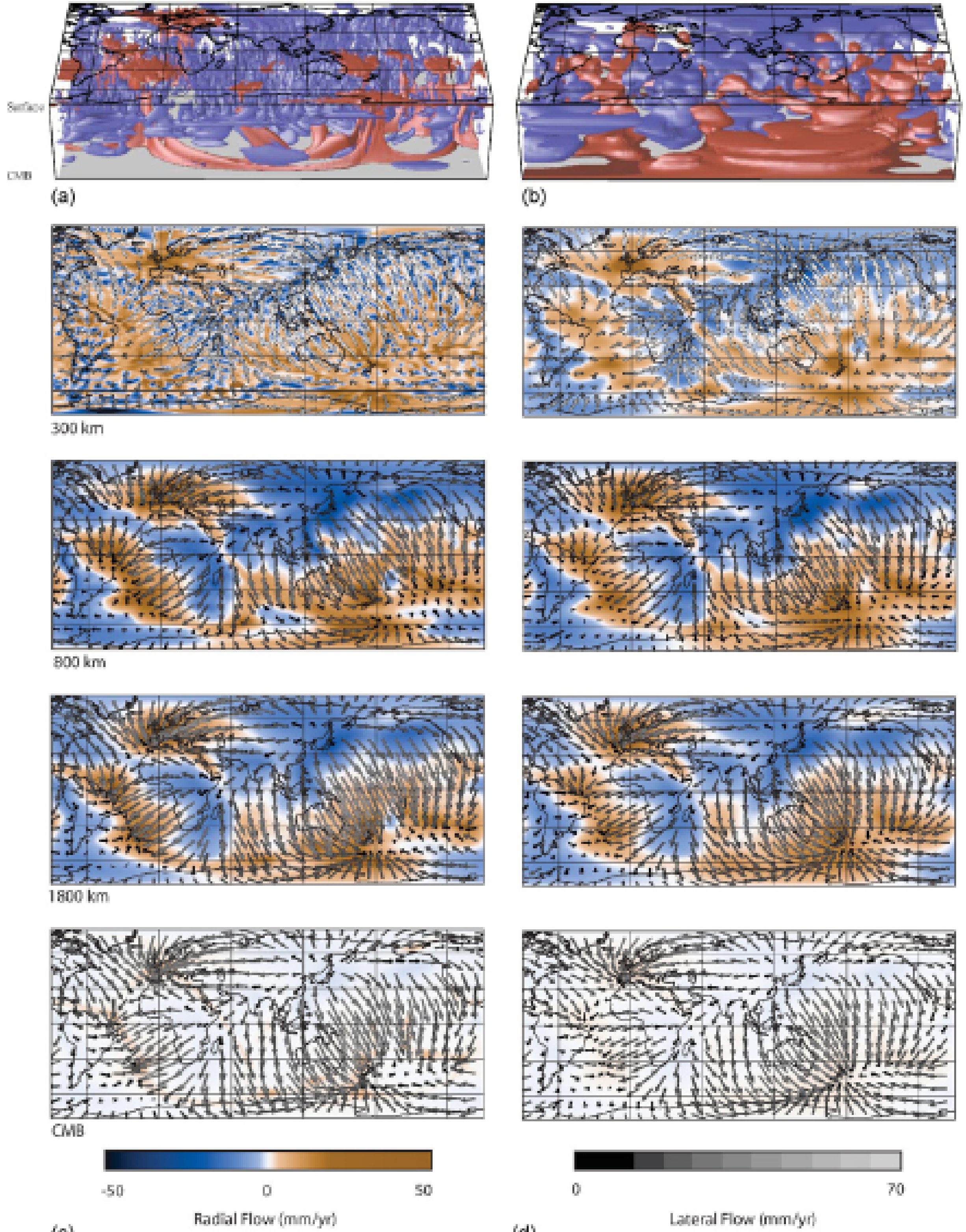

Bull et al. (2010)

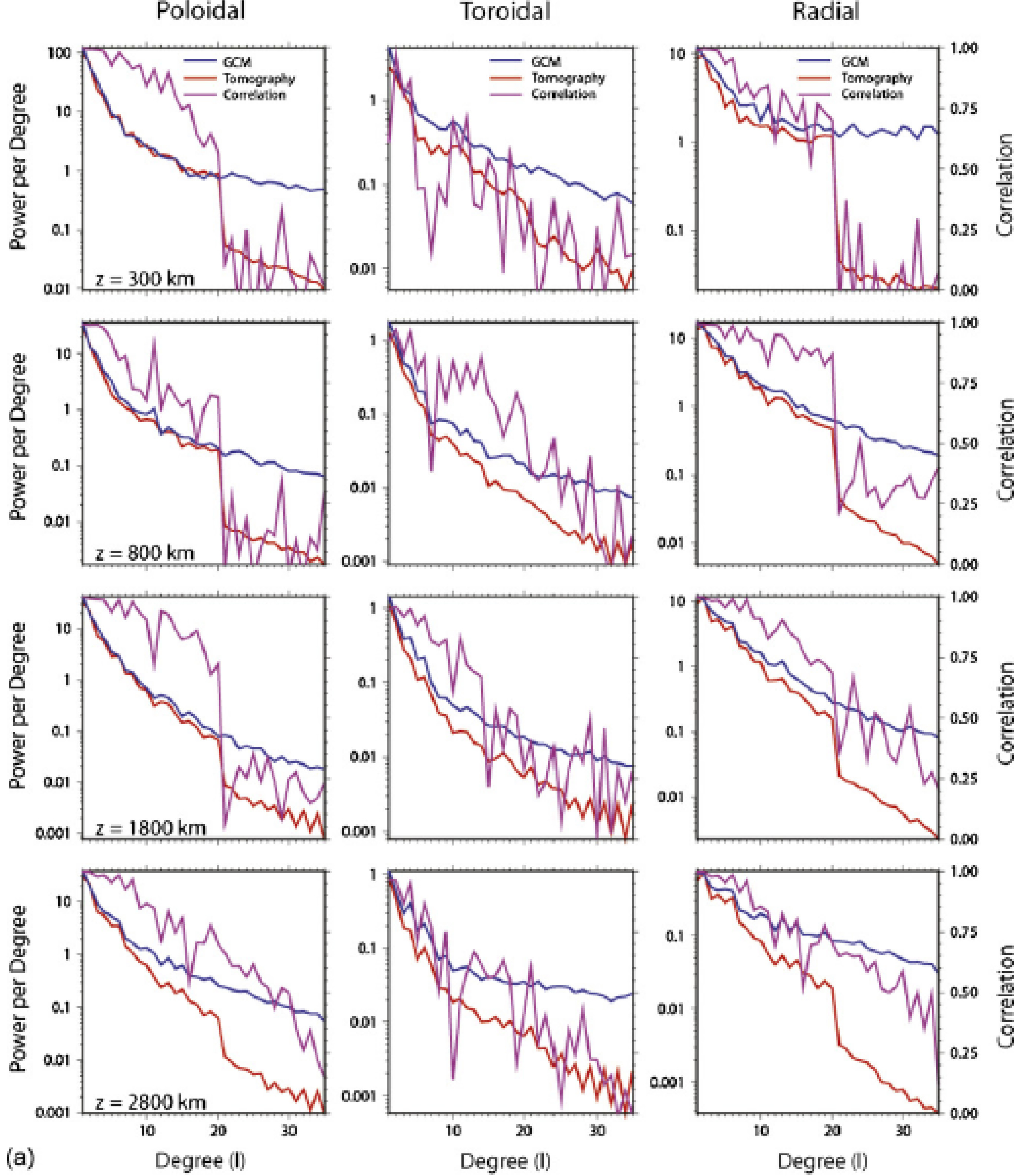

Bull et al. (2010)

Can we improve the subduction models with circulation computations?

Sensitivity to plate reconstructions

⇒ global 3-D convection model

⇒ plate-history prescribed at surface

⇒ run forward from thermal steady state

Bunge & Grand (2000)

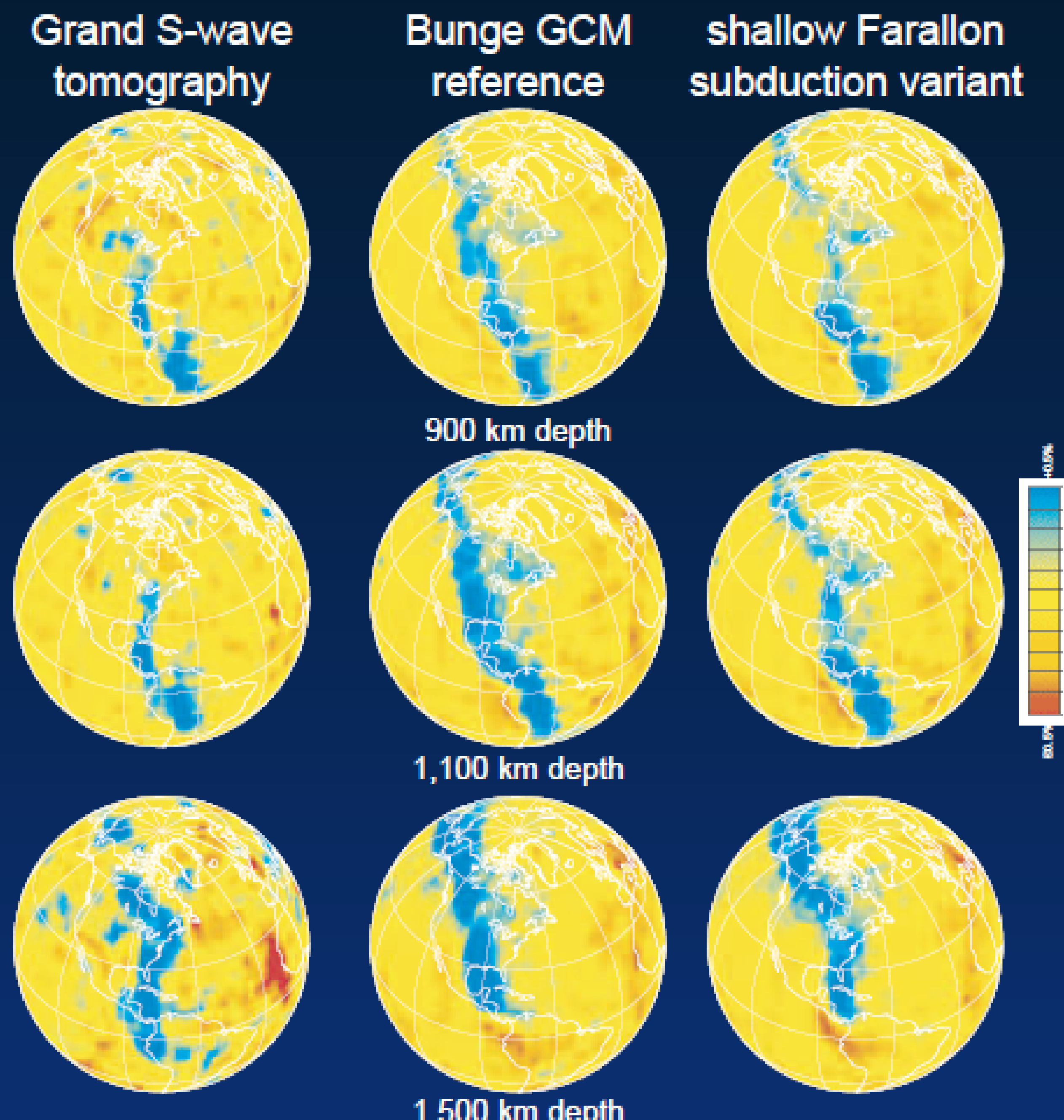

→ geological hypothesis testing feasible

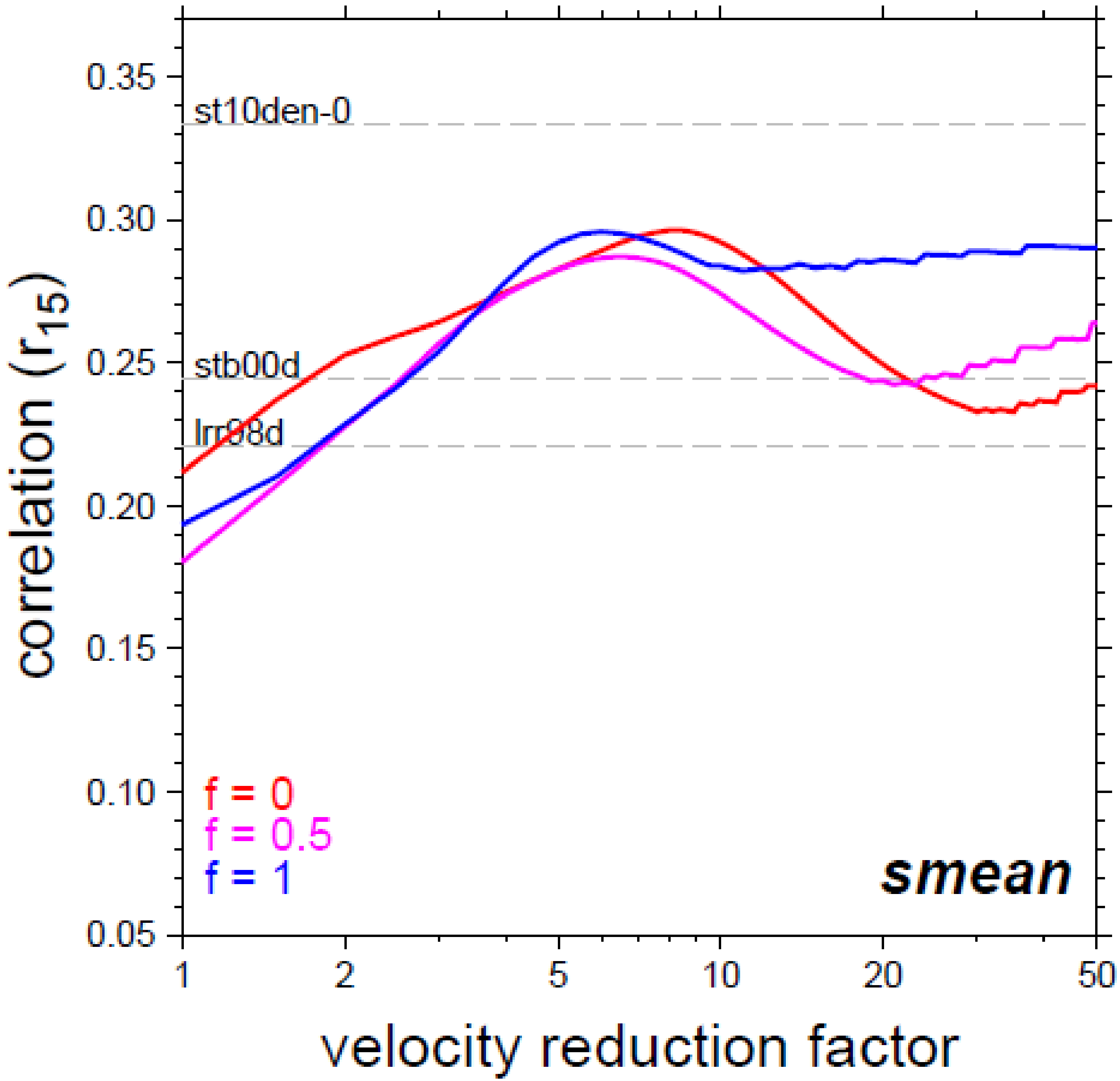

st10den-0
stb00d
lrr98d
f = 0
f = 0.5
f = 1
smean
correlation (r_{15})
velocity reduction factor
0.35
0.30
0.25
0.20
0.15
0.10
0.05
1
2
5
10
20
50

Adjoint methods

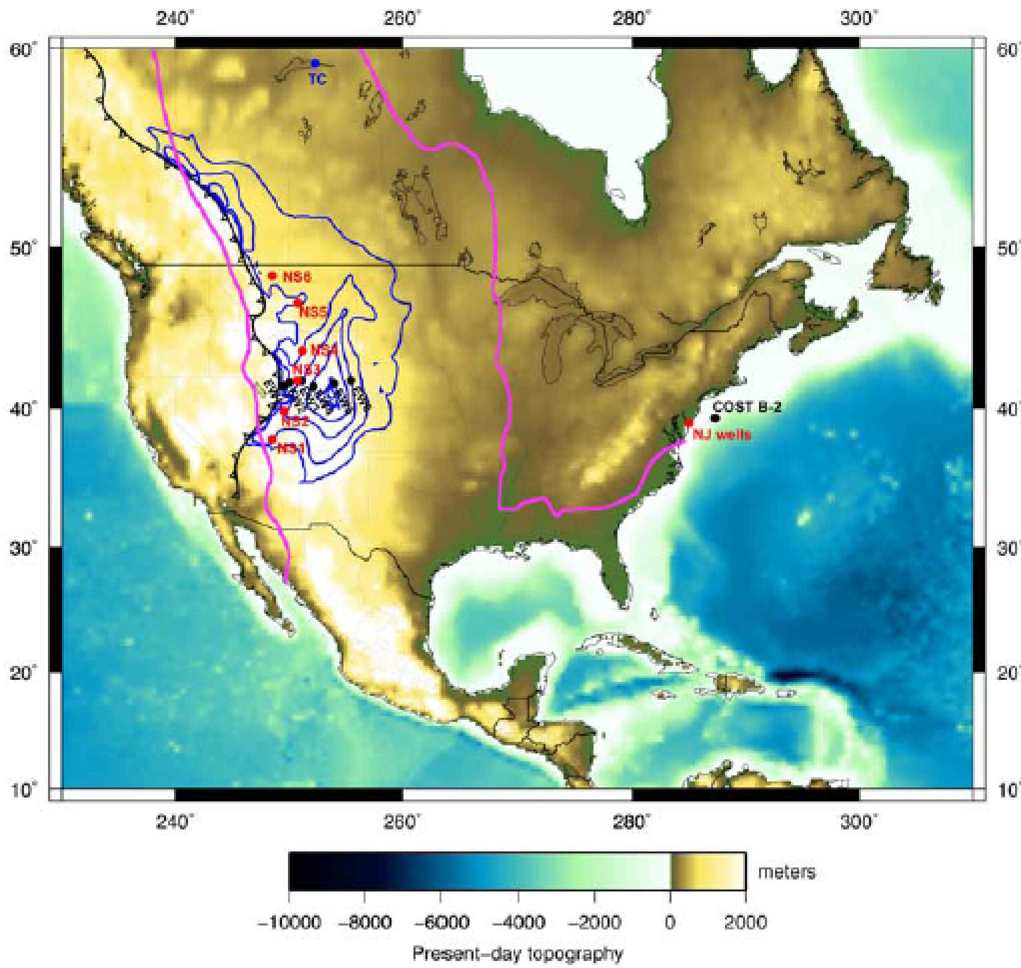

Figure 1. Position of data constraints used in the study. Pink line shows reconstructed 95 Ma paleoshoreline [*Smith et al.*, 1994], blue contours show total Late Cretaceous isopach [*Cook and Bally*, 1975] with 2000 ft contour interval, and black line shows position of the Sevier thrust belt [*Cook and Bally*, 1975]. Black and red dots, marked as EW1–EW6 and NS1–NS6, indicate location of boreholes of tectonic subsidence curves [*Liu et al.*, 2005; *Pang and Nummedal*, 1995]. Red dot marked NJ wells shows position of wells located on the New Jersey coastal plain [*Miller et al.*, 2005], and black dot marked COST-B2 indicate position of the offshore well used by *Watts and Steckler* [1979] for sea level curve derivation. Blue dot marked TC indicates location of East Lake Athabasca thermochrology study of *Flowers* [2009].

Spasojevich et al. (2009)

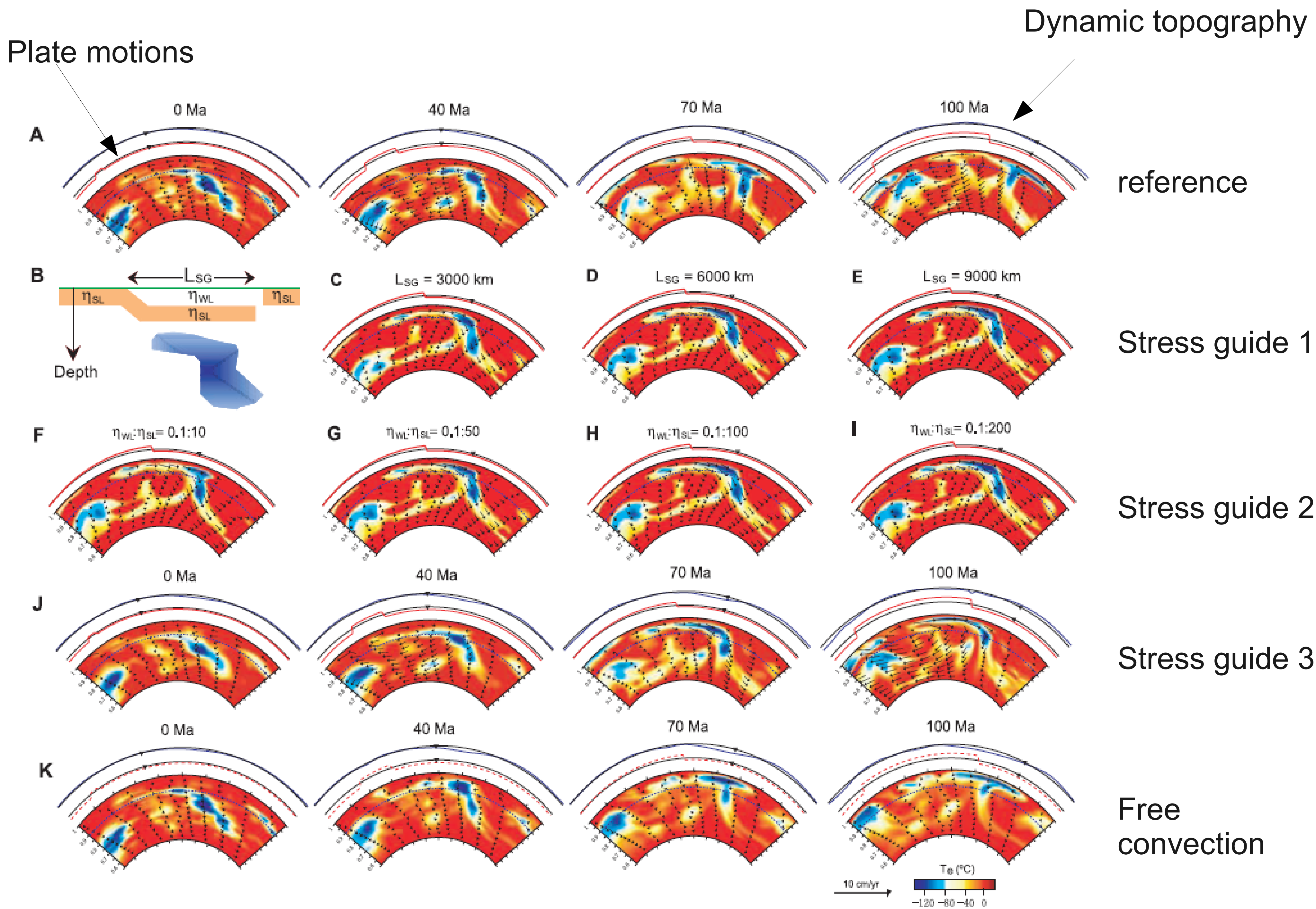

Spasojevich et al. (2009)

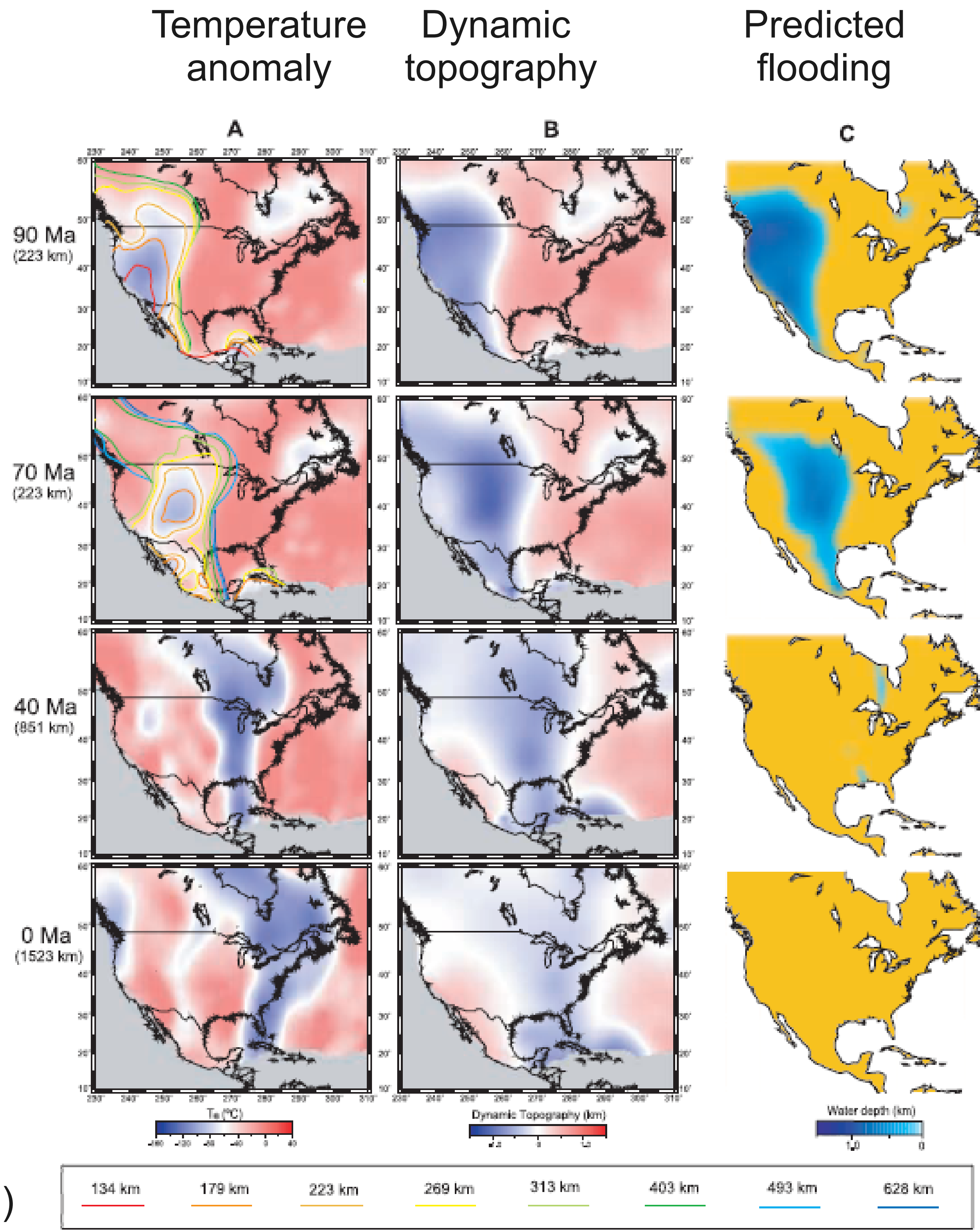

Spasojevich et al. (2009)

Some comments on plate motions from global models

Observed & Predicted Plate Motions in NNR Reference Frame

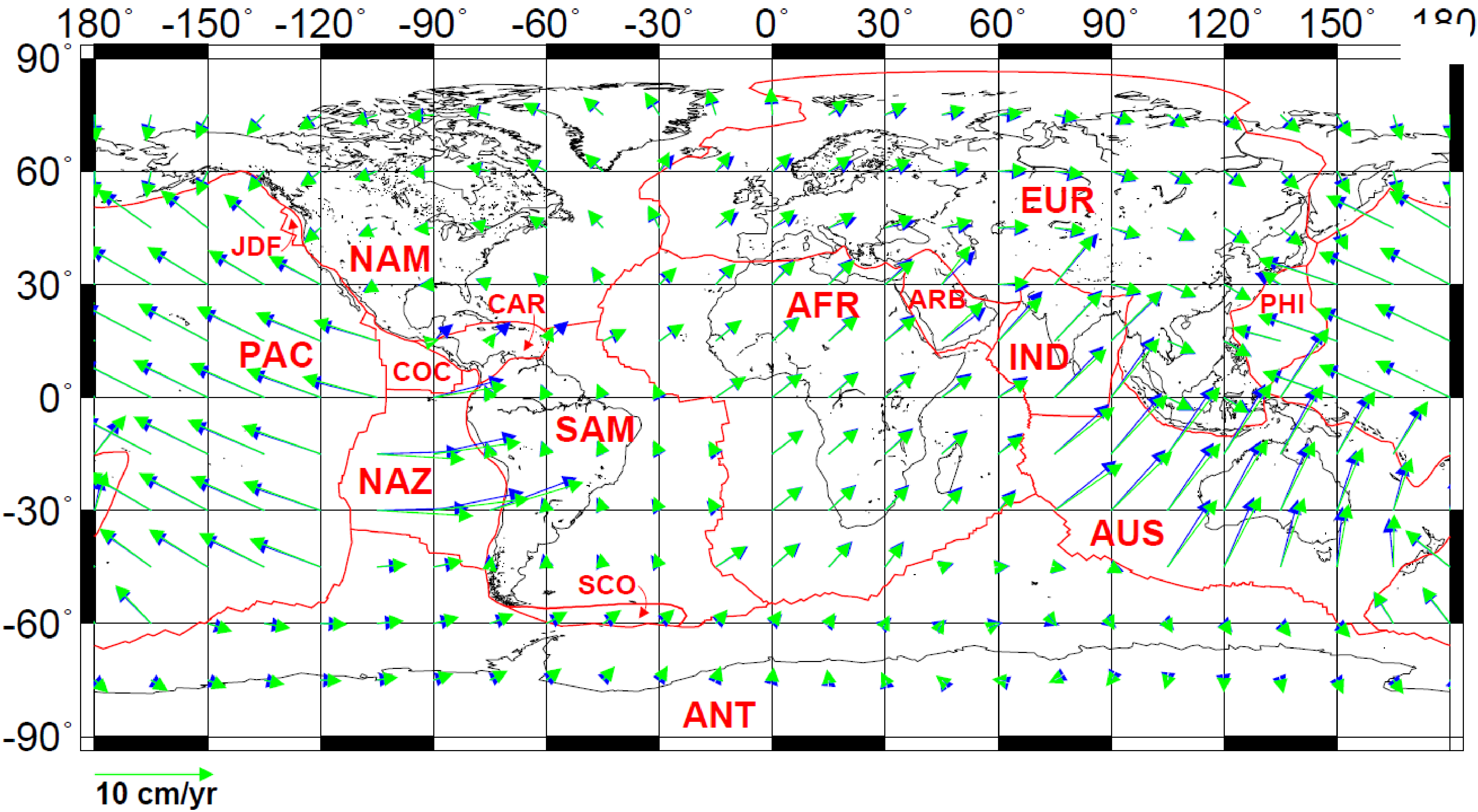

Forte (2007)

only upper mantle slabs

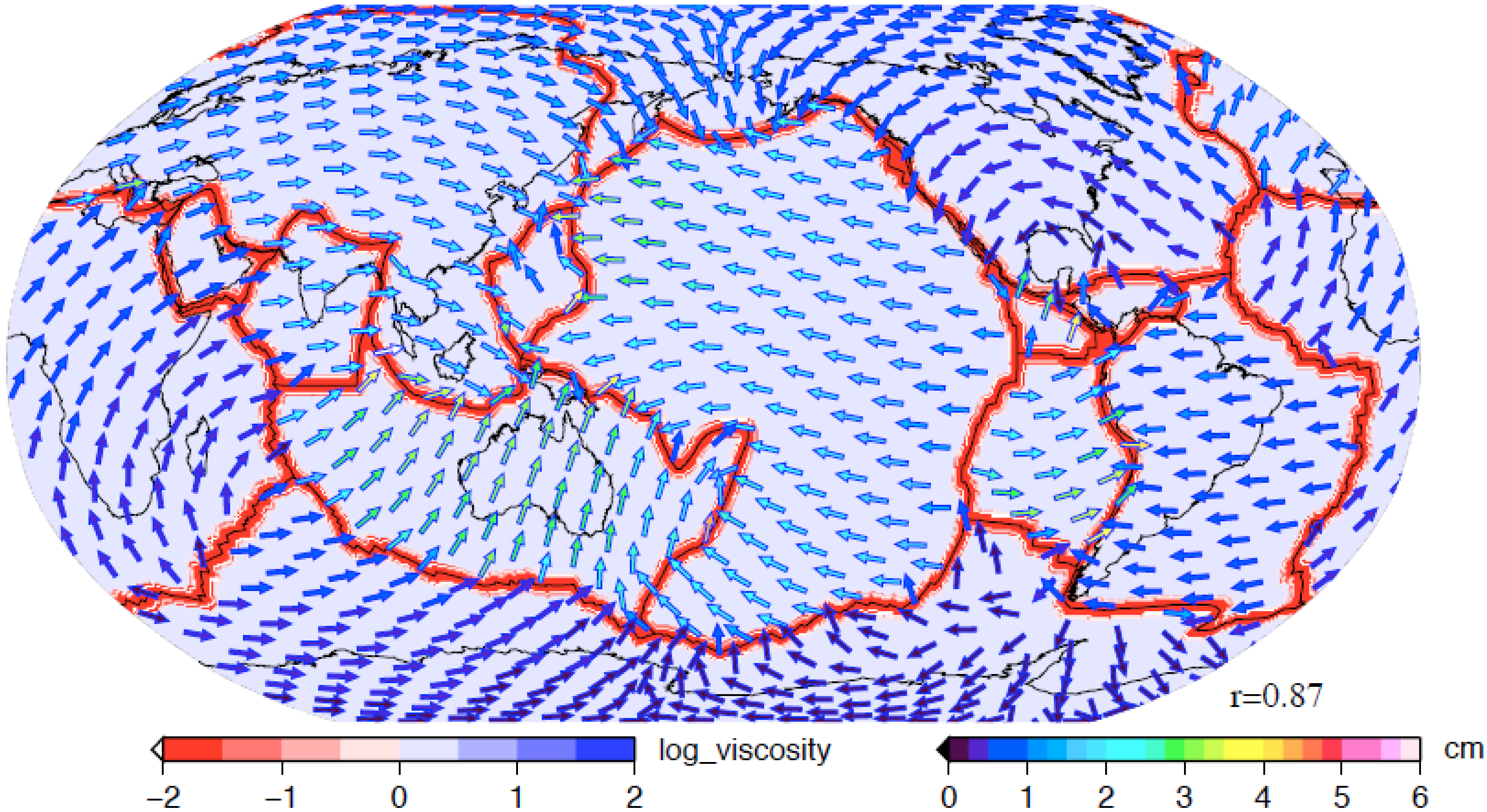

Ghosh et al. (2010)

upper mantle slabs plus tomography in lower mantle

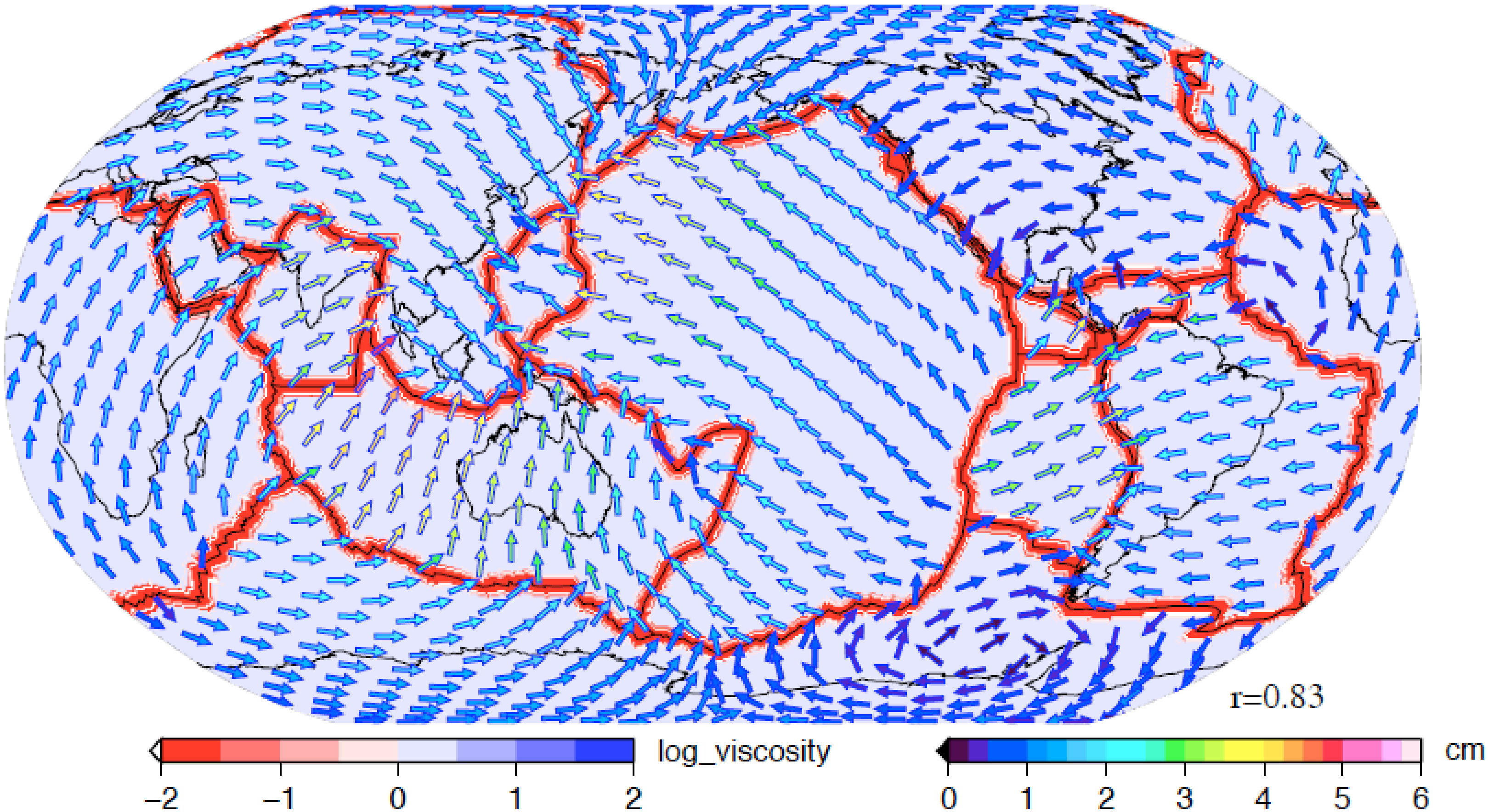

Ghosh et al. (2010)

upper mantle slabs plus low velocity anomalies from tomography plus lower mantle tomography

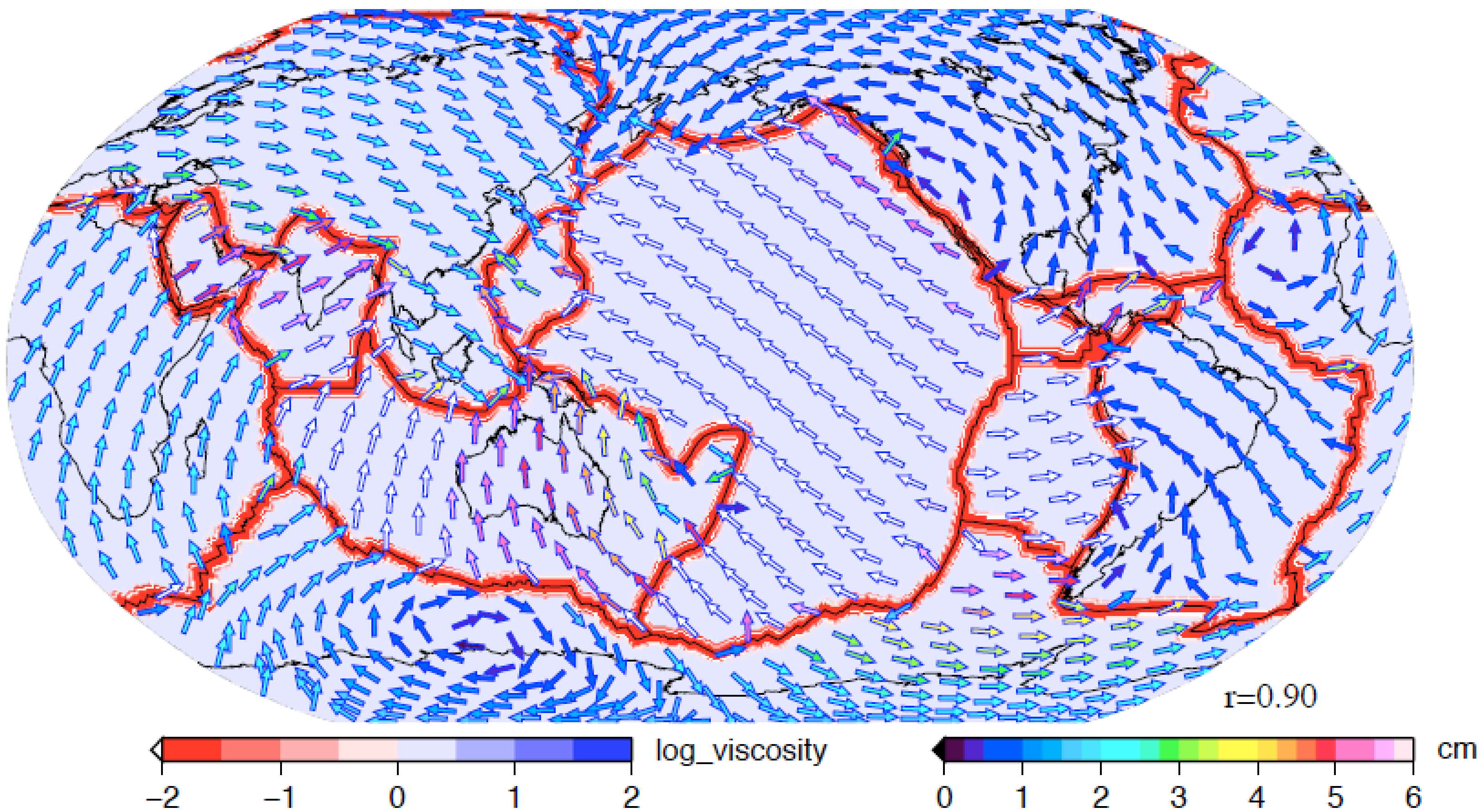

Ghosh et al. (2010)

full tomography in top 100km and lower mantle plus upper mantle slabs from below 100km

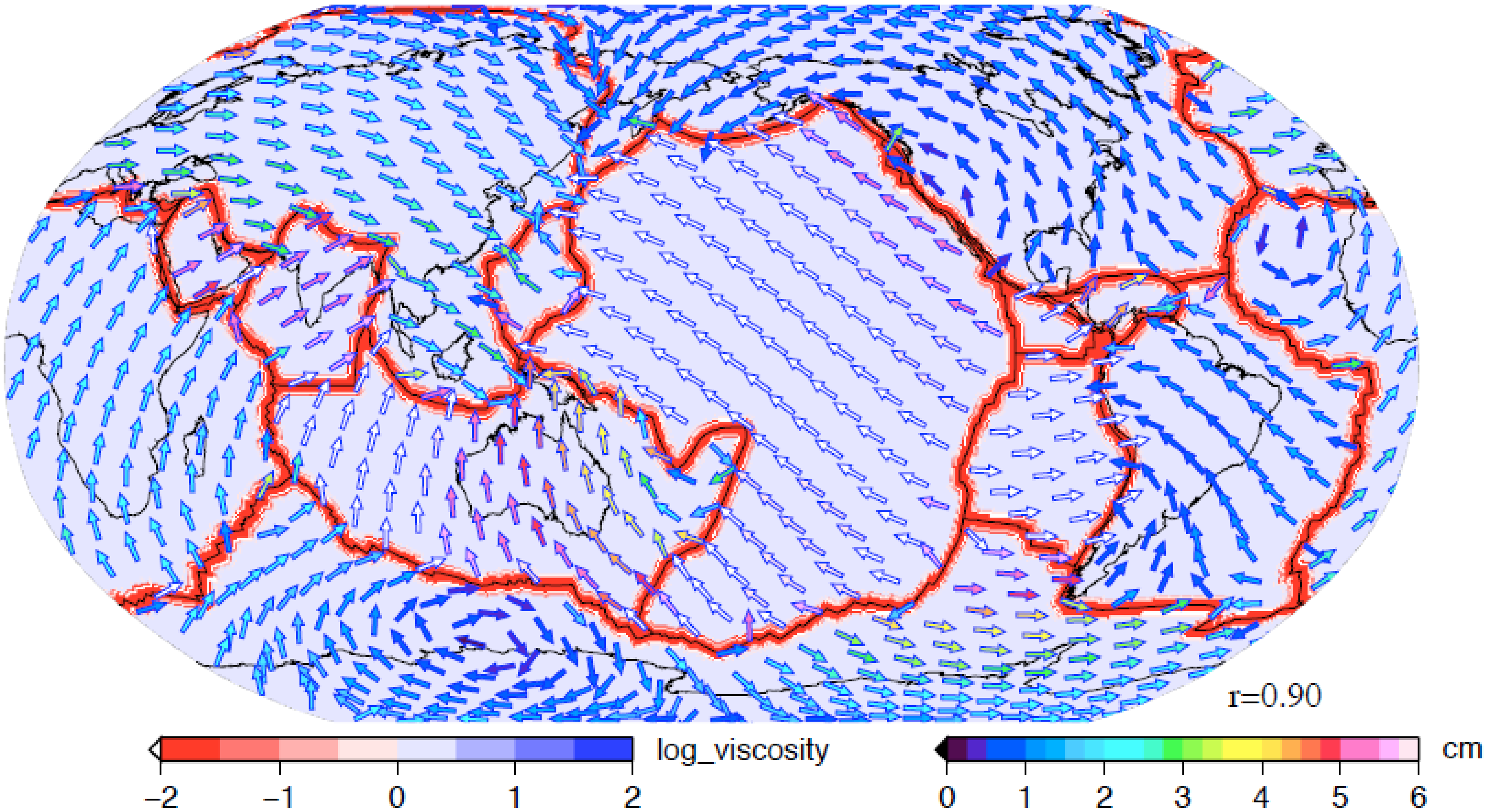

Ghosh et al. (2010)

Driving the plates

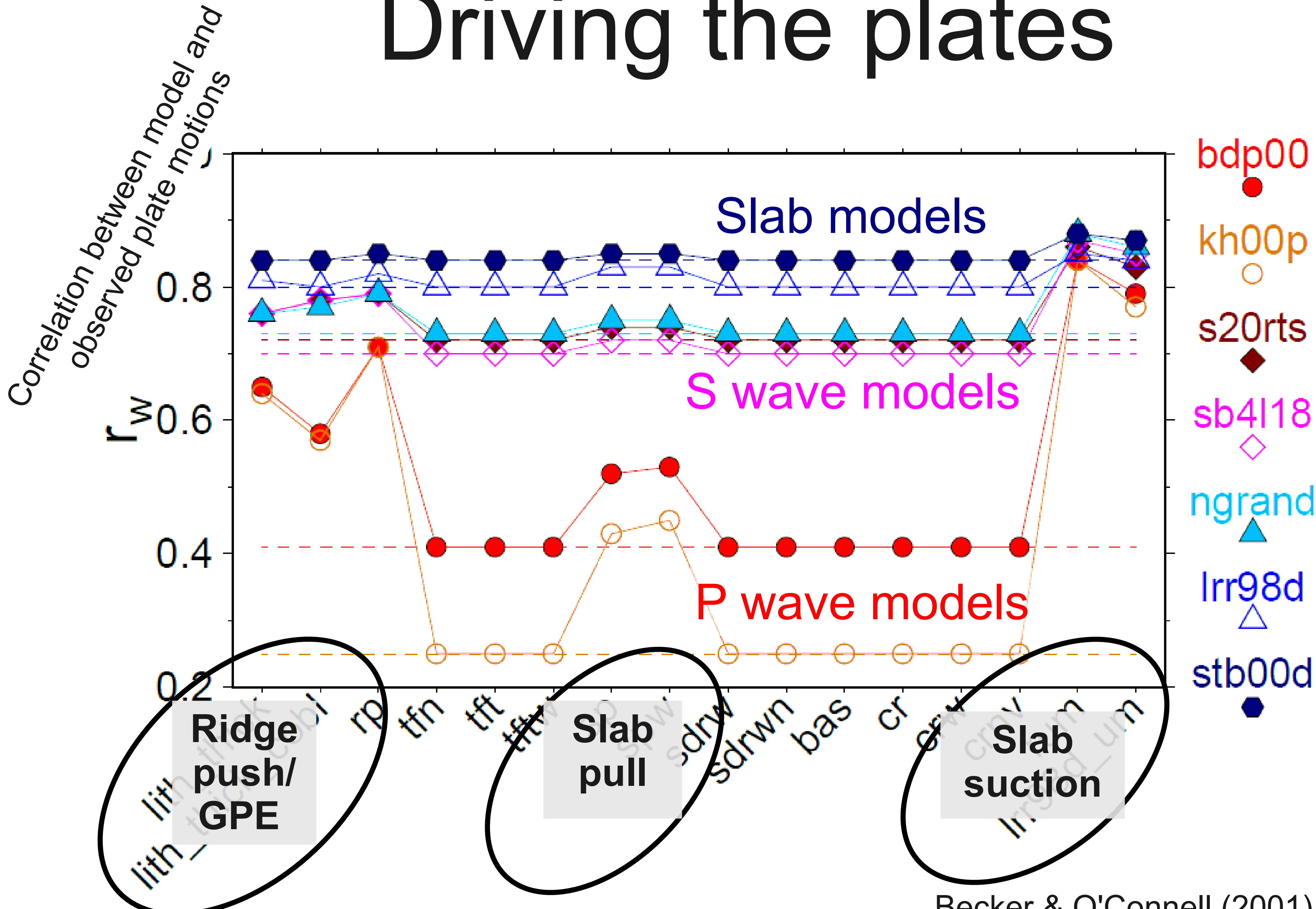

Becker & O'Connell (2001)

Ricard & Vigny (1989); Lithgow-Bertelloni & Richards (1998); Zhong et al. (2000); Becker & O'Connell (2001); Conrad & Lithgow-Bertelloni (2002); Becker (2006)